POLITECNICO DI TORINO

Master's Degree in Mechanical Engineering

Master's Degree Thesis

Development of a lightweight and modular steering system for a highly efficient competition prototype vehicle

Supervisor

Prof. Andrea Tonoli

Candidate

Stefano D'Agostino

April 2022

Abstract

The aim of this Master's Thesis was to design and develop a steering system to be integrated into the Muc022 prototype vehicle, which was designed and built within the TUfast Eco Team, the energy-efficient urban concept vehicle section of the racing team at Technische Universität München. This project, as one of the primary systems of the new TUfast Eco Team prototype, aimed not only to achieve high standards of functionality and efficiency, but also to blend in perfectly with the constituent design choices made beforehand and to reduce the weight component as much as possible in order to increase the competitiveness of the vehicle, which will be called upon to take part in the prestigious Shell Eco Marathon competition.

When sizing each component, the right compromise between efficiency, safety and weight impact was sought, always within the geometric and constructional constraints imposed by the preliminary design choices of the entire car and the primary and secondary systems linked to the steering system.

In this context, particular attention was paid to identifying the geometries and distances between the constituent elements and the points of connection and communication with the suspension system, the wheel hubs and the structural elements of the monocoque, in order to achieve and outline a kinematic system that would guarantee a steering profile as close as possible to that of Ackermann steering.

The steering system, which is particularly innovative in its design as it is based on a core of pulleys communicating by means of a wire, also required an evaluation of the forces involved based on the tension of the wire itself in relation to the torques necessary to allow the wheels to rotate around their kingpin axle.

Other aspects of the steering system involved reducing the driver's efforts to steer the vehicle, influencing the design of components such as the steering column and its associated bearings.

The structural aspects and layout issues always went hand in hand with the rest of the design, but at each step increasing the know-how and knowledge of the system, both personally and for the whole team.

Table of Contents

1 Introduction

1.1 Motivations and Goals Definition

Research oriented to performance and competitiveness. Teamwork and collaboration for the development of a finished product, which looks strongly to the future. Being protagonists of the current change of direction that is affecting the whole automotive world towards total electrification. The personal challenge of pushing the limits of technical specifications imposed by a regulation. All these are the strongest motivations that pushed me to undertake this research and Thesis work.

Each element within a more complex and broader system has its own function and affects overall efficiency. Developing a steering system that is functional and at the same time aligned with technical requirements is an extremely motivating challenge. Reduce the overall weight, improve the driver's driving feedback, adapt geometrically to the systems that live around the steering system and collaborate with it. Perform the most precise steering in relation to the travel speed. All these objectives are results that give professional personal satisfaction, but also of team satisfaction, because they constitute the source of the awareness of being a solid support for the whole vehicle and for all team members.

Doing this then within a team and a project strongly devoted to electrification, to trace new routes and navigate the future is the added value of being the designer of a steering system for this group. The conversion to electricity represents a unique opportunity for Europe to take a step forward and win the race for the climate, giving priority to the most efficient, sustainable and affordable methods to decarbonise the economy.

Electricity, powered by renewable energy, is the most efficient and economical solution: it is clean, sustainable and offers high performance, as well as being the only solution for a truly clean energy system.

The benefits affect all stakeholders: customers become more aware of energy use, while the automotive world evolves towards higher efficiency standards.

An alternative vision and design of the steering system, motivated by the pursuit of performance, competitiveness and regulatory requirements, can represent an attempt to go beyond the standard architectures used in the automotive industry and open new horizons for innovation and change.

1.2 TUfast Eco Team and Shell Eco Marathon

TUfast is a registered company, based in the Technische Universität München, born in 2002. It is an organization of students with a shared passion, the passion for motorsports. Every year team members take up the challenge of developing, designing and building all new Formula Student race cars: in this way they have the opportunity to practically

experience the world of motor vehicles and motorsport, intertwining the knowledge acquired through study with a real and formative multidisciplinary experience, refining qualities and skills that cannot be taught in the classroom, such as team building, collaboration, adapting to situations, finding solutions in a short time and taking on the weight of important responsibilities.

In 2009 the world of TUfast was expanded with the creation of a new team: the TUfast Eco Team.

The TUfast Eco Team is a close-knit team of students who are highly motivated and focused on the development of highly efficient vehicles, who wish to be involved in the development of autonomous software, to actively face and experience the latest developments in electromobility so as to gain valuable knowledge and practical experience through numerous opportunities. The goal of the TUfast Eco Team is the development of innovative solutions through interdisciplinary cooperation.

In the first years of its life, the TUfast Eco Team developed highly efficient prototypes able to define new limits in terms of energy consumption and characterized by extreme outer shapes and layouts, to reduce as much as possible the resistance to motion: eLi family.

However, since 2017 the team's design interest has shifted towards urban-concept vehicles, more stimulating from the point of view of a design that must also accompany a series of devices typical of road machines to the pure competitive aspect. These new urban concepts are certainly closer and projected to the future of the automotive world, and for this reason constitute the new fulcrum of life in the TUfast Eco Team.

Unfortunately, the pandemic due to the spread of Covid-19 has also negatively affected TUfast E.T., initially blocking and then completely cancelling the development of cars for 2020 and 2021. The latest model currently in existence is therefore the muc019 (2019) and the new project in which this Thesis was also developed, muc022 found itself starting between general uncertainty and above all with a completely updated team, with 95% of new members and without a valid know-how behind it, as a guide.

In addition, the Shell Eco Marathon also took advantage of the two-year period in which the competition was not held or was held in virtual form, to update the regulations and introduce substantial changes that made the muc019 and its predecessors no longer suitable as an example and starting point for the muc022.

My challenge and the challenge of the new team was therefore doubly complex: starting from a blank sheet, with no lines drawn previously, with many new features and requirements never addressed in other models, and also aimed at creating a new database, a new information centre for the members of the future, to avoid for this to happen again.

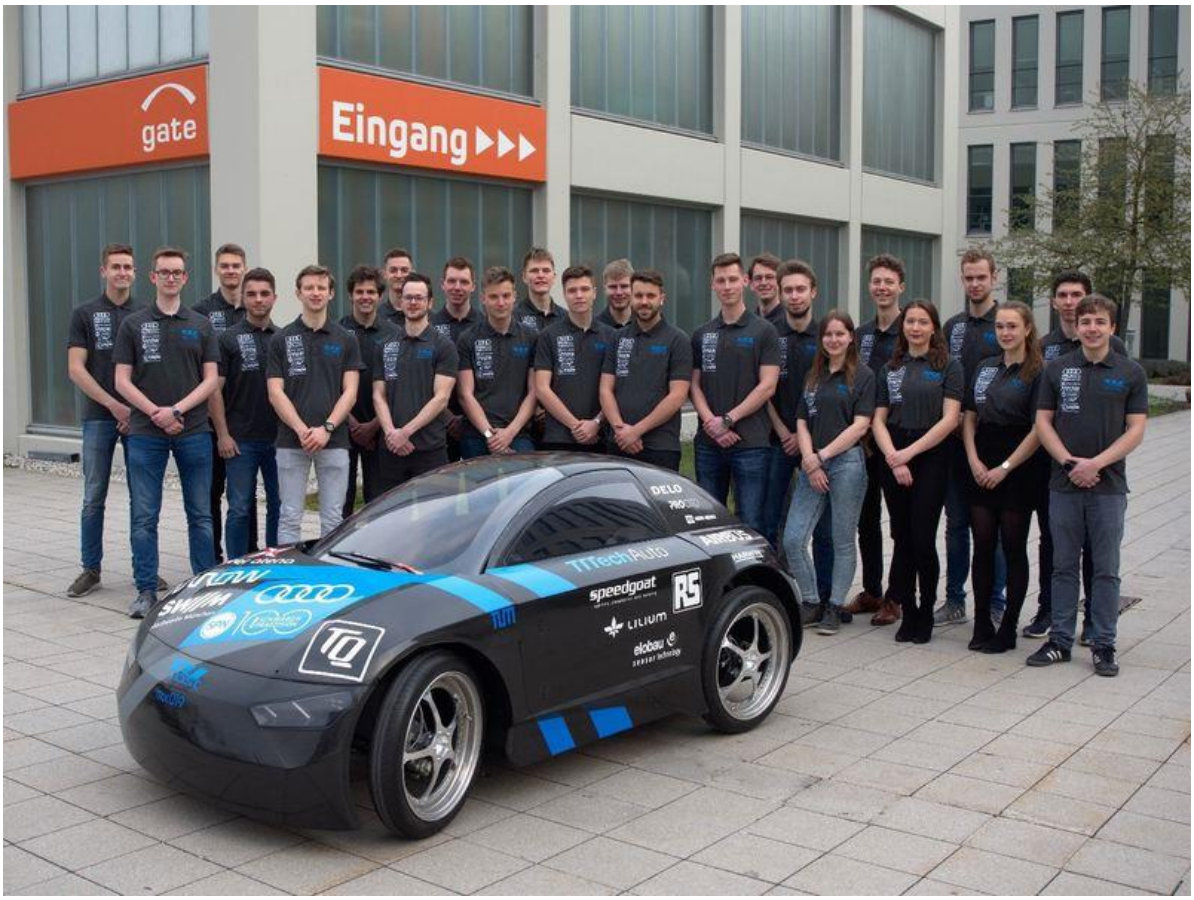

Figure 1-1: TUfast Eco Team and MUC019 (TUfast, 2019)

All the vehicles produced by TUfast Eco Team have always taken part in the most important university competition for high efficiency vehicles, the Shell Eco Marathon. The Shell Eco Marathon, organized and supported by the company of the same name, is a world-class motorsport competition, given that the European and American races are organized annually, and has more than 80 years of history. It was born in 1939 as a bet among Shell employees to see which of them could cover the greatest distance with a gallon of fuel. Since 1985 it has been transformed into the university competition it is today, assuming a unique calibre and importance. Also in this case, the global pandemic from Covid-19 caused the cancellation of the 2020 edition and virtualized the 2021 edition. At the time of writing this Thesis, the 2022 edition has strong chances to compete, but in addition to the technical regulation, no details on the location, date and track have yet been published.

Figure 1-2: Three Urban Concept vehicles at Shell Eco Marathon (Shell, n.d.)

1.3 Structure of the Thesis

Chapter 2 deals in depth with the "State of the Art" and the progressive innovations and architectures introduced in the Steering Systems design sector, while Chapter 3 moves from the general to the specific, presenting the technical and management requirements at the basis of the development of this Thesis project and the related constraints imposed.

The heart of the discussion is contained in chapter 4, where the design procedures, calculations and choices made to model the Steering System are presented. This analysis is developed in steps, passing through the different phases of kinematic definition, dynamic evaluation and CAD modelling.

Before the conclusion, Chapter 5 is used to present ideas and suggestions for further improvements to the system realised.

2 State of the Art

An in-depth study of the historical evolution of the steering system up to today's standards is necessary in order to be able to approach the design of the system in the best possible way, with a solid basic knowledge and with a set of information useful for plotting the course and developing modern research. The different and progressive innovations in both mechanism architecture and kinematic theories will be presented.

2.1 Historical Evolution of the Steering System Architecture

The automobile was invented more than 100 years ago. An important part of it, the steering system, has evolved internally over time, adapting to structural changes in vehicles and technological progress. Over time, the steering system has required an ever greater dynamism of the system and greater flexibility and modularity. The primary function of the steering system is now as it was then to allow the driver to control the vehicle to follow the desired trajectory.
In the early days, when the automobile was just being invented, the driver turned a handle or rail with a steering shaft in hand to steer. The automobile had a pinion steering gear, which was the earliest ancestor of automobile steering gears. The ratio of steering gearing was 1 to 1. It needed much power to drive.

Figure 2-1: One of the first steering systems. The pilot operated on a lever and not on the usual steering wheel (late 1800s)

When the pre-positive engine of the car was developed in 1891, the weight of the front part of the car was increased, so the vibrations of the steering system transferred to the driver by turning the handle or rail started to become too intense and ended up tiring the driver too much.
The single hinge steering mechanism used at the time, which was still quite rudimentary, had to be improved.
In order to avoid the aforementioned problems, the number of hinges was increased; the multi-hinge mechanism naturally increases the degree of freedom and controllability, while avoiding vibrations.
The rack-and-pinion steering gear design went to theorisation later, and was precisely worked out, and has since been formally applied in cars, albeit evolving over time. Parallel link mechanism patent was filed, thus improving the skeleton of links that constituted the system and bringing it closer to the modern technique of integrated automobile steering.
Parallel link mechanism had a vertical hinge which fixed attachments of steering shaft and wheels with bodywork. There was a tie-bar which connected the attachments of steering shaft one another. A special steering rack controlled the tie-bar moving to the right and left and made the inner wheel and outer wheel turn. The mechanism with a gear reducer made the automobile system more flexible to control, and insulated vibration. The handle and rail were replaced by circular steering wheel. And the circular steering wheel with a steering shaft moved to the right or left.
The flexibility and controllability of the cars steering system with the renewal of automotive technology and have been continuously improved.

Figure 2-2: The 1974 Ford Mustang II, the first American car to have a Rack and Pinion Steering System

Mechanical steering gears have diversified over time, reaching the configurations that are commonly adopted today: the rack-and-pinion gear, the worm gear and the recirculating

balls gear.
In the recent past, alongside these solutions and indeed in order to overcome their limitations and disadvantages, power steering has found widespread use. Power steering opened up a new path, different from the traditional mechanical steering system. In America, power steering gears were applied in some limousines as early as the 1950s.
A more detailed analysis of these newly introduced solutions is therefore proposed below.

2.2 Modern Steering System Architectures

Figure 2-3: Components of steering assembly (Porsche 997)

The Figure 2-3 illustrates the generic architecture of modern steering systems, highlighting the components and functional elements that, despite differentiation and continuous evolution, are always present. The interface element with the driver is the steering wheel, through which the driver can define the trajectory of the vehicle and transfer the torque applied through his arms to the system. The steering wheel is connected to the steering column, which is a structural element and transmits torsion and rotational feedback. Usually, the steering column is then connected through a universal joint to an intermediate shaft, which acts as an input shaft for the steering gear mechanism. However, in simpler applications and for smaller vehicles, such as student competitions, the steering column communicates directly with the gear mechanism. The steering gear mechanism is the heart of the system, the site where the rotational input from the steering wheel is transformed into a rotation signal directed to the wheels. This happens because this gear mechanism is connected to two circular bars called tie rods and allows their translation in space. The two tie rods are connected by two ball joints to the steering arms, extensions often modelled from the same wheel hub. The translation of the tie rods is transmitted to the steering arms and therefore to the wheel hubs and is therefore responsible for the rotation of the wheels in

order to follow a curved trajectory. Most of the developments on the steering system concentrate on the steering gear mechanism part, we can evaluate different configurations.

2.2.1 Conventional Configurations for the Steering System

A rack and pinion steering system consists of a pinion (a circular gear) with a rack (a linear gear). The system works by converting a revolving motion into linear motion. Most cars, small trucks, and SUVs come equipped with a rack and pinion system.
The rack and pinion steering system weighs less than a recirculating ball gearbox, which helps improve gas mileage. The size and weight of a rack and pinion system make it a better fit for front-wheel-drive applications because manufacturers can install it right next to the transverse drivetrain. It is easier for manufacturers to tailor rack and pinion gearboxes to fit specific wheelbases and handling packages.
BMW produced the first rack and pinion gearbox in 1930s and the first American automotive manufacturer to use rack and pinion steering in production was Ford, which used it for the 1974 Mustang II and the 1974 Pinto. While AMC adopted the system soon after for the 1975 Pacer, GM and Chrysler would not manufacture cars with rack and pinion steering until the 1980s.

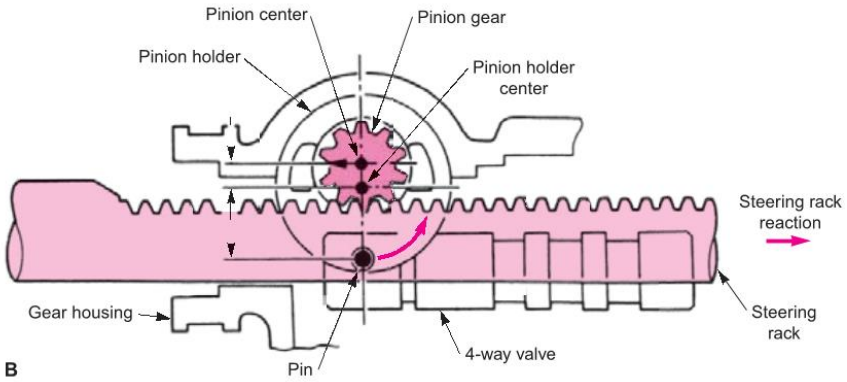

Figure 2-4: Rack-and-pinion steering system cutaway showing the pinion shaft and the rack (Auto Suspension and Steering, A4, 3rd Edition, p. 177)

In worm gear type of steering mechanism, the steering column or input shaft has a worm gear attached to it at its end. It meshes directly with a sector gear. It is so called because it is only a section of the full gear. When you turn the steering wheel, the steering shaft turns the worm gear. The sector gear rotates around its axis as its teeth move along the worm gear and moves the so-called Pitman arm. Sometimes the manufacturers provide a screw for backlash adjustment to move the sector closer or away from the worm gear. This controls the backlash between the sector and worm threads or teeth. Usually the Pitman arm is connected to the end of an intermediate element, which therefore rotates with it, while at the other end the two tie rods are connected, which therefore translate in space and move the steering arms and wheel hubs.

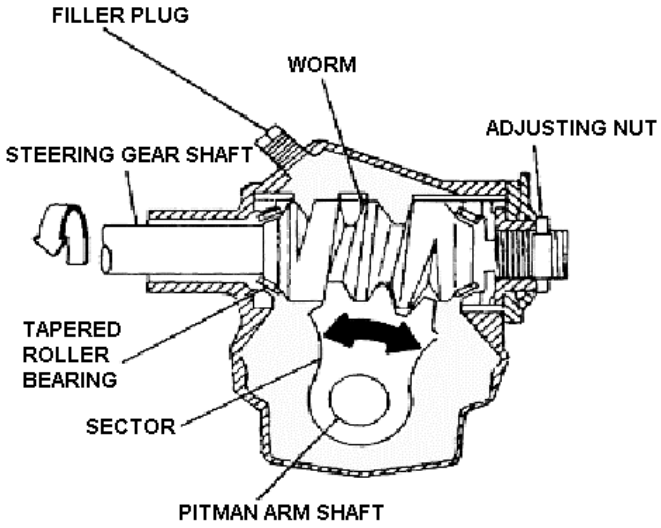

Figure 2-5: Exploded view of a worm-and-roller steering gear assembly (Toyota n.d.)

The main disadvantages of the steering worm gear mechanism are certainly linked to the development of friction phenomena that lead to an evident wear of the components and for which a good lubrication is necessary, but also to the presence of a certain clearance between the teeth of the worm shaft and the sector gear: when one surface of a tooth of the sector gear is in contact, the other is not, due to the presence of this clearance that is necessary to allow the correct reciprocal rotation. However, when the pilot encounters two close bends, one to the right and the other to the left, and therefore has to change direction of rotation of the steering column and consequently of the worm shaft, the first part of the rotation is done just to recover this clearance, so the response of the system is not really ready.

The recirculating balls steering system was created in response to the problems presented by the worm gear mechanism and is in fact its direct evolution. The architecture also includes a worm shaft connected to the steering column and a sector gear connected to the Pitman arm. However, these two elements are not directly in contact, but interface with a ball nut rack threaded internally and externally. The transmission of motion between the worm shaft and the nut rack is via a series of spherical balls. In this way, friction phenomena are replaced by a rolling contact that considerably reduces wear. In addition, the clearance responsible for the response delay has also been eliminated. On the other hand, this system is certainly bulkier and heavier due to the presence of the bulky ball nut rack and balls.

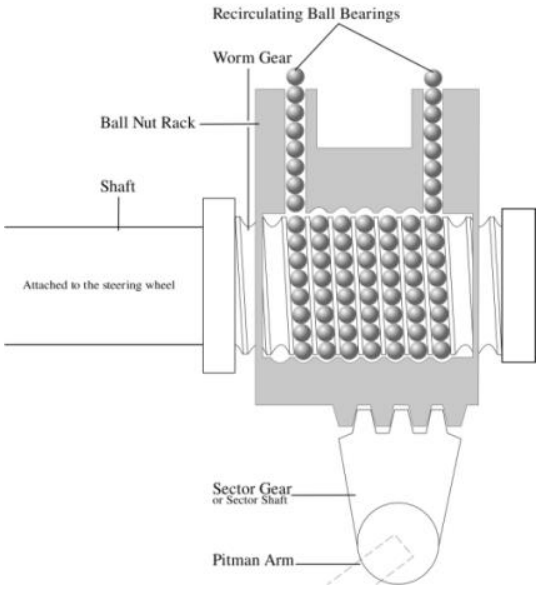

Figure 2-6: A diagram of a recirculating ball mechanism

2.2.2 Power Steering

The power steering is not just a special steering system gear mechanism, but a complete redesign of the entire system, again based on the architectures previously seen. Without power steering, steering manoeuvres of very heavy or low-speed vehicles could be very complex and require excessive effort from the driver; power steering dramatically reduces this effort. Power steering was first introduced on the Chrysler Imperial in 1951 and has since become indispensable, not only increasing driving comfort but also making the system more responsive overall. The only high-performance cars that don't have power steering today are the Acura NSX, the Lotus Elise and the Alfa Romeo 4C, but just like college competition vehicles they have very little weight and very narrow tyres.
The prevailing type of power steering from the 1950s to the early 2000s was hydraulic assist. A hydraulic power steering (HPS) uses hydraulic pressure supplied by an engine-driven pump to assist the motion of turning the steering wheel. Although it has been used in the automotive industry for over 50 years, it does have its drawbacks: there's wasted energy, since the pump is running continuously, even when the vehicle is driving straight and there's no assist needed. Plus, the hydraulic fluid needs to be replaced periodically, and if any of the hydraulic lines springs a leak, it not only makes a mess, but the power assist is lost. However, it's still possible to steer a car without the power steering working.

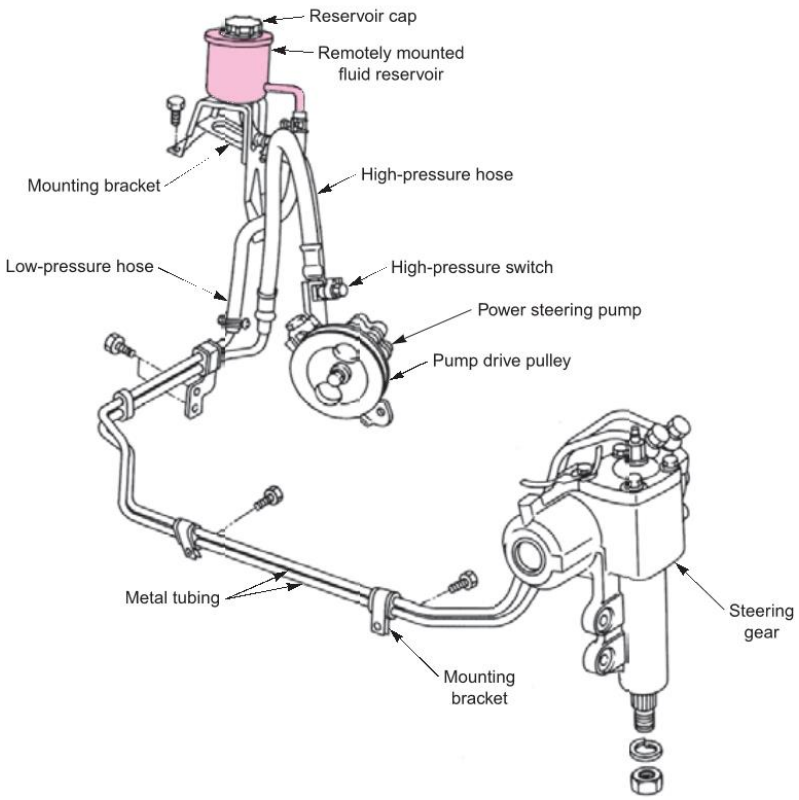

Figure 2-7: Power steering pump which uses a separate, remotely mounted fluid reservoir (Auto Suspension and Steering, A4, 3rd Edition, p. 186)

Electric power steering (EPS) is the norm on today's new cars. EPS bases its operation on the presence of a motor that drives and channels energy from the car's electrical system to assist steering. This electric motor can be located directly on the rack in a more elaborate and expensive configuration or connected to the steering column. Sensors detect the torque, or effort, that the driver is applying at the steering wheel, and a computer decides how much assist needs to be added. In most systems, the computer changes the steering effort based on the vehicle's speed: at parking speeds, the steering is light and easy to turn, while at highway speeds, the effort amps up, giving the driver a feeling of greater stability and control.
The benefits of providing assist electrically are multifold: it improves fuel economy by a few percent, as the electric motor only acts when necessary; moreover, the losses and fluid maintenance present for the HPS are also overcome. The EPS also enables several other functions that are taking the car to a new step: autonomous driving. Thanks to electric power steering, it is possible to control self-alignment problems of the wheels and steering wheel and thus compensate in those situations where the car autonomously tends not to follow a perfectly straight trajectory. Thanks also to the extensive information from the sensor system, the EPS can perform steering manoeuvres autonomously and with great control, thanks to the electric motor, especially when parking. Electric power steering is one of the technologies that will enable and already enables self-driving cars.

2.2.3 Four-Wheel Steering

A very special architecture that is not extremely common among cars is the four-wheel steering, used by some vehicles to improve steering response, increase vehicle stability while manoeuvring at high speed, or to decrease turning radius at low speed. In an active four-wheel steering system, all four wheels turn at the same time when the driver steers. In most active four-wheel steering systems, the rear wheels are steered by a computer and actuators. The rear wheels generally cannot turn as far as the front wheels and there are controls to switch off rear steering.

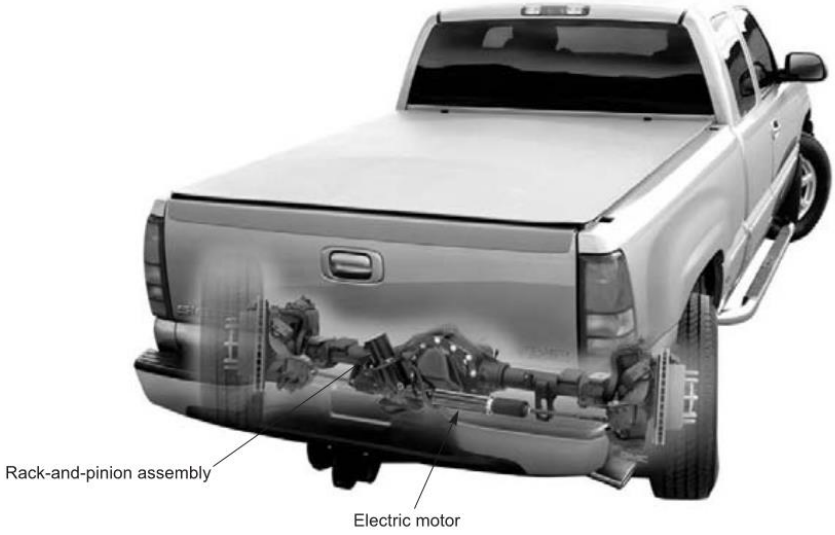

Figure 2-8: The four-wheel steering components installed on the rear axle of this truck include a stepper motor and a rack-and- pinion steering gear (Auto Suspension and Steering, A4, 3rd Edition, p. 199)

At low speeds, for example when parking, the rear wheels steer in the opposite direction to the front wheels, thus reducing the turning radius, a critical parameter especially for large vehicles with a large wheelbase. The car follows the trajectory better and is more agile. While at high speeds the front and rear wheels rotate in the same direction, reducing the body sideslip and therefore increasing the stability of the vehicle. The rear wheels at high speed balance out oversteer and the car is more stable, basically because the steering force is shared between the front and rear axles.
A few types of vehicle use only rear-wheel steering. In cars, rear-wheel steering tends to be unstable because, in turns, the steering geometry changes, hence decreasing the turn radius rather than increasing it. Rear-wheel steering is meant for slower vehicles that need high-manoeuvrability in tight spaces, for example fork lifts.

2.2.4 Steer-by-wire

It is an electronic power steering system. When we talk about by-wire systems, we are talking about systems in which the mechanical connection between the control element and the hydraulic or mechanical actuator is replaced by a distributed, fault-tolerant mechatronic system, one that is able to guarantee the correct operation of the system even in the event of

one or more faults. The aim of steer-by-wire technology is to completely remove as many mechanical components, steering column, intermediate shaft, gear mechanism, as possible. Completely replacing conventional steering system with steer-by-wire has several advantages, such as: the absence of the mechanical components mentioned above simplifies the design of the system considerably and allows much more space to be managed for the location of the engine block. Furthermore, not having the steering column means having less rigidity at the steering wheel, which means that in the event of an accident, the damage resulting from the impact of the steering wheel against the driver will be reduced. Finally, the whole system is more flexible and adaptable to different situations and different steering responses and feels. Currently no car in production relies totally on steer-by-wire technology for safety and cost reasons. However, progress in this direction is remarkable and it will be the most common new steering system in the future.

2.3 Steering System Kinematics

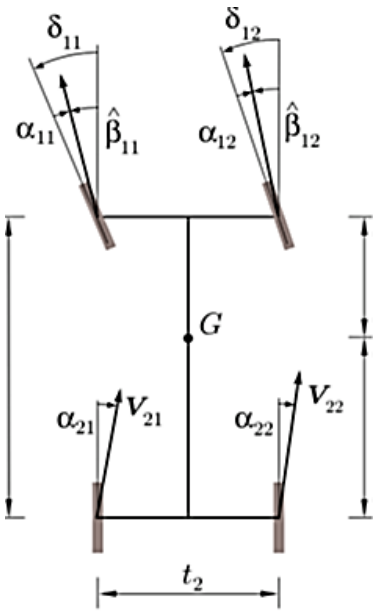

Figure 2-9: Fundamental angles and vectors in steering kinematics (Motor vehicle mechanics, Vigliani A.)

When defining the design choices of a steering system, it is essential to evaluate the kinematics to be achieved in order to favour one steering mode over another. In this sense, it is fundamental to evaluate the quantities that come into play in the kinematics of a vehicle. With reference to the Figure 2-9:

- δ_{ij} steering angle of each wheel
- v_{ij} velocity of each wheel
- α_{ij} sideslip angle of each wheel

The steering angle δ_{ij} is the angle formed between the car's x-axis and the x-axis of each individual wheel whenever it is rotated to follow a curve, while the sideslip angle α_{ij} is the

angle formed between the wheel's x-axis and the wheel's speed vector v_{ij}.

When a rigid body moves along a curved trajectory, it is possible to identify one and only one centre of rotation, a point in space that is fixed throughout the journey and around which the body practically rotates. Of course, this is also possible for a vehicle.

Suppose then that we have a car travelling along a curved trajectory at a very low speed. Under these assumptions any sideslip angle α_{ij} is negligible, as a result of the fact that the travel velocities v_{ij} of the individual wheels become very small.

To find the centre of rotation of a vehicle, we find the point of intersection of the two straight lines perpendicular to the speed vectors of the two front wheels (in the more general case of a 2-wheel steering system) and assess where this point is in relation to the extension of the rear axle (see Figure 2-11).

In the light of this, it is clear that the parallel-wheel steering kinematics used centuries ago cannot be used to follow the path of a curve.

2.3.1 Parallel Wheels Kinematic

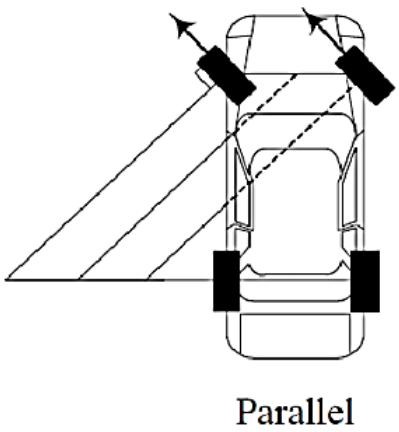

Figure 2-10: Kinematics of a car turning with parallel wheels (Motor vehicle mechanics, Vigliani A.)

If you look at the Figure 2-10, you can see that when you draw perpendiculars to the wheel speeds, the wheels never meet. There is no unique centre of rotation and this is not physically possible in a rigid body. In fact, no car today steers with parallel wheels, i.e. with equal steering angles between the inner and outer wheels, because it is clear that the two wheels follow trajectories with different radii. Having the wheels parallel when steering would lead to serious instability and slippage of the wheels. It is therefore necessary for the steering system to provide a different steering angle between the inner and outer wheels. This concept gave rise to the need to introduce a mechanism capable of differentiating the angles of the two wheels of the steering axle.

2.3.2 Ackermann Kinematic

The need for the two front wheels to steer at different angles is reflected in Ackermann's kinematics. To achieve kinematically correct steering, the axles passing through the hubs of the two front wheels must join at a point, the centre of instantaneous rotation, which is positioned on the extension of the rear axle.
This is the only way to achieve a pure wheel-rolling condition, with no sliding in the contact area between the tyre and the road.

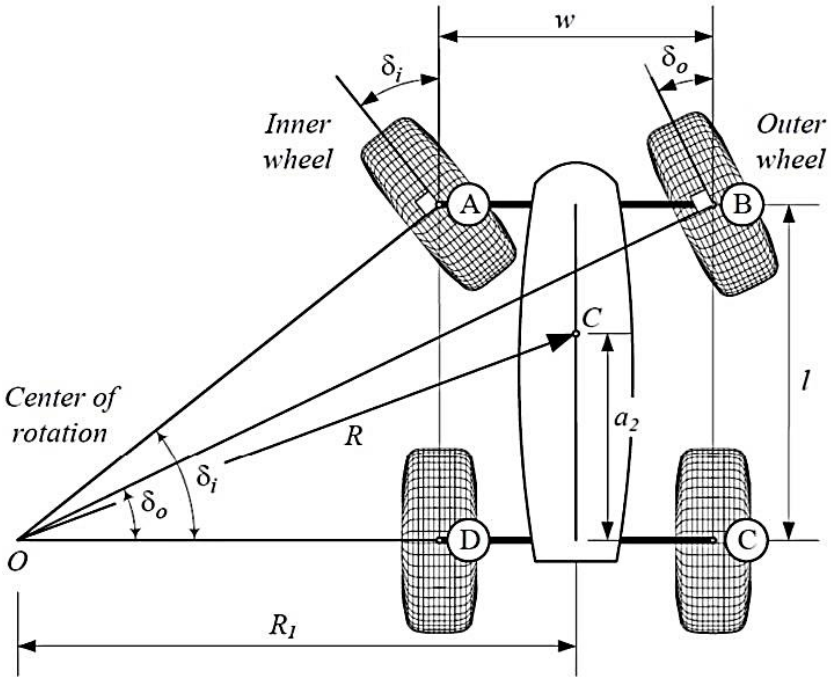

Figure 2-11: Ackermann Kinematic (Motor vehicle mechanics, Vigliani A.)

The following quantities are defined:

- δ_i steering angle of wheel on internal trajectory
- δ_o steering angle of wheel on external trajectory
- l wheelbase or distance between front and rear axle
- w length of front axle

From the image above, one can see the fundamental relationships between the geometric parameters in Ackermann Kinematics.

First of all, the steering angle of the wheel travelling on the inside trajectory must be larger than that of the wheel travelling on the outside trajectory:

$$\delta_i > \delta_o \tag{2-1}$$

Furthermore, between the two angles exists the important relation:

$$\frac{1}{tan\delta_o} - \frac{1}{tan\delta_i} = \frac{w}{l} \tag{2-2}$$

This is the so-called Ackermann steering relation.

In order to perform this type of kinematics correctly, the most commonly used solution is the Jeantaud or four bar linkages mechanism.

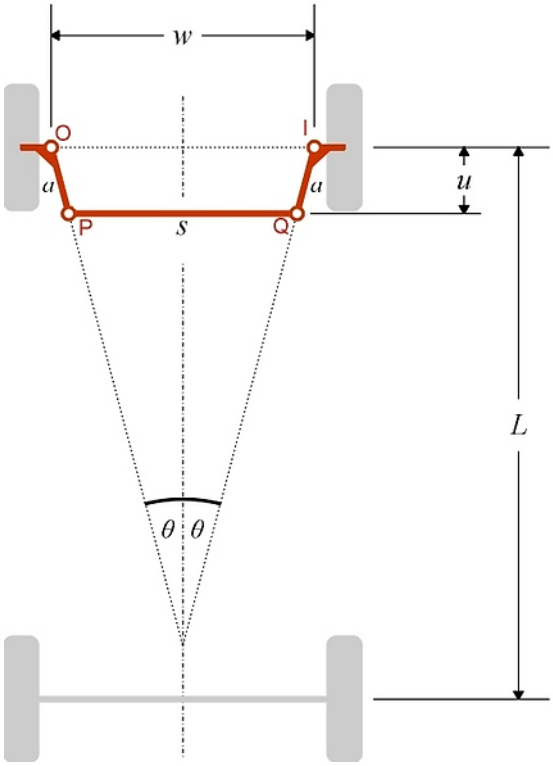

Figure 2-12: Schematization of the Jeantaud mechanism (Motor vehicle mechanics, Vigliani A.)

As can be seen from the Figure 2-12, this mechanism consists of four bars, three real and one virtual (the frontal axis) which closes the quadrilateral. The bars are connected to each other and to the wheels by ball joints.
By acting on the geometrical parameters of this mechanism, such as the length of the bars, the length of the front axle and the angles allowed to the spherical joints, it is possible to change the values of the internal and external steering angles, until the angles that satisfy the Ackermann Steering relation are achieved. And that was the executive principle behind this Thesis project.
Media interest in Ackermann's kinematics has exploded recently following the controversy surrounding the introduction of the DAS (Dual Axis Steering System) by the Mercedes F1 team during pre-season testing in 2020. This innovation made it possible to vary the steering geometry of the front wheels in motion, exploiting the axial displacement of the steering wheel, operated by the driver. Mercedes was thus able to change the Ackermann angle, which is normally a fixed parameter that can only be modified when the car is stationary through structural and geometric changes, as the car travels along the track, making the car more suitable for each part of the track.

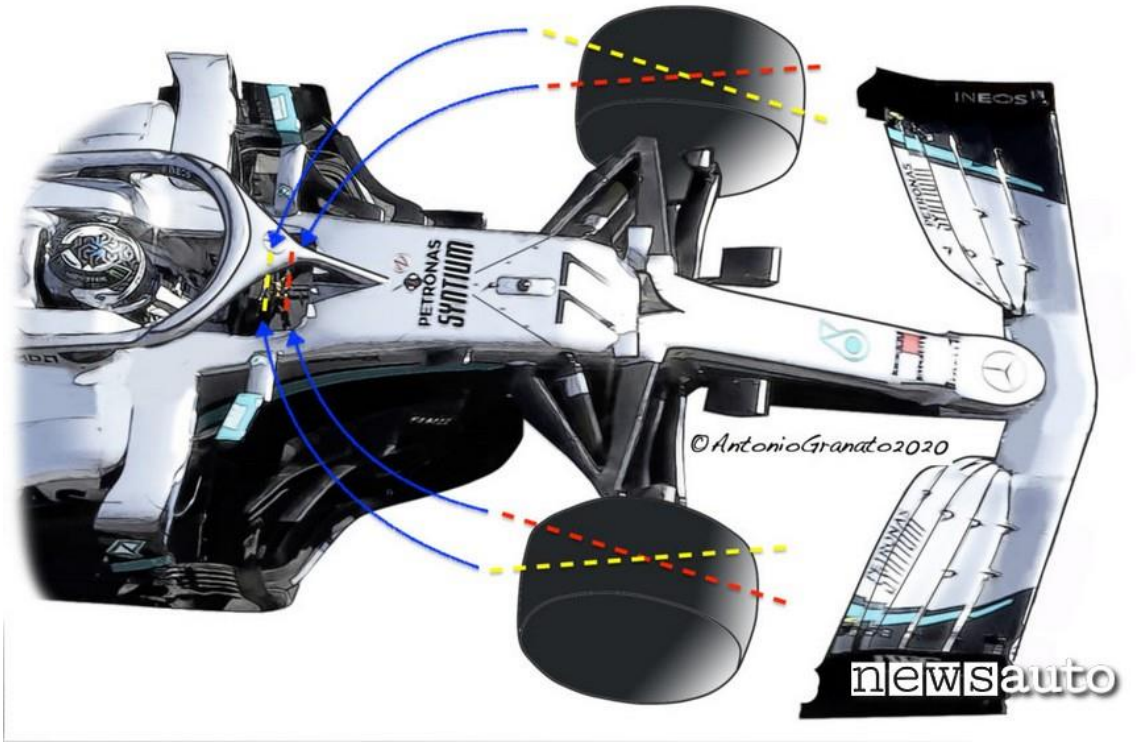

Figure 2-13: Operation of the Mercedes F1 DAS system (2020) (newsauto n.d.)

An article published in "The Royal Society of London" (Vol. 56, No. 1, Jan 2002) reveals that the original idea of a differentiated steering was initially conceived by the English physician, philosopher and naturalist Erasmus Darwin (grandfather of the most famous Charles), who lived north of Birmingham in the second half of the 1700s.
Every year the scholar was forced to face over 15,000 kilometers on bad roads to visit his patients, aboard carriages that at the time were equipped with a very rudimentary steering system, made by rotating the entire front axle, with the wheels constrained to the axis itself.
A configuration that led to two fundamental problems. The first was that the wheels had to be quite small in order to swing under the carriage frame, and this feature caused enormous inconvenience on the holes, where it would be preferable to have a rolling radius as large as possible to alleviate vertical shaking. The second problem was related to safety during very sharp turns: in this phase, in fact, the footprint of the wagon became triangular and a hollow or a stone was enough to cause the carriage to overturn.
To alleviate the danger and inconvenience during his travels, Darwin therefore decided to develop a new concept, where the axle was fixed and the wheels rotated around their own independent axis, no longer being parallel to each other. Furthermore, Darwin realized that to avoid slippage the wheels had to turn around the perimeter of a circle, whose common centre was placed in correspondence with the extension of the rear axle. It was undoubtedly the invention of modern steering. It is estimated that Darwin had five carriages built with the new steering system, of which three were donated to illustrious personalities, including Prince Edward, younger brother of King George III, and wealthy friend Edgeworth, who did his utmost to make known the system, showing it to the London Society of Arts in 1769, receiving several appreciations.

Darwin, on the other hand, never made an effort to publish his idea, worried that his reputation as an inventor might somehow ruin his reputation as a doctor.
He limited himself to using his own carriages on a daily basis, with the new steering system, testing them for over 30,000 km, thanks to the help of the many servants, of whom a high social class figure such as a doctor in the 1700s had at his disposal.
But the coach builders, informed of the existence of Darwinian steering, considered its realization and repair in case of failure too complicated, and for these reasons they decided not to apply it to their models: it was thus that Darwin's idea was soon forgotten after his disappearance in 1802.
It was revived only 15 years later, in 1817, by the German craftsman Georg Lankensperger, who chose to file the patent in England.
He entrusted the task to his friend Rudolph Ackermann, an expert publicist.
It was curious that, at the time of filing, Ackermann gave his own name to the invention, of which in reality he was only an agent: the official title of the patent was "Specification of Rudolph Ackermann axletrees".
He was soon accused of stealing the invention, charges from which he defended himself by admitting that he was not the inventor but only the agent of Lankensperger, from whom he had received the mandate to file the patent.
Unlike Darwin, Ackermann did a lot to make the invention known, exploiting his knowledge in publishing (he was the founder of "The Redipository of Arts, Literature, Fashions, Manufactures, etc .."), but clashed with the usual opposition from manufacturers, not very accustomed to innovations and worried about the overall reliability of the system.
The text of his patent also had some fundamental errors, in fact he misinterpreted the original concept of Erasmus Darwin and perhaps these inaccuracies were the cause of the delay in dissemination and practical application.
In fact, the patent image showed a decidedly abrupt and exaggerated steering, as much as 62 degrees, so that the centre of rotation of the front wheels coincided with the hub of the inner rear wheel, and not with the extension of the rear axle, as shown in Figure 2-14. An error that most likely made it more complicated to guess how it worked.
It was the turn of the French engineer and builder Charles Jeantaud, in 1878, more than sixty years later, to perfect Ackermann's patent and study its practical application, making it suitable for vehicles equipped with their own traction that began to spread in those years.
Jeantaud introduced the aforementioned four bar linkages mechanism which interpreted Ackermann's theoretical steering with a high degree of precision, also resulting in a system of easy physical implementation, compact and with only ball joints, still used today, albeit evidently evolved, in the world of automotive industry.
In light of this troubled history that has spanned over two centuries, it would be more correct to speak of Darwin's invention, of Jeantaud's four bar linkages mechanism but we know that injustices in the field of intellectual property are very frequent and it was thus that Mr.Rudolph Ackermann, a publicist who served only as a licensed agent, managed to earn a virtually immortal reputation in automobile engineering.

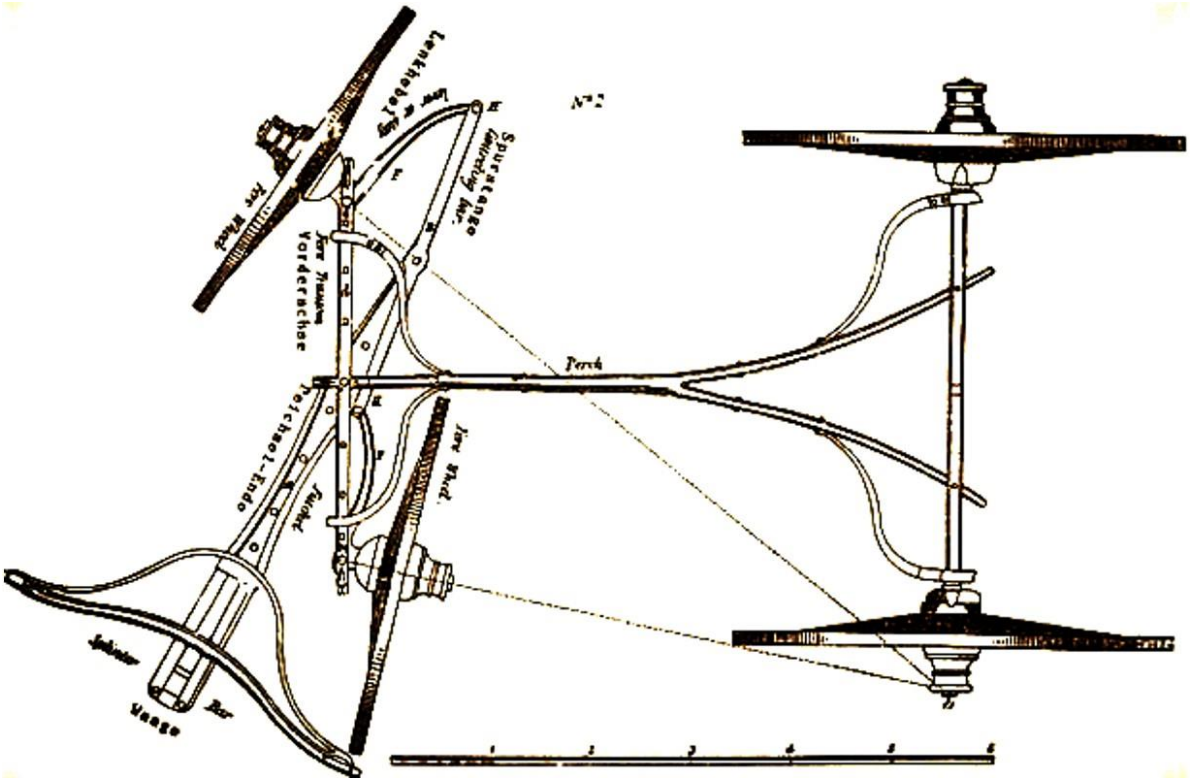

Figure 2-14: Image published in Ackermann's patent (The Royal Society of London, Vol. 56, No. 1, Jan 2002)

2.3.3 Dynamic Kinematic

When studying the vehicle statically or at very low speeds, finding the correct Ackermann angle is simple and unambiguous, while its dynamic interpretation is more complex, where external factors such as transverse load transfer and tyre side slip angles intervene.
When vehicle speed is no longer negligible, there are many parameters that need to be considered:

- The transverse load transfer, which causes the vertical load on the outer wheel to increase and the inner wheel to lighten.
- The side slip angles of the tyres (see Paragraph 2.3 and Figure 2-9) the angles formed between the longitudinal axes of the wheels and the direction of their velocity vectors, due to the elastic deformation of the tyres and whose presence is actually necessary to generate steering forces since the latter are directly proportional to these angles.
- The characteristic angles of the wheels, camber and toe-in.
- The vertical travel of the suspension, which causes the characteristic angles to vary dynamically.
- The tractive or braking forces applied to the wheels.

It is therefore evident that it becomes enormously more difficult to obtain a steering system that can achieve theoretically correct steering for any speed and any steering angle.

Considering an example, in which a car drives through a right-hand bend at a speed that causes a transversal load transfer (and therefore a rolling of the car).

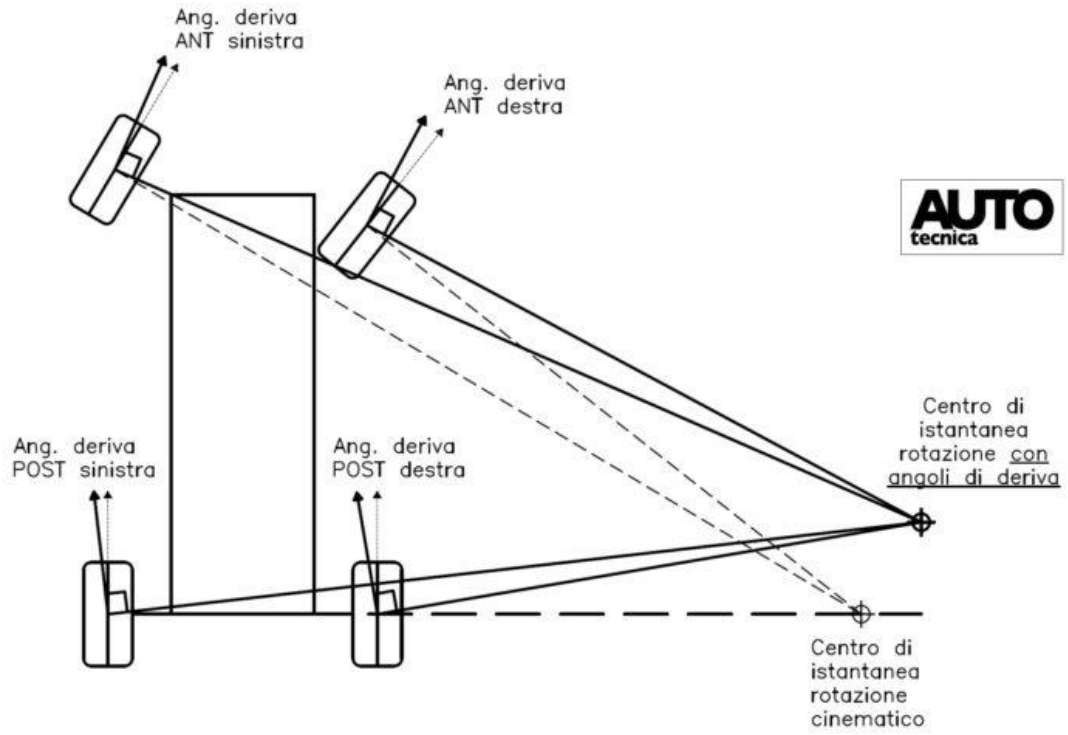

Figure 2-15: Dynamic Steering Kinematic. Due to the sideslip angles, the centre of rotation is no longer at the rear axle (AUTOtecnica n.d.)

It is therefore up to the sensitivity of the designers, based also on the type and performance targets of the vehicle, to find a geometry that is the right compromise between driveability, performance and safety.

For example, in road cars, there is a tendency to have an almost zero Ackermann angle, to facilitate congenital understeer, which increases safety for inexperienced drivers, avoiding the onset of oversteer, which is much more dangerous and more difficult to control.
In racing cars and Formula 1, where performance is maximised and understeer is barely tolerated, the correct selection of the Ackermann angle varies greatly depending on the set-up and type of track being driven. When the inside wheel contributes a lot to the overall grip, there is a tendency to exaggerate the effect, even considerably beyond the kinematic values (Pro-Ackermann). This happens, for example, when aerodynamic downforce is so high that the effect of transverse load transfer contributes less in percentage terms to the overall vertical load on the wheels.
There are also cases in which we speak of Anti-Ackermann, i.e. when the engineers choose a steering kinematic system in which the inner wheel steers less than the outer wheel: this happens when the inner wheel is significantly discharged by the load transfer and therefore its side slip angle is significantly reduced.

3 Requirements and Constraints

The analysis of the requirements was the real starting point in the design of the steering system. It was necessary to meet and consider various aspects that were constraints to embrace and exploit to the maximum of their potential. The requirements derived both from the regulatory and the performance fields and we took particular account of basic design decisions taken a priori, before I took charge of the development of this System and of this Research.

3.1 Shell Eco Marathon Regulation

The first aspect to be considered during the development of Muc022 steering system is the compliance with the rules of the competition for which the car is designed. The rules which are considered in this dissertation are the ones referred to the urban concept class of Shell Eco-marathon. “Chapter I” and “Chapter II” are the two documents issued by Shell: the first one is reporting the Shell Eco-marathon official rules while the second is focused on the guidelines of the “on-track” event. The most relevant section is the “Part 3C, article 47" related to "Turning Radius and Steering", contained in “Chapter I”. In the following, only the most important and pertinent rules will be presented and commented. As already mentioned, the following section are entirely referred to Shell Eco-marathon 2021 Official Rules Chapter 1 (Shell, 2020).

The Shell Eco Marathon regulation for 2022 requires each vehicle to steer using predominantly, if not exclusively, the front wheels. This is a first major step which excludes any possible architecture with four-wheel steering or with only rear-wheel steering.

The regulation also explicitly requires that the system be manually controlled, so that both the driver and the steering wheel communicate the intention and magnitude of the steering. Therefore, no power steering system, hydraulic or electric, as well as no autonomous steering system is allowed. In addition, the only means of interaction between the driver and the steering system must be the steering wheel, no replacement or additional control bar, lever or joypad may be present.

The last but fundamental indication provided by the regulation regarding the design of the steering system is that relating to the turning radius. The regulation dictates that the turning radius must be 6 meters or less and specifies that turning radius is meant the distance between the centre of the circle and the external wheel of the vehicle (see Figure 3-1).
The external wheel of the vehicle must be able to follow a 90° arc of 6 m radius in both directions. The steering system must be also designed to prevent any contact between tyre and body or chassis.
This specific turning radius technique is to all intents and purposes the keystone and the real starting point in defining the geometry and kinematics of the steering system.

All the other constraints will adapt and embrace this conceptual and design point of reference.

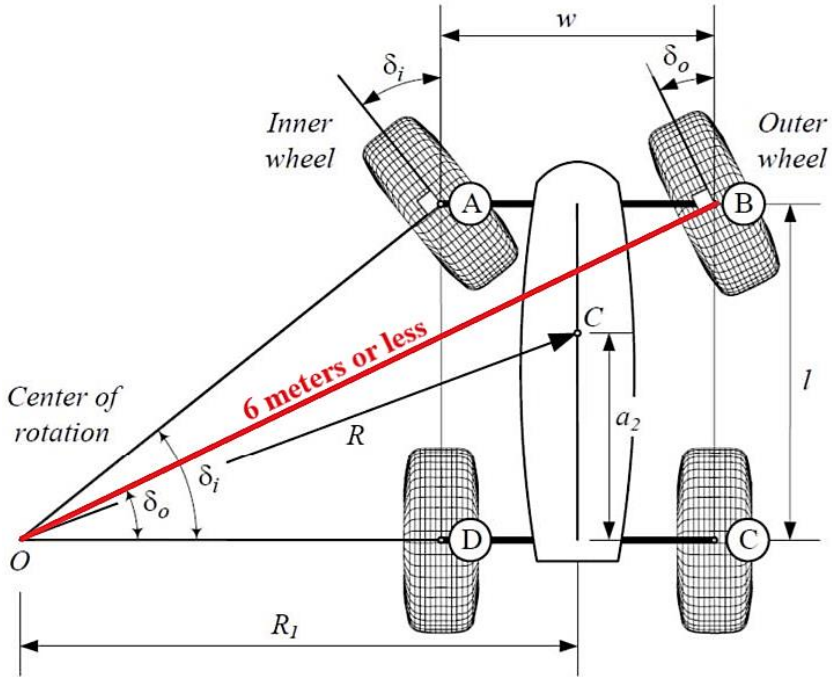

Figure 3-1: Turning radius according to the rules of SEM 2022

The Organisers reserve the right to set up a vehicle handling course to verify the following when the vehicle is in motion: driver skills, turning radius and steering precision.

3.2 Preliminary Design Choices

My joining the TUfast Eco Team coincided with the start of my Erasmus teaching experience at the Technische Universität München, so in March 2021. However, the formation of the team and the beginning of conceptual decisions regarding the new vehicle started at the end of 2020, so at the time of my arrival in the team and my taking charge of this project, I had to deal with some preliminary project decisions, made in the previous months.
The most important ones, which influenced the work described in this Thesis, are the following.

- The main dimensions of the vehicle had already been decided, in detail height, wheelbase, overall length, front track and rear track. All these dimensional parameters, in particular those referring to the front part of the car, constrain the design of the steering system, limiting its space and dimensions and influencing in particular the definition of the kinematics, as will be illustrated in Paragraph 4.2.
- Another choice already made by the team was that of propulsion. The propulsion will be electric and will be developed through a double hub motor inserted in the hubs of the two front wheels. The presence of this element is a further point of attention for the design of the steering system. In fact, no element of the system must

come into contact with these two hubs at any stage of steering. This aspect was developed in Paragraph 4.2.3.

- The last preliminary choice concerned the suspension system. The types of suspension were chosen for the front and rear of the car, and the geometry and kinematic points of the front suspension were further defined. Suspension system and steering system share among their kinematic points the one that links the tie rods to the wheel hub, so defining it a priori, even before having a basic idea of the kinematics of the steering system, was a rash decision and, as explained in Paragraph 4.2.3, it was later the subject of an inevitable modification.

The following table summarises the preliminary decisions made by the team prior to the start of development of the steering system, and which therefore influenced its design.

Vehicle characteristic	Set value	Unit of measure
Height	1000	mm
Width	1200	mm
Length	~3400	mm
Front track	1080	mm
Rear track	850	mm
Wheelbase	1550	mm
Ground clearance	100	mm
Vehicle characteristic	**Concept decision**	
Propulsion	Electric	
Traction Axle	Front Wheel Drive	
Doors	2 + Tailgate	
Seats	1	
Front Suspensions	McPherson	
Rear Suspensions	Double Wishbone	

Table 3- 1: Preliminary Concept Decisions (TUfast E.T.)

3.3 Sponsorship agreements, preliminary investments and team philosophy

The requirements to be met in developing the steering system were not only regulatory, technical or project-related. There were also constraints of a more managerial and team resource management nature, as is the case in every situation.

The main one in this sense was the sponsorship and technical support agreement taken by the team with the company Reichenbacher Hamuel, specialised in the production and use of first class CNC-machining centres and 5-axis systems (see reichenbacher.de). Using this technology, it is possible to produce incredibly advanced components that could never be produced using university means.

The sponsorship with this company was signed at the end of 2019 and involved the

manufacture and use on the next three vehicles produced by the TUfast Eco Team of a very complex aluminium component, a horizontal translation slide with associated railguide.

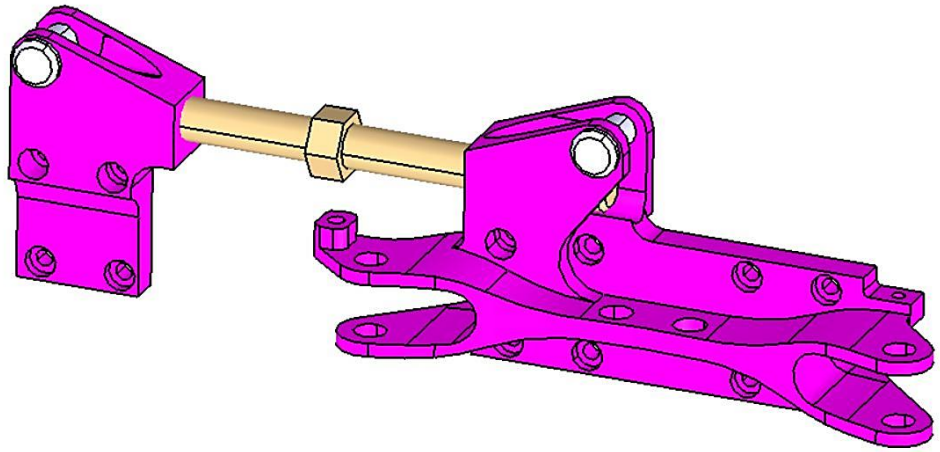

Figure 3-2: CAD model of the central translation slide. It will be one of the fundamental components of the Steering System (CATIA V5)

The component was ordered with a view to integration into the old steering systems, in order to improve their performance.
However, as is well known, the muc020 and muc021 project never saw the light of day and the Shell Eco Marathon regulations changed in the two-year period, leaving the team with a triplicate component that was very technologically advanced and expensive for the machinery with which it was made.
In these situations, the TUfast Eco Team's philosophy has always been to minimise and if possible completely avoid waste, both material and financial. It is a policy with which the team was born, which has always led to worthy results and which the Shell Eco Marathon fully espouses.
In the light of this, when I was interviewed for the position of steering system designer, the team board asked me to do my utmost to integrate this component into the new steering system in some way, thus establishing what was the biggest requirement and fixed point in the definition of the system architecture.

The team's philosophy was also applied during the development of this project and the car in other minor situations. At the beginning of the year and in the previous years, several orders for materials and components, such as carbon fibre tubes, screws, bearings and much more, had already been placed in view of two car models to be produced. All of these items had been in stock for a year and a half or more. Wherever possible, the board asked me and the whole team to make use of what was already in stock for these very general and widely applicable components.

4 Steering System Design

In the following chapter the phases, processes, conceptual operations, choices and calculations that are at the basis of the development of an extremely light weight steering system model for a highly competitive vehicle from the energy point of view, such as the muc022, will be specifically described.
The discussion will be divided into four macro-areas that represent the four main consequential moments that have affected the development of this Thesis project and that, at different times and periods, have added the necessary pieces to achieve the predetermined result. These four phases are:

1. The definition of a basic architecture on which to develop and model the Steering System;
2. The definition of the kinematics underlying the system;
3. The definition of the dynamic actions within the system and the dimensioning of its constituent elements;
4. The final implementation using CATIA V5 (software) of the models and CAD drawings of the Steering System.

Each paragraph will therefore detail the procedures, results and problems that emerged in each of the above-mentioned phases.

4.1 Definition of the Basic Architecture

The first step necessary for the design of the steering system is certainly to think of a functional basic architecture with respect to the set targets. In this sense, the respect of the constraints mentioned in Chapter 3 is fundamental to set the contours of the architecture sought. The approach taken in this perspective has been to integrate the constraints present, not as obstacles to an idea to be limited, but as protagonists of the idea itself.

The main constraints among those mentioned in the previous chapter that must be taken into account in this preliminary phase of modelling an architectural idea are the use of the central sled, the subject of the sponsorship agreement, the primary search for lightness in the system with consequent total reduction in weight, and compliance with the rules of the Shell Eco Marathon 2022 for which the system must be entirely mechanical and the steering performed in its entirety only by the front wheels. The dimensional constraints, which are the result of the design choices made by the team in the phase prior to my entry (see also chapter 3), are of equal importance, but will be developed and verified in the subsequent phases of kinematic and dynamic analysis.

The weight reduction requirement cuts out any classic Rack and Pinion steering architecture (see Paragraph 2.2.1), which is too heavy. The previous TUfast models all used this type of steering mechanism, which is in fact the most traditional. Figure 4-1 is just a picture of the

Steering System of an earlier TUfast model based on the Rack and Pinion mechanism. However, the weight of the rack and pinion in the solutions of the previous years reached 1.5÷2 kg, tolerable with the old regulations on car weight, but no longer suitable for the new competition rules that allow vehicles to stay under 70 kg overall. In this situation a weight of the rack and pinion in the order of that of the previous years would represent alone 2÷3% of the total, a value absolutely not tolerable thinking also that to this weight for the steering system the weights of the other components of the system should be added. The idea of trying to make a smaller rack and pinion in order to save weight was not even considered, given that their dimensions depend mainly on the forces generated by the tyres, which in turn are linked to the speeds the vehicle can reach and the steering angles it has to perform, all values that are almost identical between the previous models and the muc022.

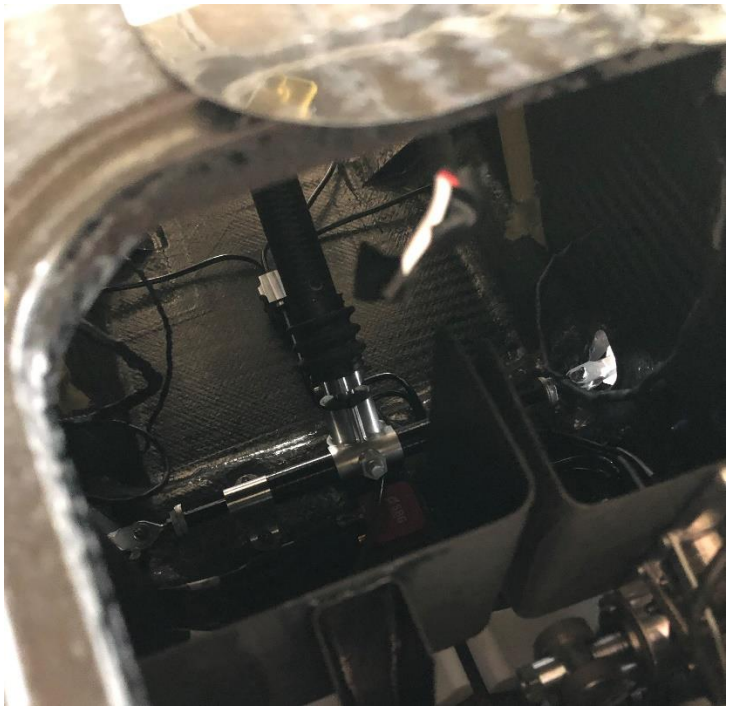

Figure 4-1: Detail of a Rack and Pinion Steering System

Added to this is the required presence of the central slide. The general idea at the time the sponsorship agreement was signed was to create a more advanced rack that would be integrated with the central slide and thus exploiting the toothed coupling with the pinion, would set it in motion and with it the two tie rods. The project and the idea were then abandoned due to pandemic by Covid-19 as already mentioned in Paragraph 1.2 and at the dawn of this new project, it was no longer possible to implement this idea because it meant adding further weight to the already excessive weight of the rack and pinion. It was therefore necessary to find a different idea, one that completely abandoned the traditional mechanism.

The subject was obviously the focus of several team meetings, where we tried to gather ideas and propose alternative solutions. However, the idea that was then validated came to me when I looked through the team's archives and drives.

In the past, the TUfast Eco Team participated in the Shell Eco Marathon not in the urban-concept category, but in the prototype category. These vehicles are extremely elongated and tapered, as can be seen in Figure 4-2. The driver is placed horizontally on the inside in horizontal position.

Figure 4-2: The eLi15, one of the first prototypes created by TUfast E.T. (2015, TUfast)

These vehicles are normally equipped with three wheels, two steered forwards and one at the rear. The weight of these vehicles is incredibly low, and all the solutions and systems applied in them point and aim in this direction; for example, the eLi15 prototype weighs just 24 kg. Seeing how the team has designed the steering system for these ultralight vehicles in the past was the inspiration for the new muc022 architecture. Below are two figures of the eLi15's steering system.

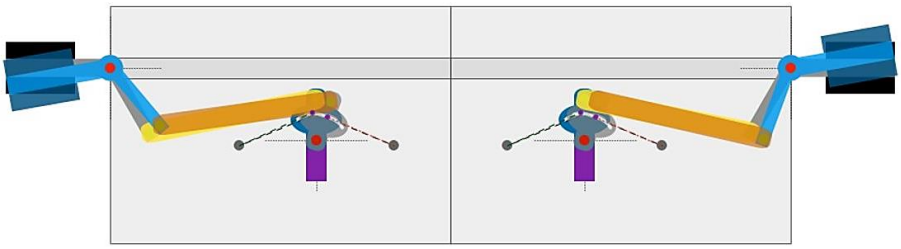

Figure 4- 3: Steering system eLi15-lower part, Conceptual drawing (2015, TUfast)

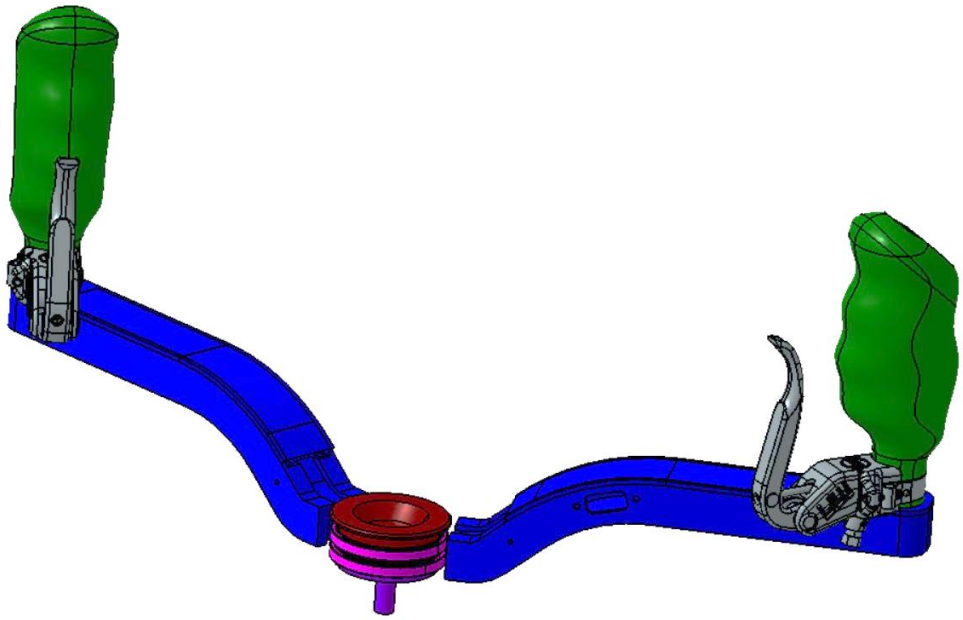

Figure 4-4: Steering system eLi15-upper part, CAD drawing (2015, TUfast)

The two tie rods shown in Figure4-3 (the elements in orange) are moved by two flanges (the elements in grey) capable of rotating around a pin (red dot). The two flanges are in turn set in rotation by the stretching of cables connected to them. These cables terminate inside the grooves of the fuchsia pulley in Figure 4-4. This pulley is then inserted into a case which is integral with the handlebar used as a steering wheel by the rider. In this way, the rider rotates the handlebars when approaching a bend, stretches the cables and moves the flanges and with them the tie-rods connected to the wheels. The idea from looking at these drawings was to adapt this system to an urban concept vehicle. The idea was to use a pulley integral with the driver's control element, in the case of the muc022, the steering wheel, around which a cable would be wound, and two other pulleys would be used to direct it towards the central slide and connect it. When the pilot would have rotated the steering wheel, the rotation would have been transmitted via the steering column to the first pulley, which by rotating, together with the two secondary pulleys would have rotated the cable and this would have dragged with it the central slide that would have started to slide along the rail guide.

The central slide would then move the tie-rods and the wheels with them.
The following image represents the architecture at the end of the Steering System development project. Obviously, the achievement of this architecture represented below is subsequent to the dynamic and kinematic computation and the dimensioning of the various components illustrated later in this chapter. The objective of the presentation at this point of the discussion of the final result of this Thesis project is obviously to provide a clearer and more outlined image of what, through subsequent studies, it is intended to achieve.

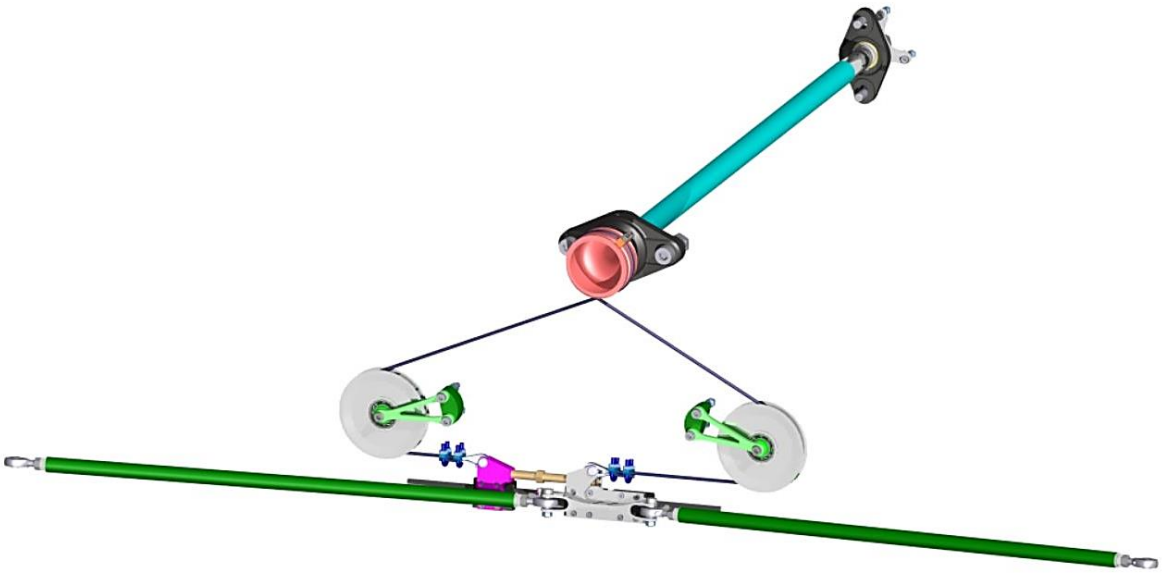

Figure 4-5: muc022 Steering System (isometric view) (Final CAD Drawing, CATIA V5)

The use of cables and pulleys will considerably reduce the weight of the system. In addition, by simply removing the cable from the pulleys and unhooking them from their mounts, the whole steering system is modular and can be easily moved.
This architectural idea was quickly approved by the whole team.

4.2 Steering System Kinematics

Once the architecture of the system has been defined, with an initial identification of the components that will make it up, it was fundamental to define the geometric and kinematic part to support the dynamics of the system itself. The definition of the kinematics for a steering system is, as illustrated in Paragraph 2.3, the starting point and at the same time the synThesis of a series of needs. The choice of target and kinematics from those normally adopted and illustrated above (parallel wheels to be excluded a priori, Ackermann Kinematic, Dynamic Kinematic) takes account of many factors, and depending on the option taken into consideration will also include relative advantages and disadvantages.

4.2.1 Kinematics selection

The choice of Kinematics for the steering system of the muc022 was an issue that was immediately the focus of many team meetings held in the initial concept-design phase, even before I joined the team as Steering System Designer. The starting idea, taken from the muc019 model, was from the outset to move towards an Ackermann Kinematic and try as much as possible to stay close to this configuration. This choice, which I supported, is clearly the most obvious given the scope of application of this particular steering system, together with the requirements foreseen and illustrated in Chapter 3. The speeds that the muc022 will have to sustain are relatively low, the entire powertrain is developed to perform at a maximum of 40 km/h, which will almost certainly not be reached during the Shell Eco Marathon 2022. In addition, the track has an urban and city layout, so there are many more times when the car will be travelling at near-zero speeds than when it will be racing down a straight line at 30km/h. There are also parking manoeuvres.

It is therefore clear that the Ackermann Kinematic, designed for near-zero or very low speeds, in which the slip angles of the front wheels become negligible, is the optimal solution that performs well in a wider range of situations.

4.2.2 Calculation of Ackermann angles

Having defined the objective kinematics was a major step forward in the design. The Ackermann kinematics in fact imposes specific angles for the inner and outer wheels (with the inner being greater than the outer) and these angles are defined as a consequence of the main geometric parameters of the car, which as seen in Paragraph 3.2 were set in the context of the concept-decisions team meetings in the initial phase of the design of the entire vehicle, to satisfy performance parameters in aerodynamics, structural design, feasibility in the manufacturing area, while also respecting the limits and standards imposed by the SEM2022 regulations. These geometric constraints were joined by the most important regulatory constraint, which is the real starting point for any speculation on the muc022 steering system, that of the turning radius.
In spite of, and indeed taking into account, the dimensions chosen for the vehicle, it must be able to perform a curve with a turning radius, i.e. with a distance between the centre of rotation and the centre of the outermost wheel, of at least 6 m. From this information, correlated with the dimensions and spatial encumbrances of the car, it is possible to define the δ_{int} and δ_{ext} steering angles for the inside and outside wheel, which the steering system must guarantee in order to perform exactly the kinematics of Ackermann kinematics, our objective.

The methods for calculating these angles from the geometric factors and the turning radius just mentioned are given below with reference to Figure 3-1 reproduced below for clarity:

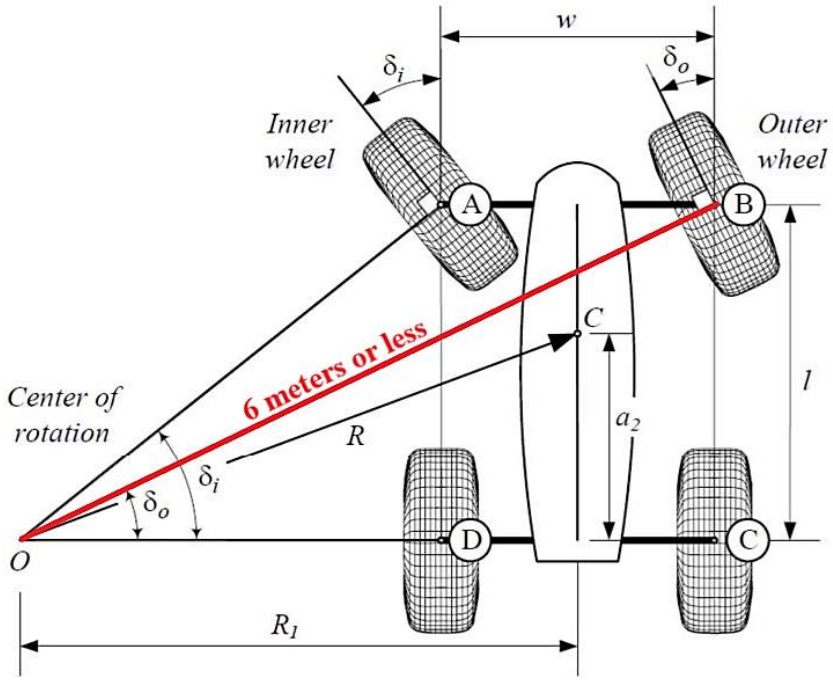

Figure 4-6: Turning radius according to the rules of SEM 2022

$$\delta_{ext} = arcsin\left(\frac{l}{R_{max}}\right) \quad (4\text{-}1)$$

$$\delta_{int} = arctan\left(\frac{l}{R_{max}cos\delta_{ext} - w_r}\right) \quad (4\text{-}2)$$

Term and value	Description
l=1550 mm	Wheelbase [mm]
$\boldsymbol{R_{max} = 4000 \div 6000\ mm}$	Turning radius as distance between the centre of rotation and the centre of the outermost wheel [mm]
$\boldsymbol{w_r = 850\ mm}$	Rear track length [mm]

Table 4-1: Descriptive table of quantities appearing in the equations

In the first approach to the calculation of these angles, a turning radius of 6 m was used in accordance with the regulations. The calculation was subsequently repeated for a turning radius of 5 m, 4.5 m and 4 m, to assess the safety margin with respect to the minimum design limit imposed. Table 4-2 is given here with the values of the δ_{int} and δ_{ext} angles obtained, varying the turning radius.

R_{max} (Turning Radius)	δ_{ext}	δ_{int}
6 m	14,97 deg	18,19 deg
5 m	18,06 deg	22,88 deg
4,5 m	20,15 deg	26,24 deg
4 m	22,82 deg	30,73 deg

Table 4-2: Values of Ackermann steering angles as a function of turning radius

Obviously, researching and defining a kinematics for a smaller turning radius means guaranteeing that the car is absolutely able to turn then for the greater turning radius required, but it also means having greater steering angles required that the steering system must perform as visible in table 4-2, therefore greater forces in play that could modify the sizing of some steering system components and their relative weight. Moreover, although evident and present, this problem is marginal if compared to the fact that, as we will see in the next section of this Master's Thesis, increasing the steering angles to be performed leads to a greater discrepancy between the theoretical Ackermann kinematics and then the real one we obtain. In the light of all these reasons, which will be further analysed, the final choice, after several moments of confrontation with the members of the team in an attempt to balance the disadvantages of reducing the design turning radius with obtaining a good safety margin with respect to the minimum design conditions imposed, led to the choice of a turning radius of 4.5m, thus having to perform two theoretical Ackermann steering angles of $\delta_{int} = 26{,}24\ deg$, $\delta_{ext} = 20{,}15\ deg$, for the inner and outer wheel.

4.2.3 DMU Kinematic Simulation: Theoretical vs Real Ackermann Kinematics

As already pointed out in Paragraph 2.3.2 and taken up again in the preceding paragraphs, the Ackermann kinematics is influenced by the geometry and spatial dimensions of the car, therefore by the dimensions of the wheelbase and front and rear axle. Using this information and knowing the desired turning radius it is possible to obtain the Ackermann angles for which it is necessary to steer the inner and outer wheels.
However, in section 2.3.2 we saw that in order to actually perform these angles and therefore achieve steering in accordance with Ackermann's kinematics, it is necessary to have a steering system whose geometry is based on Jeantaud's 4-bar-linkages mechanism. The dimensions of each of the four sides of the Jeantaud parallelogram cannot be random but must be chosen specifically because they then influence the kinematics and steering angles during execution.

In the pre-design architecture of the muc022 steering system, these four sides are:

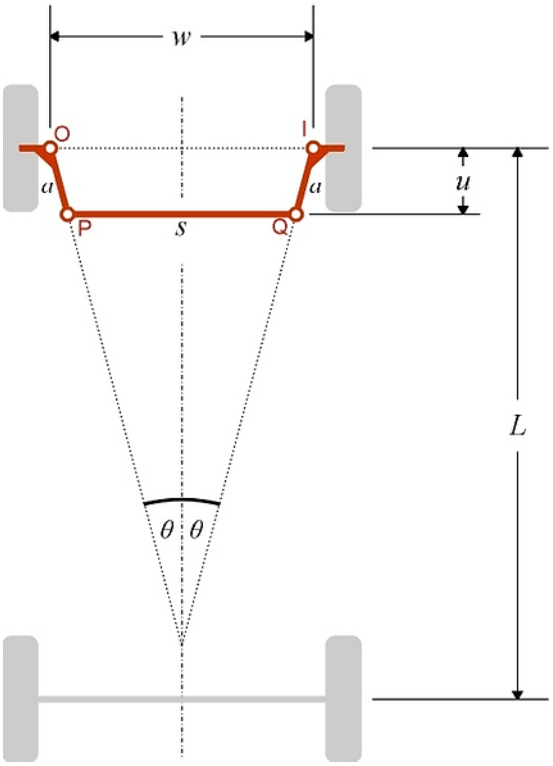

Figure 4-7: Schematization of the Jeantaud mechanism (Motor vehicle mechanics, Vigliani A.)

w: front axle length, a dimension set during the concept-decisions phase, therefore a design constraint.

s: central slide length; the central slide, as already mentioned, is the fundamental element for the use of the steering system in the architecture designed for the muc022. As it is made by Reichenbacher Hamuel using advanced cutting machinery, its dimensions are already defined and set, including obviously its length. Another design constraint.

a: length of the tie rods, the connecting element between the central slide and the wheel knuckle. This length obviously depends on the coordinates of its two ends. One end is connected in a special housing on the central slide, so its position is fixed. The position of the other end, on the other hand, has been defined taking into account various aspects such as the kinematics and geometry of the suspension and the size of the powertrain in the wheel hub. Evaluations in this regard are addressed in the following paragraphs.

Not knowing the exact position of the tie rod-knuckle connection point did not allow the length of the tie rods to be known and thus close the Jeantaud mechanism. Each different position corresponded to a different length of the tie rods and therefore a different Jeantaud parallelogram and therefore two different Ackermann angles with respect to the objective ones calculated in Section 4.2.2.
Since, as just mentioned, this position was affected by several constraints and generated very complex scenarios, in order to quickly and functionally evaluate the effects on the kinematics of each modification to the tie rod-knuckle connection point, it was decided to proceed by means of a software analysis.

The software used is DMU Kinematics. DMU Kinematics is a particular CATIA V5 workbench, a supplementary function that allows the kinematics of complex systems with numerous degrees of freedom to be simulated, tracing them back to components of more or less complex geometry linked together by certain types of joint (Revolute, Cylindrical, Planar, Prismatic, Spherical, Rigid, Universal). The choice of the joint type, combined with the elements it connects, describes and defines the degrees of freedom of the system, so in the correct description of the system to be analysed it is essential to choose the correct joint that connects two components. Once the construction of the system and the combination of the parts have been performed and constrained, the actual kinematic simulation can be carried out. The system is set in motion by entering the value of a degree of freedom of your choice, and the software reproduces the kinematics by outputting the value of all other degrees of freedom as the one entered changes.
In the application described in this Master's Thesis, the parameter inserted in input (the degree of freedom of which the spectrum of values was set) was the internal steering angle, in particular the one for a steering radius of 4.5 m, $\delta_{int} = 26{,}24\ deg$, with the aim of evaluating what value the external steering angle δ_{ext} (the output of the simulation) acquired.
The whole process was iterated several times with the different possible positions of the tie rod-knuckle connection point defined in the brain-storming phase on the respect of the constraints illustrated with the other team members. In this way, it was possible to evaluate which position would lead to an external steering angle that corresponded to or was as close as possible to the theoretical value according to Ackermann kinematics (20,15 deg).

The first necessary step was therefore to construct the geometry of the system to be analysed within the programme. All that was important for the simulation was that the dimensions of the sides of the Jeantaud parallelogram we defined earlier were precise (i.e. the length of the front axle, the width of the central slide, the lengths of the two tie rods) and that the type of joint linking the two elements was correct. For these reasons, the particular shapes that each component will then assume were not required and, in order to streamline and speed up the simulation, everything was reduced as much as possible to simple geometric figures, respecting the dimensions and features necessary to install the joint (for example, the spherical joint can be set through DMU Kinematics only if one element has a sphere and the other connected element a spherical cavity).
It is then reported in detail how the various components of the system to be simulated were represented. Wherever possible, for the sake of clarity, an image is also shown of how the component was finally drawn at the end of the project and Thesis work.

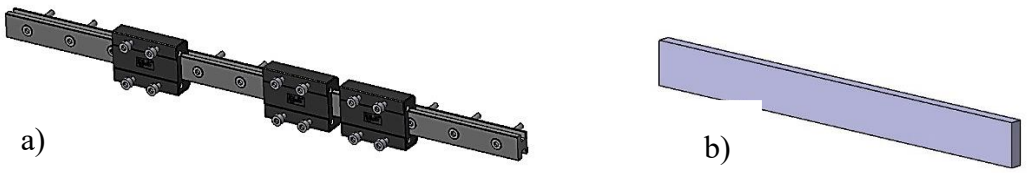

Figure 4-8: a) CAD model of the real rail guide (CATIA V5) b) CAD model of the simulacrum of the rail guide (CATIA V5)

The rail guide is the element on which the central slide slides under the action of the tensions of the wire wrapped around the pulleys. It also performs a support function as it is the element by which the lower part of the steering system is fixed to the monocoque. It is a standard element, which has always been combined with the central slide and recommended by the same company that made the central slide. It will be fixed to the monocoque by means of 12 M3x20 screws.
It has a very simple shape and for this reason it has been approximated to a parallelepiped; its function in the simulation is that of reference for moving the central slide. And for this it is stuck in space.

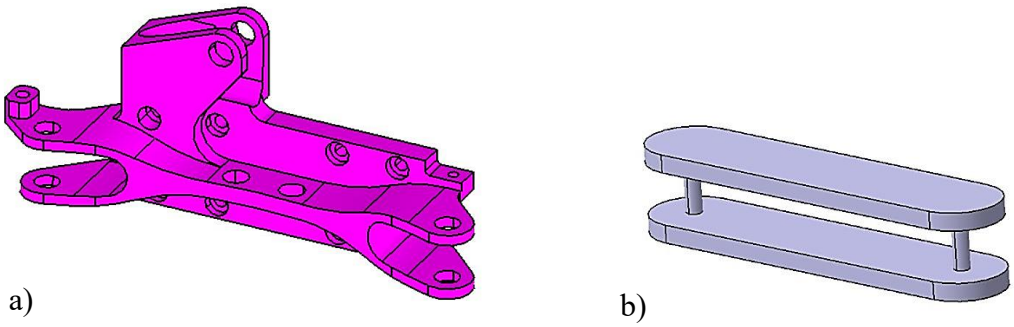

Figure 4-9: a) CAD model of the real central sled (CATIA V5) b) CAD model of the simulacrum of the central sled (CATIA V5)

The central slide is one of the key elements of the steering system architecture and at the same time represents one of the design constraints. As already seen in Chapter 3, it is part of a commercial and technical agreement between the team and a sponsor company specializing in laser cutting. In the architectural idea of the steering system, this is the element that slides along the rail guide and onto which the two tie rods are attached, which then change their position with the movement of the same slide. Despite its very complex shape for the kinematic simulation that we went to realize, only the fundamental geometric dimensions are interesting: length, width and type of joint in contact with the ends of the tie rods, i.e. two universal joints.

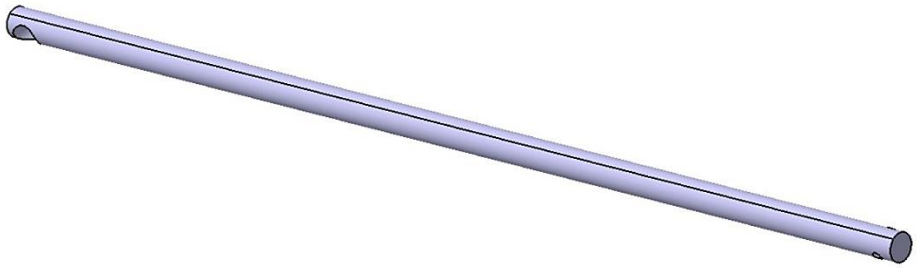

Figure 4-10: CAD model of the simulacrum of the two tie rods (CATIA V5)

The two tie rods are two cylindrical elements that connect the central slide to the wheel knuckle. They are the oblique sides of the Jeantaud quadrilateral and are therefore fundamental for defining the kinematics of the system. The different iterations of the kinematic simulation are aimed precisely at defining the dimensions of the tie rods, modifying each time the connection point with the knuckle and therefore the length of the tie rods. On the tie rod end in connection with the central slide we have, as already specified, a universal joint, while on the other end, the one in connection with the knuckle, the joint is spherical, as it takes up the spherical connection bearings, particular devices used in the industrial world for the connection of tie rods to knuckles.

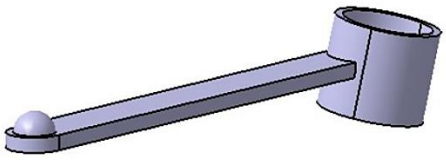

Figure 4-11: CAD Physical modelling of the steering arm (CATIA V5)

The steering arm is a necessary element for simulation purposes, as it imposes a dimensional constraint on a very important parameter, which is the distance between the tie rod-knuckle connection point and the kingpin axle, the virtual axis around which the vehicle wheels rotate. Normally this element is incorporated in the knuckle itself and its design and shaping phase takes into account other aspects such as possible deformation due to the heat source that is the electric motor, as well as possible interference with the rims and other systems surrounding it. In this iterative simulation phase, its length, which is the only important parameter for the kinematics of the steering system, was modified from time to time. Since the design of the knuckle was the responsibility of another subgroup within the team, once I had finished my kinematic evaluations and identified the position of the tie rod-knuckle connection, it was obviously my task to transfer this package of information to them.

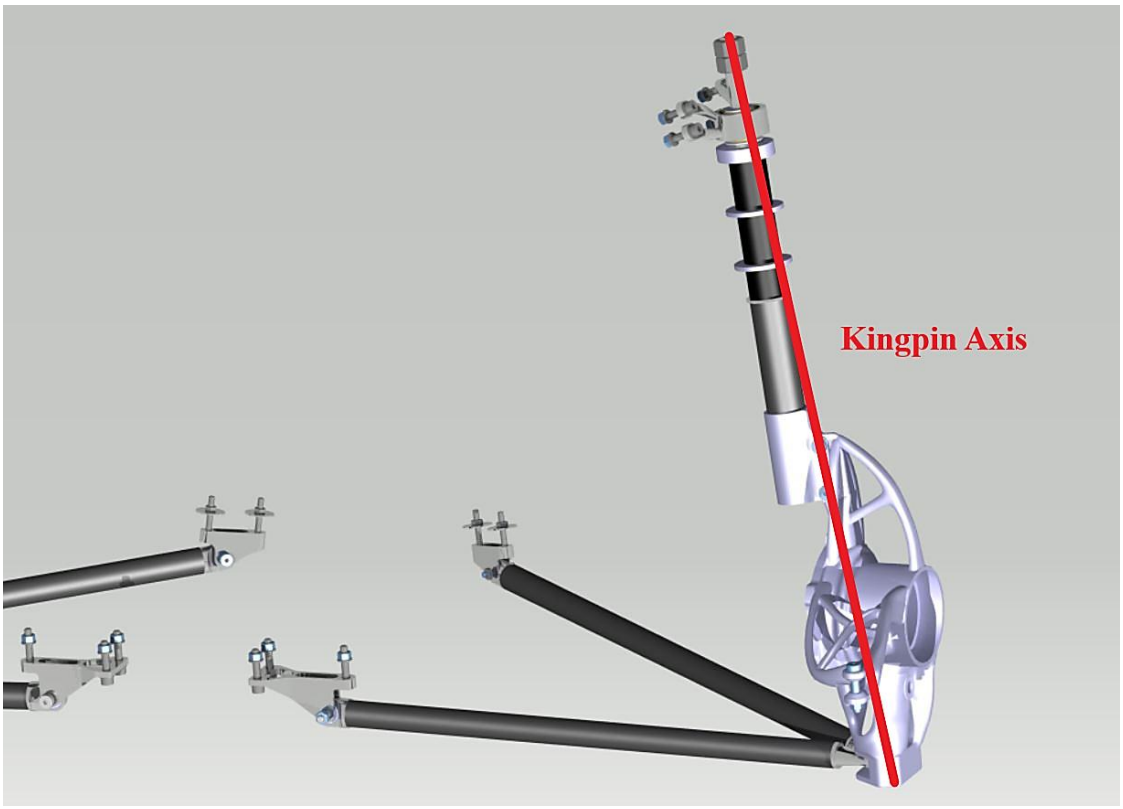

Figure 4-12: Kingpin Axis on muc022 suspension system (TUfast,n.d.)

The kingpin axis, also known as the steering axis, is the axis around which the wheels rotate to perform steering. Since it is fixed, its position in space is therefore fundamental for setting the entire set of reciprocal distances between each component of the steering system. However, it is not a real or physical component, it is a virtual axis normally identified by the line connecting the lowest point of the suspension system to the highest point as visible in Figure 4-12. As the suspension geometry had already been set before I joined the TUfast Eco Team, the data about the position of this axis and its inclination in space was passed to me by the suspension team.

Figure 4-13: CAD Physical modelling of the Kingpin Axis (CATIA V5)

For the kinematic simulation we intend to perform, however, we need a physical component; a simple geometric feature such as an axis cannot be inserted. Therefore, the solution was to create a cylinder whose axis coincides exactly with the kingpin axis and is therefore a simulacrum of it (see Figure 4-13).

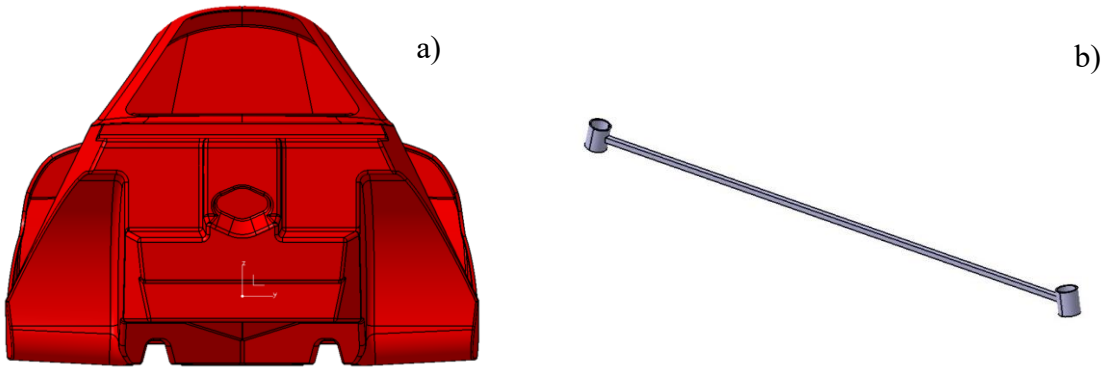

Figure 4-14: a) CAD model of the real monocoque (CATIA V5) b) CAD model of the simulacrum of the monocoque (CATIA V5)

The last parameter to be set in the kinematic simulation was obviously the length of the front axle, one of the four sides of the Jeantaud quadrilateral. In the final, real car model, this length is identified in the monocoque (Figure 4-14 a), which also connects the steering elements (steering arm, knuckle, kingpin axle) of the right with those of the left in a single system. At the time of the simulation, the shape and CAD model of the monocoque had not yet been chosen or produced, but the length of the front axle was known, which is the only dimensional parameter required at this level of kinematics and was set as part of the preliminary concept decisions at 1080 mm. With these considerations the monocoque was replaced by an element of equal length and which from a physical point of view performed the same function of coupling the left and right parts of the car (Figure 4-14 b). The joints assigned to the ends of this element are of the rotational coupling type with the simulacra of

the left and right kingpin axles. From a kinematic point of view the monocoque in the steering phase is stationary with respect to the rotating wheels; from this consideration the last constraint imposed in the simulation was the constraint of immobility in space of this simulacrum element of the monocoque.
Once all the simulacra of the various components of the architecture conceived for the steering system have been realised by CATIA V5 and coupled by means of the above-mentioned joints, the simulation on DMU Kinematics could be started.

The input parameter for the simulation was precisely the internal steering angle $\delta_{int} = 26{,}24\ deg$, necessary to perform a curve with a steering radius of 4.5 m according to the Ackermann kinematics illustrated above. Exploiting the constraints and the dimensions of the various parts, the system simulated the rotation of the inner wheel of the curve for an angle of 26,24 deg, graphically showing the displacements and movements of all the components of the system, therefore also the consequent rotation of the outer wheel. By placing virtual sensors it is possible to receive as output a numerical information of the value of this angle δ_{ext}, which to follow Ackermann's theory at the basis of the design had to be as close as possible to the value of 20,15 deg.
Being able to simulate the steering in a relatively short period of time was a fundamental tool for the corrections and the iterative process of changing the size and position of the tie rod-knuckle connection. The iterative process included the following steps:

1. First attempt simulation and acquisition of the relative δ_{ext} value;
2. Brainstorming with the team and the suspension department to define a new position of the tie rod-knuckle connection;
3. Modification of the CAD drawings in order to create new simulacra that reflected the decisions taken in the previous phase;
4. New simulation and acquisition of the new value of δ_{ext};

The iterative process was thus repeated trying to get as close as possible to the Ackermann value for δ_{ext}. In phase 2), however, the main limitations to the mobilisation of the tie rod-knuckle connection point emerged: moving the point too much in the x- direction means bringing it closer to the motor-reducer hub positioned in the centre of the wheel and with a diameter of 65 mm, so consequently it means bringing the tie rod itself too close to the hub, risking immediate or future contact as a result of deformation. Moving the point too far in the x+ direction means bringing it closer to the innermost diameter of the wheel rims and therefore risking new contact problems. On the other hand, movement in the y direction involves major changes to the shape of the knuckle body, which can only be implemented to a certain extent. In fact, modifying the length of the knuckle body in the y direction means risking moving the motor hub too far into the car and therefore creating the possibility of new contacts with the tie-rod, or else risking moving the knuckle too far outwards, leaving the area covered by the rims and the tyre shoulder, and also dirtying the aerodynamic flow to the wheels. Finally, due to the kinematic and geometric evaluations previously made on the suspension system, it was not possible to modify the z coordinate of the point, which had to be in correspondence with the xy centreline plane of the wheels.
The spatial constraints were therefore different and evident, and the margin of modification of the position of the tie rod-knuckle connection point not so wide.

Figure 4-15 shows the CAD drawing representing the tie rod-knuckle connection point (circled in red) and its relative position to the motor hub. The drawings are taken from the final muc022 designs.

Following several team meetings, various evaluations and discussions and taking all of this into account, the optimal position of the connection point was set at a distance of 147 mm along x to the centre of the wheel and its motor hub, and at a distance of 7 mm along y to the outside of the car in relation to the x-z plane of symmetry of the wheel. The z-coordinate as requested by the suspension team was not changed.

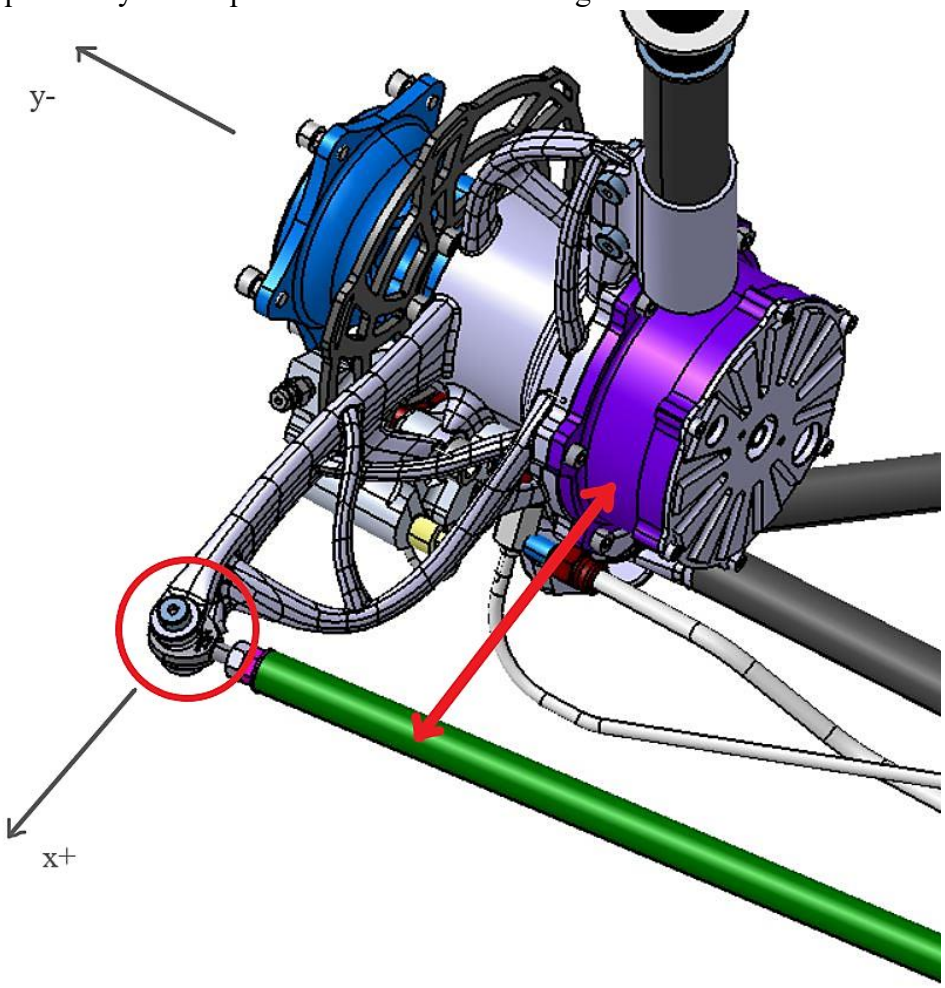

Figure 4-15: Connection point tie rod-knuckle and motor hub (Detail CAD drawing of the front mechanics of muc022, TUfast)

Simulating therefore the steering with this set of coordinates and with the relative dimensional modifications to the components, the output value of the external steering angle δ_{ext} is equal to 21.28 deg, optimal and conclusive value of the iterative process.
In this way, the kinematics of the muc022 steering system coincides with that of the Ackermann theory at 95% (with respect to the theoretical and objective angle of 20.15 deg), representing a first important success and improvement with respect to the kinematics of the muc019 steering system, coinciding with Ackermann only at 88%.

Figure 4-16 shows the system assembled by DMU Kinematics and used for simulations. In particular, a frame at the end of the steering simulation is shown.

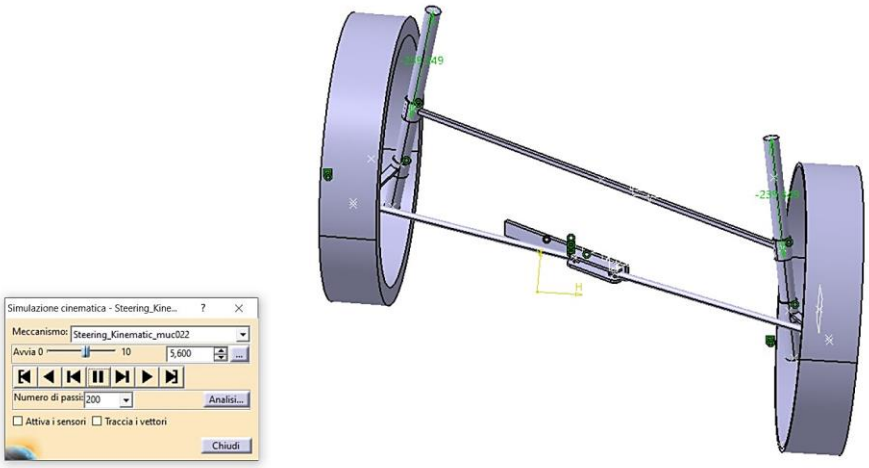

Figure 4-16: One of the frames collected during the steering simulation carried out with DMU Kinematics (CATIA V5)

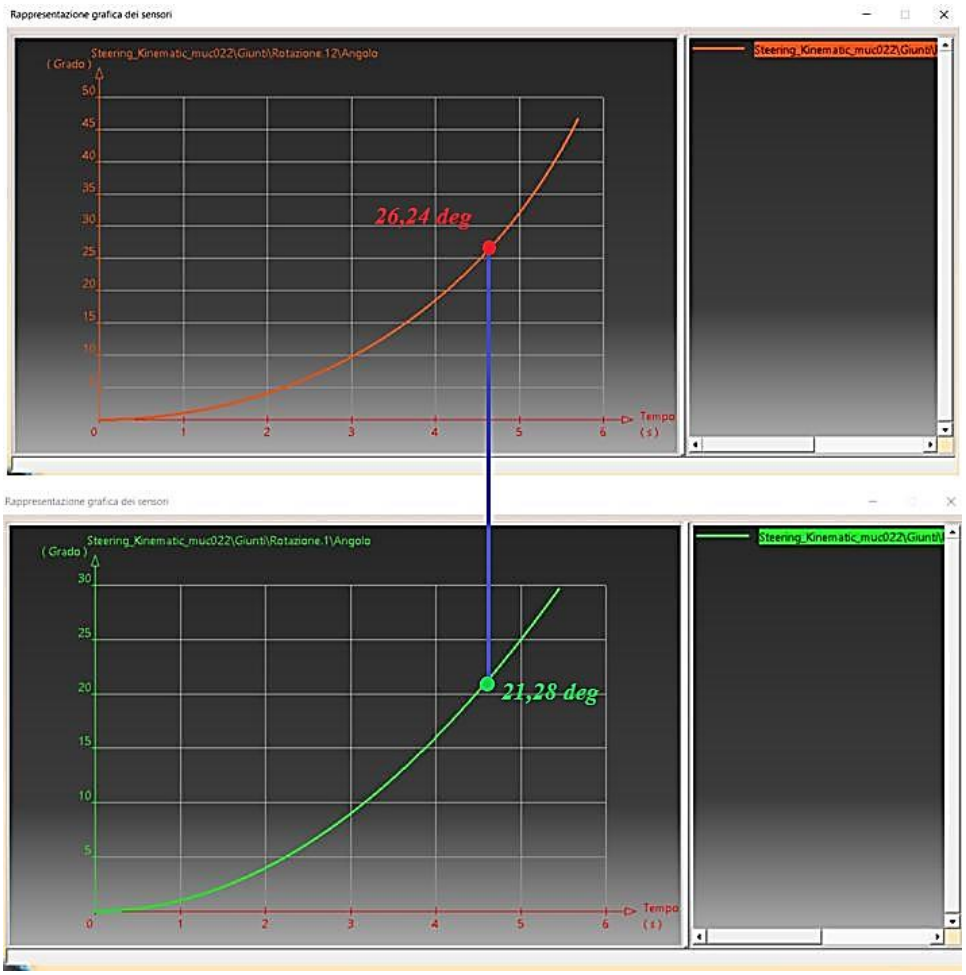

Figure 4-17: Steering angle trends in the simulation performed with DMU Kinematics (CATIA V5)

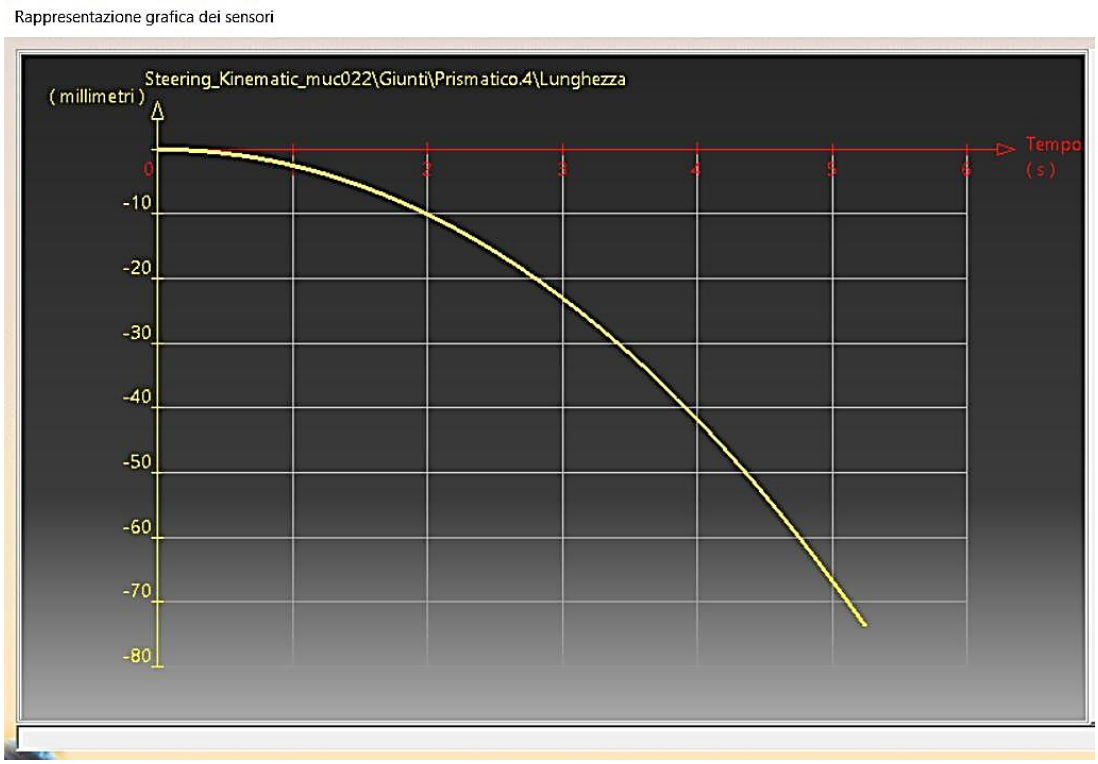

Figure 4-18: Central sled displacement trend in the simulation performed with DMU Kinematics (CATIA V5)

The graphs reported in Figures 4-17 and 4-18 are the results shown on the screen at the end of the simulation with DMU Kinematics and illustrate how, in the time instant in which the inner wheel reaches an angle $\delta_{int} = 26{,}24\ deg$ (red graph), the outer one is performing an angle $\delta_{ext} = 21{,}28\ deg$ (green graph).

A third graph provided by the simulation illustrates the value of the displacement along the y direction of the central sled in the time interval in which the wheels steer, thus linking to the information about the angles δ_{int} e δ_{ext}, also that relative to the displacement of the central sled necessary to obtain these angles. It can then be seen that the sled moves a maximum of 80 mm in one direction, so it will have a travel of at least 160 mm, which is perfectly acceptable compared to the length of the rail guide provided by the sponsor company, which is 300 mm.

4.3 Steering System Dynamics

The evaluation and dynamic design part of the steering system is one of the most delicate and important phases. Through the calculation of the forces acting on each single component, their balancing and the subsequent dimensioning of the various elements that make up the system, what has hitherto been an idea is given a numerical and dimensional form. The input for the start of each dynamic analysis derives from the kinematic study illustrated in Paragraph 4.2 that led to the definition of the limit steering angles required to satisfy the technical and regulatory requirements ($\delta_{int} = 26{,}24\ deg$ and $\delta_{ext} = 21{,}28\ deg$). From these results, the performance target to be pursued through the dynamic action is that the steering system must be able, through the transmission of forces from the

steering wheel to the tie rods, to allow the rotation of the wheels for at least an angle of 26,24 deg around the kingpin axis, overcoming the forces between the tyres and the asphalt.

4.3.1 Mathematical modelling of the relationship between forces acting on the tyres and steering angles

The steering system must be designed to be able to transmit the torque applied by the driver to the steering wheel to the wheels and then make them rotate around the kingpin axis. Based on the steering system architecture described in Paragraph 4.1, the torque applied by the driver must make the pulley system rotate under the action of the wire and thus set the central slide in motion. Moving the central sled means moving the tie rods connected to it, then applying a force F_{steer} on the wheel knuckles, at a certain distance or arm (r_{steer}) from the kingpin axis, thus generating a left and right steering moment ($M_{steer,l}$ $M_{steer,r}$).

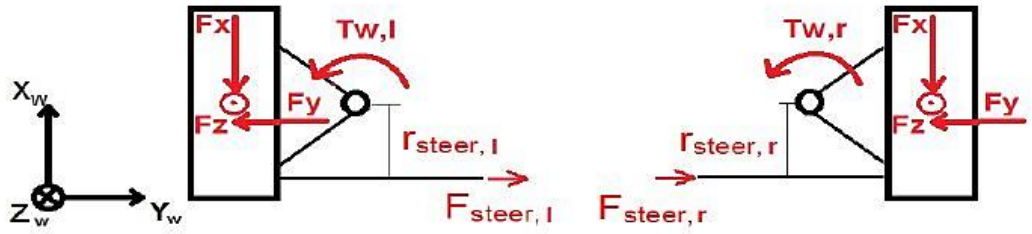

Figure 4-19: Steering torque as function of left and right kingpin moment

$$M_{steer,l} = F_{steer,l} * r_{steer,l} \quad (4\text{-}3)$$

$$M_{steer,r} = F_{steer,r} * r_{steer,r} \quad (4\text{-}4)$$

These steering moments must overcome the reactions and forces that arise between the tyres and the asphalt, which can be broken down into three components F_x, F_y, F_z. Each of these components has a point of application and therefore a distance from the kingpin axis r_x, r_y, r_z that define a corresponding moment (M_x, M_y, M_z).
The sum of these moments, for the left and right wheels, must then be equalised by the sum of the left and right steering moments:

$$M_{steer,l} = -M_{x,l} - M_{y,l} - M_{z,l} = -(F_{x,l} * r_x) - (F_{y,l} * r_y) - (F_{z,l} * r_z) \quad (4\text{-}5)$$

$$M_{steer,r} = M_{x,r} - M_{y,r} + M_{z,r} = -(F_{x,r} * -r_x) - (F_{y,r} * r_y) + (F_{z,r} * r_z) \quad (4\text{-}6)$$

And so:

$$M_{steer} = M_{steer,l} + M_{steer,r} = (F_{x,r} - F_{x,l})r_x - (F_{y,l} + F_{y,r})r_y - (F_{z,l} - F_{z,r})r_z \quad (4\text{-}7)$$

Therefore, net of the contributions deriving from the right or left wheel, therefore internal or external, it is possible to conclude that the steering moment that our system must generate is a function of the tyre-asphalt contact forces and the distances of the point of application of these forces from the kingpin axle: $M_{steer} \propto M_{steer}(r_x, r_y, r_z, F_x, F_y, F_z)$.
The objective of this phase of the project was therefore to find a mathematical relationship linking all these quantities.

The model introduced in the following paragraphs is based on the geometric relationships between the various planes of the wheel (vertical and horizontal plane of symmetry, plane of contact with the asphalt) and the kingpin axle. Some of these distances are well-defined geometrical parameters which are part of the configuration of the architecture of the suspension system.
The meaning of some of the symbols and parameters that are later included in the treatment and definition of the model is explained below.

Term	**Description**
Kingpin inclination σ	inclination of kingpin axis in y-z plane (see Figure 4-20)
Caster angle $\boldsymbol{\tau}$	inclination of kingpin axis in x-z plane (see Figure 4-20)
Camber angle γ	inclination of wheels y-z-plane (see Figure 4-20)
Toe angle $\boldsymbol{\varepsilon_t}$	tilt of wheels in x-y-plane (see Figure 4-20)
Effective kingpin angle λ	effective three-dimensional kingpin angle as sum of inclination and caster angle: $\lambda = \sqrt{\sigma^2 + \tau^2}$
Pneumatic trail t	the longitudinal distance between wheel centre and lateral force acting point on tire contact patch plane
Caster trail e	the longitudinal distance between where the steering axis hits the ground and the wheel centre
Scrub radius $\boldsymbol{r_c}$	the lateral distance between where the steering axis hits the ground and the wheel centre (negative if on outside of the wheel)

Table 4-3: Geometric parameters describing the geometry of the suspension and steering system

There are also two parameters that will return frequently in the discussion, which are simply the caster offset on wheel centre height (e_w) and kingpin offset on wheel centre height (r_w), indicated by the subscript "*w*".

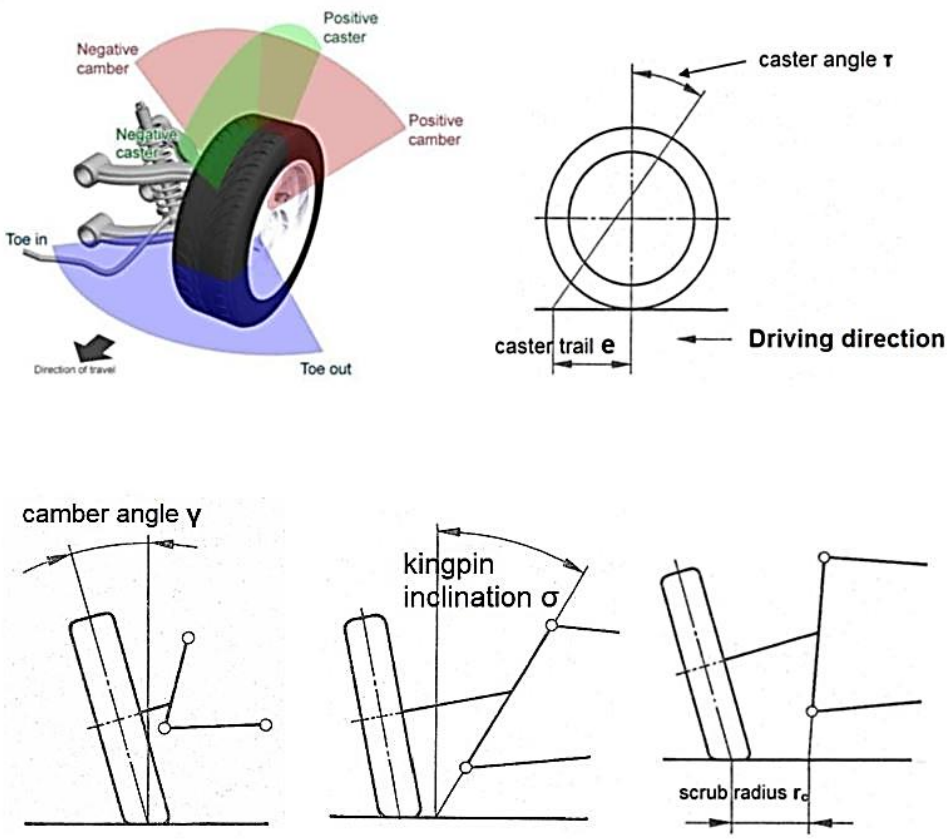

Figure 4-20: Main geometric parameters that describe the geometry of the suspension system and steering system

By subdividing the coordinate system into three sub coordinate systems for kingpin axis, wheel and contact patch plane on the road, as it has been done in Figure 4-21, one can describe the geometric relations between its components and the degrees of freedom of the whole system.

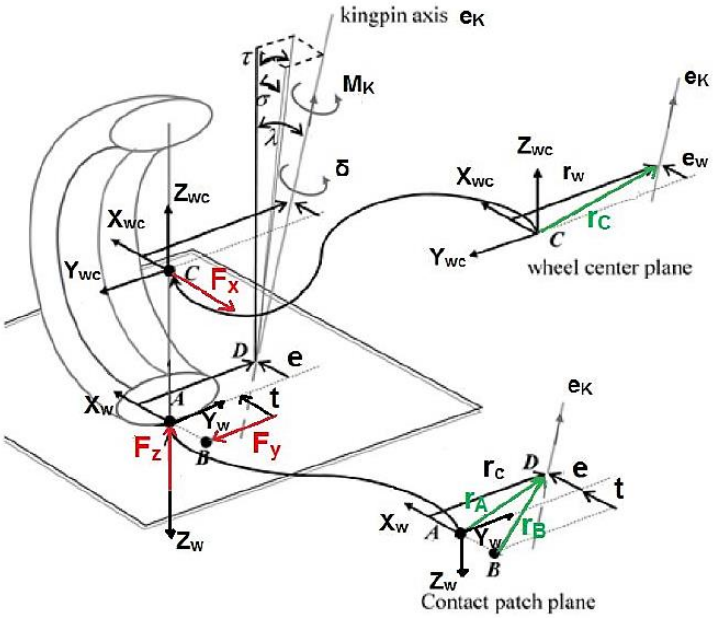

Figure 4-21: Sub coordinate systems for kingpin axis, wheel and contact patch plane on the road

Despite the three sub-coordinate-systems, displacement vectors r_i, tire forces F_i and kingpin vector e_k are in the vehicle coordinate system $X_V\ Y_V\ Z_V$ in equations 4-8 4-9 4-10. Since tire forces F_i are generally described in tire coordinates, they must be transferred in vehicle coordinates.

$$M_x = (r_C \times F_x) \cdot e_K \tag{4-8}$$

$$M_y = (r_B \times F_y) \cdot e_K \tag{4-9}$$

$$M_z = (r_A \times F_z) \cdot e_K \tag{4-10}$$

with:

$$r_A = -\begin{pmatrix} e\cos\delta + r_C \sin\delta \\ e\sin\delta - r_C\cos\delta \\ 0 \end{pmatrix} \tag{4-11}$$

$$r_B = -\begin{pmatrix} (e+t)\cos\delta + r_C \sin\delta \\ (e+t)\sin\delta - r_C\cos\delta \\ 0 \end{pmatrix} \tag{4-12}$$

$$r_C = -\begin{pmatrix} e_w\cos\delta + r_w \sin\delta \\ e_w\sin\delta - r_w\cos\delta \\ 0 \end{pmatrix} \tag{4-13}$$

The longitudinal force F_x can be sufficiently described by the force acting on the wheel centre. Differently to vertical and lateral force, does the wheel radius not affect the kingpin moment due to longitudinal forces. For the side slip force F_y and vertical force F_z the force acting point at the tire-to-ground contact patch must be considered. For each force acting point, the displacement vector (as can be seen in previous equations) is defined, from which the moment around the kingpin axis is calculated.

Equation 4-14 shows the transformation between forces in the vehicle coordinate system $X_V\ Y_V\ Z_V$ and wheel coordinate system $X_w\ Y_w\ Z_w$ using transformation matrix. The kingpin axis vector e_K is given in equation 4-15 for vehicle coordinates.

$$\begin{pmatrix} F_x \\ F_y \\ F_z \end{pmatrix}_V = \begin{pmatrix} \cos\delta & \sin\delta & 0 \\ -\sin\delta & \cos\delta & 0 \\ 0 & 0 & 1 \end{pmatrix} \begin{pmatrix} F_x \\ F_y \\ F_z \end{pmatrix}_w \tag{4-14}$$

and

$$\text{Kingpin axis unit vector } e_K = \begin{pmatrix} \tan\tau\cos\lambda \\ \tan\sigma\cos\lambda \\ -\cos\lambda \end{pmatrix} \tag{4-15}$$

Using those relations, the kingpin moments due to longitudinal, lateral and vertical tire forces can be simplified to 4-16, 4-17 and 4-18.

$$M_x = F_x r_w \cos\lambda \tag{4-16}$$

$$M_y = F_y(e+t)\cos\lambda \tag{4-17}$$

$$M_z = F_z(-e\sin\delta + r_C\cos\delta)\tan\tau\cos\lambda + F_z(e\cos\delta + r_C\sin\delta)\tan\sigma\cos\lambda \tag{4-18}$$

As can be seen from equation 4-16 to 4-18 does only the kingpin moment M_z due to vertical

forces change with steering angle δ.

The relationships sought through this treatment and mathematical modelling are thus obtained and there is a correlation between the moments acting around the kingpin axis and the distances and geometric parameters dependent on the point of application of the tyre-asphalt contact forces. In order to know these moments and from them derive the equivalent steering moment M_{steer}, it is necessary to know the value of the same forces F_x, F_y, F_z.

The longitudinal and lateral forces (F_x, F_y) that the tyres develop with respect to the asphalt are essential to enable the vehicle to move forward, brake and steer; they represent the vehicle's method of communication with the external environment. To understand how they work, the Brush model is normally applied.

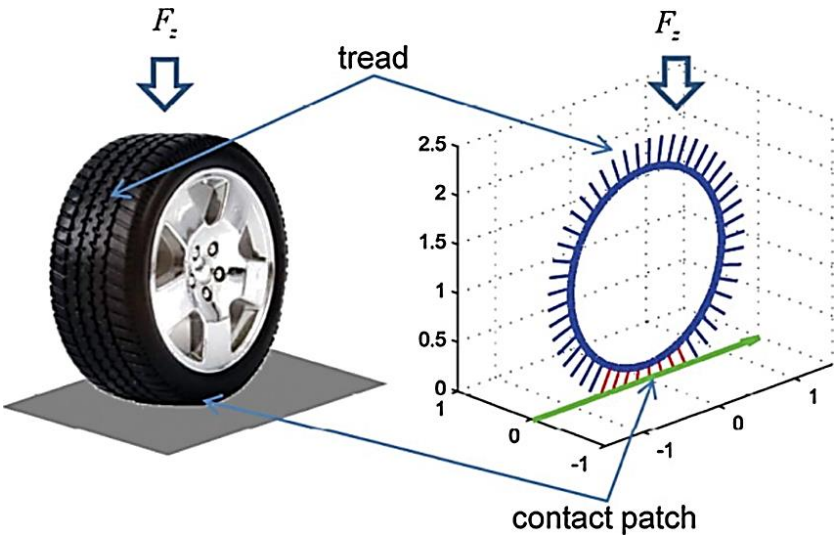

Figure 4-22: Tire and brush model (Ann Arbor, Department of Mechanical Engineering, The University of Michigan)

Using the Brush model, the tyre is reduced to a brush where the carcass represents the mass of the tyre and the rubber is modelled by the bristles, elastic and deformable parts (see Figure 4-22). These bristles resist circumferential deformation, but do not resist radial deformation and can therefore be flexed to the right or left simulating the deformation of the tyre rubber. This deformation obviously only occurs if a vertical load is applied to the brush.

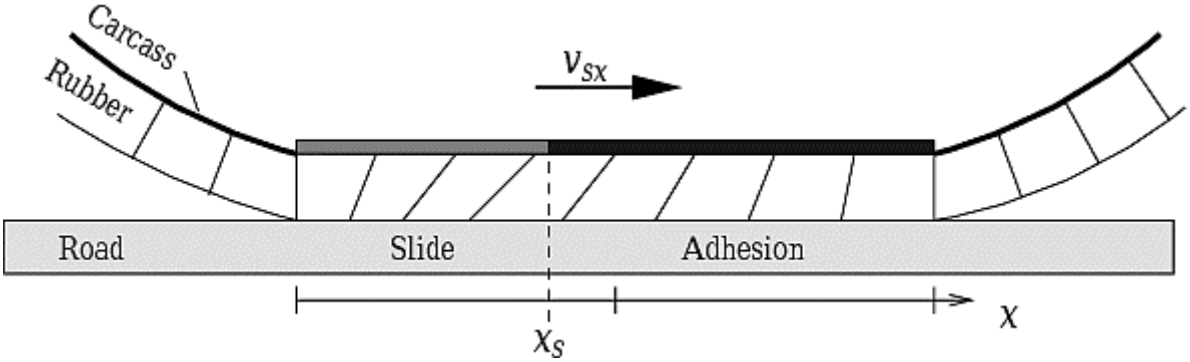

Figure 4-23: Brush model applied to longitudinal displacement (J. Svendenius, B. Wittenmark, Brush tire model, 2003)

If we imagine to apply a vertical load and to move the brush in a longitudinal direction, the effect will be that the various bristles will start to deform and that longitudinal stresses $\tau_x = -C_k \cdot s \cdot \xi$ will be generated at their tips, where C_k is a simple proportionality constant whose value is based on the assumption that the deformation of the bristles is linear and directly proportional to the longitudinal stresses, \xi is a spatial measurement of how much the brush is moved in the longitudinal direction and finally s is the slip, a fundamental parameter in this relationship and which derives from a relationship between the longitudinal speed of the wheel and the speed of rotation of the same.
As long as the longitudinal tensions are below the value of the friction tensions the brush and therefore the wheel is in a condition of adherence, when this limit value is exceeded we enter the slip region.
The set of longitudinal stresses τ_x has the macroscopic effect of generating longitudinal forces F_x.

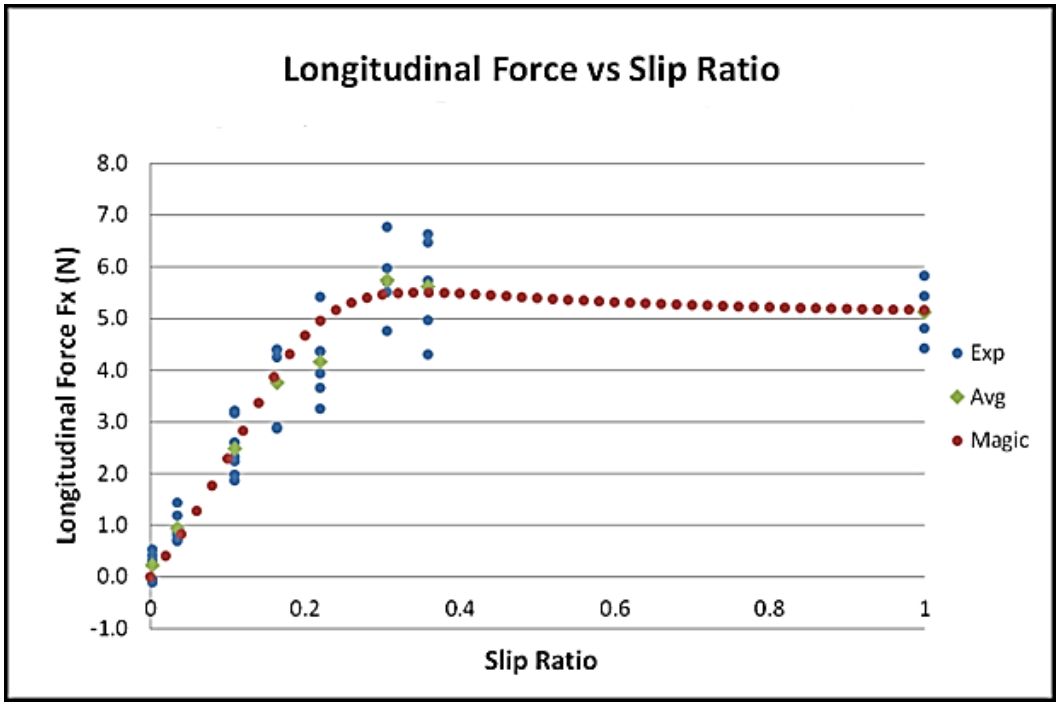

Figure 4-24: Plot of Longitudinal force vs Slip ratio

In Figure 4-24, it is possible to evaluate the trend of the force $F_x = -C_x s$ whose value is therefore linked to the slip s and therefore to the speed of the vehicle. The slope of the curve, on the other hand, depends on the factor C_x, called longitudinal tire stiffness, a parameter that encompasses the influence of the microscopic deformation of the tyre (of the bristles) as a function of the required longitudinal movement. C_x is therefore a characteristic parameter that changes from tyre to tyre.

The same Brush model can be used to understand the origin of lateral deformations.

In this case, one imagines rotating the brush around a vertical axis, while at the same time applying a vertical load. As a result, the bristles are again deformed, but this time in the lateral direction. More and more deformation of the bristles can be observed, until the maximum deformation is reached after which the bristle tips lose contact with the ground

and the slip region is entered (see Figure 4-25). The intensity of the deformations is obviously linked to the generation of lateral stresses $\tau_y = -C_k \cdot \alpha \cdot \xi$, where the new parameter α is the slip angle (see Paragraph 2-3), which contains information on the amount of rotation required to the brush (tyre).

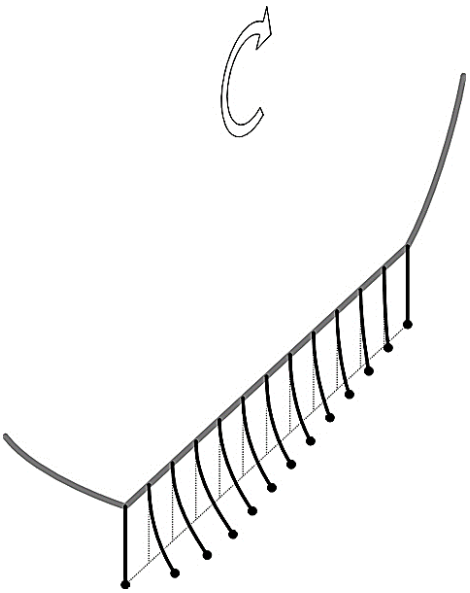

Figure 4-25: Trend of lateral deformations of the bristles (Motor vehicle mechanics, Vigliani A.)

The macroscopic effect of the lateral stresses τ_y is the generation of the lateral forces F_y.

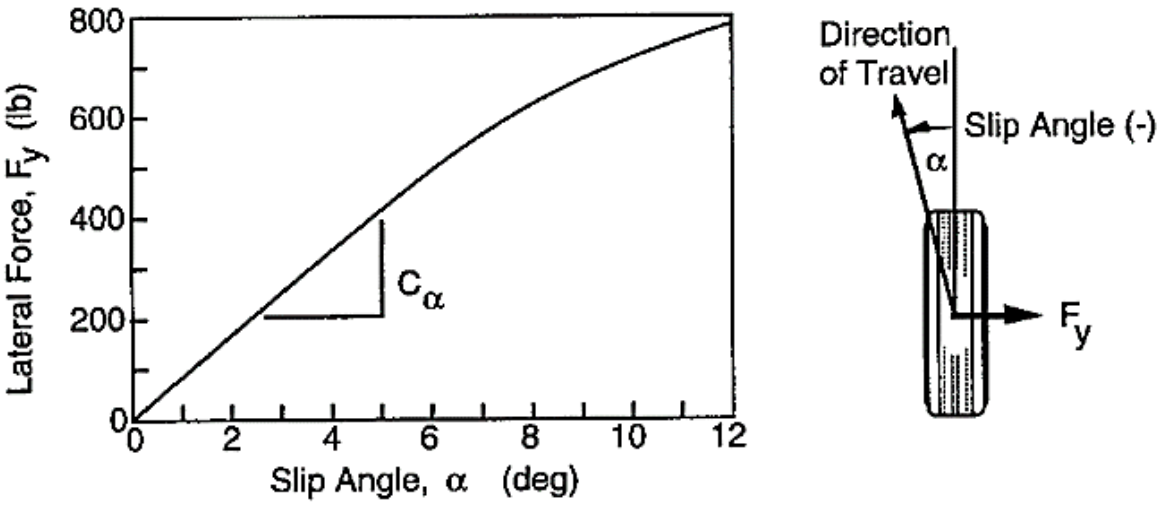

Figure 4-26: Plot of Lateral force vs Slip angle (Motor vehicle mechanics, Vigliani A.)

In Figure 4-26, it is possible to evaluate the trend of the force $F_y = -C_\alpha \alpha$ whose value is therefore linked to the slip angle α. The slope of the curve depends instead on the factor C_α, called cornering stiffness, a parameter that encloses the influence of the microscopic deformation of the rubber (of the bristles) as a function of the required rotation. C_α is therefore a characteristic parameter that changes from tyre to tyre.
In the light of the theoretical discussion just presented on the generation of the tyre-asphalt contact forces, it can be said that the forces F_x, F_y that are the object of research together

with F_z are dynamic forces that vary their value as a function of the vehicle speed, of the wheel rotation speed, but also and above all as a function of the particular tyre type, given the preponderant dependence on the longitudinal tyre stiffness C_x and on the cornering stiffness C_α.
This information is usually encapsulated in the Pacejka model, a model that linearises and combines the trends of F_x, F_y with respect to s e α, on the basis of numerous empirical evaluations.

The Pacejka template processes all the data for a specific tyre contained in the ".tir" file usually associated with the same tyre. The ".tir" file and associated Pacejka model are normally given to manufacturers by their suppliers.

The Pacejka model and its ".tir" file were undoubtedly the most difficult problem to solve and the most complex obstacle to overcome in the design of the steering system.
It all stemmed from a lack of the tyre supplier sponsor, which could no longer be recovered despite the efforts of myself and the team.
The tyres that muc022 will be using were supplied by Michelin as part of a sponsorship agreement. However, these tyres were acquired by the TUfast Eco Team around two years ago, in February 2020, to be fitted to the muc021, a project which due to the Covid-19 pandemic never saw the light of day. The tyres were then put into storage and reused for the next project, pursuing the Eco Team's philosophy of zero material and economic waste. The problem was, however, that these tyres were sent without any Pacejka 'tir' file or model and subsequently no one asked for them for a year and a half as no project was carried out or continued.
When the matter finally came to light during this project of mine, contacting Michelin for this kind of information had become impossible. After numerous reminders from us and frantic work from myself and the management team to retrieve these files, the source of all the problems was finally found. The tyres had been taken out of production and no data was immediately available as they are obviously special compounds and sizes exclusive to university competitions and therefore not subject to massive industrial production.
As a result of this situation, several team meetings were held to work out a solution strategy. Changing tyres was not an option as the rims designs had already been finalised; however, we could not wait any longer as 3-4 weeks had already been spent trying to solve this problem. So the idea I proposed, and which was eventually validated by the whole team, was to proceed with a viable alternative to knowing the longitudinal and lateral forces F_x, F_y.
In fact, while researching the Pacejka model, I had thought of an alternative solution for calculating the moments around the kingpin axis without having the model available. The solution found was to dimension the forces in parking condition. The parking condition, i.e. with the vehicle practically stationary and speed close to zero, is the worst condition for steering, the one in which the system is required to generate a greater steering force to overcome the static friction that binds the wheels to the ground.
“The reference benchmark for the evaluation of this maximum steering wheel torque is the static parking manoeuver” (Weinberger, Bargende -Internationales Stuttgarter Symposium: Automobil und Motorentechnik- 2017).

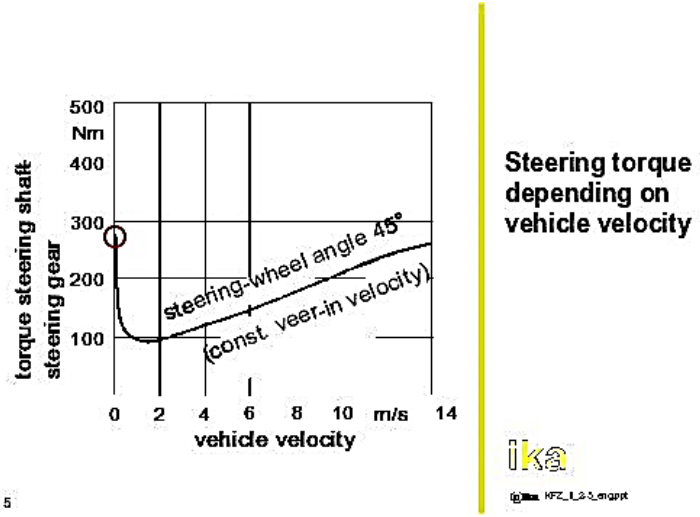

Figure 4-27: Steering Torque depending on vehicle velocity (Euromotor, Automotive Engineering II)

In the light of these observations and the problematic situation that had arisen, the team decided to proceed in this way, basing the design of the steering system on the calculation of the forces required for steering in the worst possible case, thus ensuring that there was a margin of coverage for all other possible scenarios.

4.3.2 Sizing of the various Steering System components

As explained in the final part of paragraph 4.3.1, the procedure for calculating the forces acting on each single component and therefore useful for their dimensioning starts from evaluations made on the parking condition scenario. In this situation the car is practically stationary, therefore the speed of the car is close to zero, therefore no longitudinal force is generated to move the car. In the same way also the vectors defining the wheel speeds are null, therefore as can be seen from Figure 4-26 no slip angle is defined and therefore also the lateral contribution cannot be considered. The only component of the forces present, and which is independent of the tyre characteristics and therefore assessable even without the Pacejka model, is F_z, the vertical load.

The vertical load is distributed between front and rear axle, F_{zf} F_{zr}. The interest in the design of the steering system is obviously focused on the front axle load, which in turn is split between the right and left wheel $F_{zf} = F_{zf,left} + F_{zf,right}$ with $F_{zf,left} = F_{zf,right}$ in the parking condition scenario.

$F_{zf,left}$ $F_{zf,right}$ are then calculated:

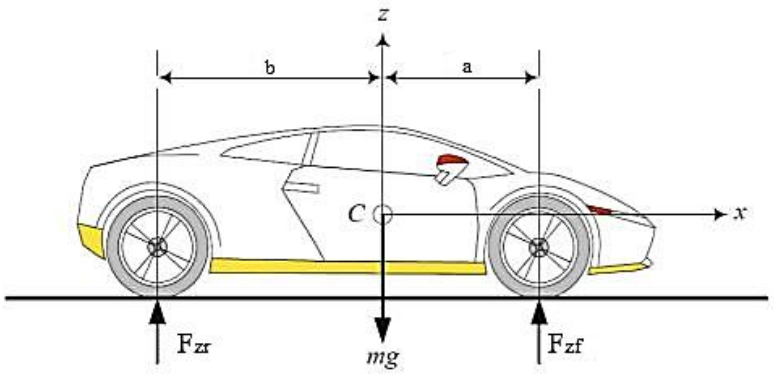

Figure 4-28: Vertical force distribution on a car in parking conditions (Dynamic structural analysis of a propeller shaft, Instituto Politécnico Nacional)

The following equations are defined from Figure 4-28:

$$F_{zf} + F_{zr} = mg \quad (4\text{-}19)$$

$$F_{zf}(a+b) = mgb \quad (4\text{-}20)$$

Term and value	Description
$m = 140\ kg$	Total mass of the vehicle (vehicle mass + driver mass) [kg]
$a = 736\ mm$	Distance of the front axle from the center of gravity of the car [mm]
$b = 814\ mm$	Distance of the rear axle from the center of gravity of the car [mm]

Table 4-4: Descriptive table of quantities appearing in the equations

The downforce generated by aerodynamic effect is considered negligible in a car like the muc022 with an urban-concept and a top speed of 30 km/h.

From equations 4-19 and 4-20 it follows that: $F_{zf} = 721{,}257\ N$ and consequently $F_{zf,left} = F_{zf,right} = 360{,}628\ N$.

Resuming then equation 4-18 we have that:

$$M_{z,left} = F_{zf,left}(-e\sin\delta + r_C\cos\delta)\tan\tau\cos\lambda + F_{zf,left}(e\cos\delta + r_C\sin\delta)\tan\sigma\cos\lambda \quad (4\text{-}21)$$

$$M_{z,right} = F_{zf,right}(-e\sin\delta + r_C\cos\delta)\tan\tau\cos\lambda + F_{zf,right}(e\cos\delta + r_C\sin\delta)\tan\sigma\cos\lambda \quad (4\text{-}22)$$

Since $F_{zf,left} = F_{zf,right}$ also $M_{z,left} = M_{z,right}$. Then assigning dimensional values to the geometric parameters that appear in equations 4-21 and 4-22:

Term and value	Description
σ=10,57 deg	inclination of kingpin axis in y-z plane [deg]
$\boldsymbol{\tau}$= 4,45 deg	inclination of kingpin axis in x-z plane [deg]
λ=11,46 deg	effective three-dimensional kingpin angle as sum of inclination and caster angle: $\lambda = \sqrt{\sigma^2 + \tau^2}$ [deg]
e=22,82 mm	the longitudinal distance between where the steering axis hits the ground and the wheel centre [mm]
$\boldsymbol{r_c}$=80,401 mm	the lateral distance between where the steering axis hits the ground and the wheel centre (negative if on outside of the wheel) [mm]

Table 4-5: Descriptive table of quantities appearing in the equations

The value of all these geometric parameters already presented in paragraph 4.3.1 was easy to measure, having previously set the tyre size and suspension geometry and therefore the position of the kingpin axis in space. (See Figure 4-10 for more clarity).
The result was therefore $M_{z,left} = M_{z,right} = 2{,}699\ Nm$.
At this point, taking up the equation 4-21 and 4-22:

$$M_{z,left} = M_{steer,l} = F_{steer,l} * r_{steer,l} \quad (4\text{-}23)$$

$$M_{z,right} = M_{steer,r} = F_{steer,r} * r_{steer,r} \quad (4\text{-}24)$$

So:

$$F_{steer,l} = \frac{M_{z,left}}{r_{steer,l}} \quad (4\text{-}25)$$

$$F_{steer,r} = \frac{M_{z,right}}{r_{steer,r}} \quad (4\text{-}26)$$

with $r_{steer,l} = r_{steer,r} = 140{,}539\ mm$ the result will be $F_{steer,l} = F_{steer,r} = F_{steer} = 19{,}203\ N$.

To support the mathematical model presented in Paragraph 4.3.1 and the design choice in the parking condition scenario, the Sharp and Granger Model is shown.
R.Sc. Sharp and R. Granger developed an empirical formula for static torque prediction around the kingpin axis in stand-still situations. It is based on a model in physical macro-scale and integrates friction forces over a circular contact patch (Sharp, Granger - Proceedings of the Institution of Mechanical Engineers, Part D Journal of Automobile Engineering- 2003).
Through various experimental tests, they arrived at the following formulation of the static torque:

$$T_{stat} = \frac{2\mu}{3} \frac{F_{z,stat}^{1,5}}{\sqrt{\pi p_0}} \quad (4\text{-}27)$$

Term and value	Description
μ=0,70	Tire-to-road friction coefficient (suggested value by Sharp and Granger Model)
$\boldsymbol{F_{z,stat}} = 360{,}628$ N	The vertical load acting on a wheel of the front axle in static conditions, $F_{z,stat} = F_{zf,left} = F_{zf,right}$ [N]
$\boldsymbol{p_0 = 5\ bar}$	The pressure inside the tires [bar]

Table 4-6: Descriptive table of quantities appearing in the equations

Using the above data, the static torque $T_{stat} = M_{z,left} = M_{z,right} = 2{,}550\ Nm$.
With $r_{steer,l} = r_{steer,r} = 140{,}539\ mm$ *the result will be* $F_{steer,SG} = 18{,}144\ N$.

We can therefore see that the two results relating to the forces transmitted by the single tie rod are very close (($F_{steer} = 19{,}203\ N$ e $F_{steer,SG} = 18{,}144\ N$)) and this confirms the validity of the mathematical model developed in this project, the final result of which will be adopted in the subsequent phases as more conservative and therefore in favour of safety.

The knowledge of F_{steer}, as will be seen later in the set of equations 4-28 to 4-31, leads to the calculation of the tensions acting on the conducting and driven branch of the wire wound around the pulleys and subsequently to the evaluation of the constrained reactions to which the supports fixing the pulleys to the monocoque are subject.
As far as the dimensioning of the pulleys is concerned, we have chosen to follow the rules of good design which apply to the design of cable-pulley systems.
First and foremost, the type of cable available to the team's supplier depended on the type of application (aeronautical, mooring lifting, bridge cranes). For basic applications such as the steering system, the recommended cable is a commercial steel cable consisting of 28 outer wires, each 0.33 mm in diameter and arranged around seven textile cores; the overall diameter is d=3mm (Ceccantini s.r.l. -Cables and Ropes Catalog- www.ceccantini.it/ cataloghi/nuovocatalogo/02-funi.pdf, p.32).
As far as the diameter of the pulleys is concerned, the supplier's tables indicate a range within which optimum values have been found taking various aspects into account (Ceccantini s.r.l. -Cables and Ropes Catalog-www.ceccantini.it/cataloghi/nuovocatalogo/02-funi.pdf, p. 17):

d cable diameter
D minimum pulley diameter

Driving pulleys	Secondary or return pulleys
$\boldsymbol{\frac{D}{d} \geq 20}$	$\frac{D}{d} \geq 20 \div 25$

Table 4-7: Good design indication for sizing pulleys (Ceccantini, n.d.)

In the architecture of the steering system for the muc022, the driving pulley is the first pulley, the one connected to the steering column, while the other two pulleys are secondary.
The first pulley is the one that has a greater axial length and therefore a more elongated shape, as it is connected to the steering column with a special insert. The following Figure is included for clarification purposes about the insert, but it is obviously a detail of the pulley

CAD drawing that was only created in the final phase of the project.

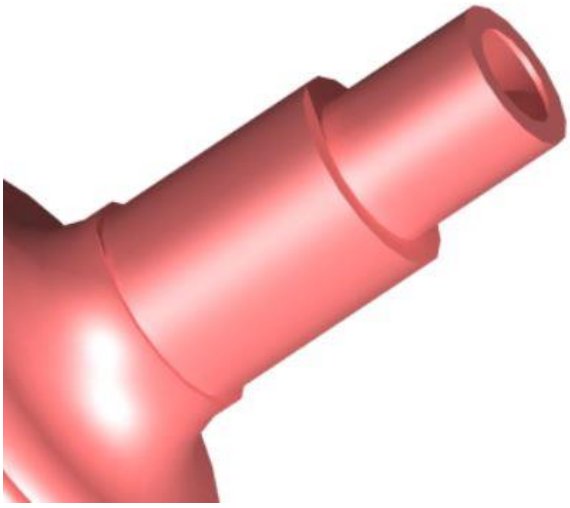

Figure 4-29: Detail of primary pulley, connection insert (Final CAD drawing)

Due to its particular shape, the space occupied by this element is larger than that of the other two pulleys. The space reserved for the system at the front of the car is mostly occupied by the electrical systems and the batteries, which are arranged at a height just in front of the central pulley as can be seen in Figure 4-30. Furthermore, the plane of the three pulleys is not vertical, but is inclined by a few degrees as you move towards the bottom of the car, as it follows the plane of the monocoque. This means that there is slightly more space in front of the secondary pulleys than is available in front of the primary.

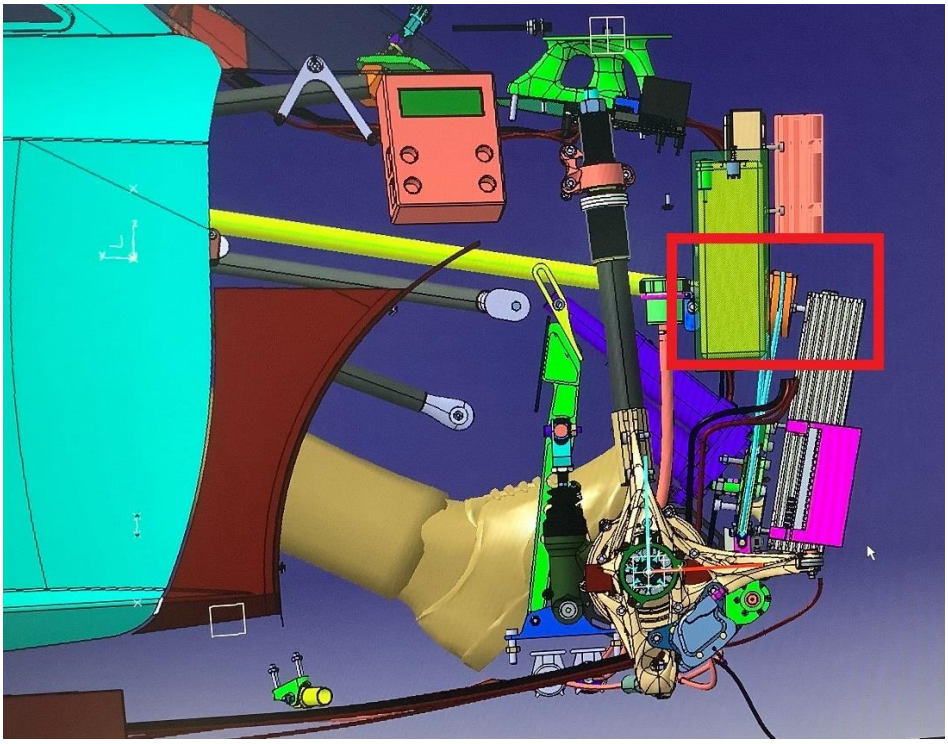

Figure 4-30: Disassembled front assembly. As can be seen in the red box, the primary pulley is completely immersed in the battery pack.

The constraints that emerged for the positioning and choice of the diameter of the primary pulley in relation to the indicated cable were therefore the distance with respect to the battery pack, the necessary alignment with the inclined plane of the monocoque created by the vehicle body team and the respect of the standard of good design indicated by the supplier and shown in Table 4-7.
Aligning the plane of the monocoque with that of the pulley, in order to ensure a safe distance from the battery pack, the choice of diameter was to set the limit of the margin allowed by the standard and then define a ratio $D/d=20$.
The result is that the minimum diameter selected for the first pulley is $D_1=60$ mm.
D is the minimum diameter, i.e. the diameter on which the cable rests, net of the height of the shoulders that identify the groove and whose calculation is included later in this paragraph.
The secondary pulleys, on the other hand, are not driven and as illustrated above, have more space around them. This implies greater freedom in following the supplier's good design standard (see Table 4-7), and to remain fully within the range indicated the minimum diameter chosen was $D_2=D_3=70$mm $(D/d=23{,}33)$.
To the diameters D_1 D_2 D_3, in order to complete the sizing of the pulleys, the heights of the shoulders that identify the groove in which the cable runs of d=3mm must be added. Also in this case there is a specific supplier's standard that defines the value (Ceccantini s.r.l. - Cables and Ropes Catalog-www.ceccantini.it/cataloghi/nuovocatalogo/02-funi.pdf, p. 18):

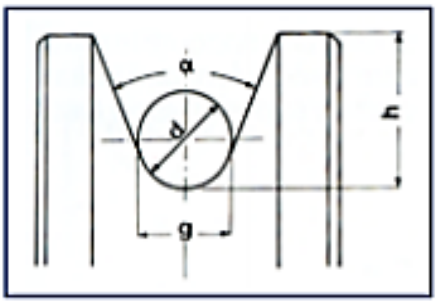

Figure 4-31: Pulley groove dimensions (Ceccantini n.d.)

Term and Value	Description
d=3 mm	Cable diameter
g=1,08d	Throat diameter
h=1,75d	Optimal shoulder height
h_{min}=1,41d	Minimum shoulder height
α=45÷60 deg	Angular width of the throat

Table 4-8: Pulley groove dimensions (Ceccantini n.d.)

If we apply the standard to the three pulleys, we obtain:

1st Pulley (Driving)	2nd pulley (Secondary)	3rd pulley (Secondary)
D_1=60 mm	D_2=70 mm	D_3=70 mm
g=3,24 mm	g=3,24 mm	g=3,24 mm
h=5,25 mm	h=5,25 mm	h=5,25 mm
h_{min}=4,23 mm	h_{min}=4,23 mm	h_{min}=4,23 mm
α=45 deg	α=60 deg	α=60 deg
D_{1ext}=68,5÷70,5 mm	**D_{2ext}=78,5÷80,5 mm**	**D_{3ext}=78,5÷80,5 mm**

Table 4-9: Final dimensions of the three pulleys

The internal diameter of the pulleys, on the other hand, which is not relevant to the calculation of the stresses, was defined later, after the sponsor-meeting phase, which will be explained later, in which the supports for each pulley were chosen instead. The internal diameters will be adapted to these supports.

Once the pulley diameters had been defined, it was finally possible to define a first spatial arrangement. The plane of the first pulley has already been identified, taking into account the distance to the battery pack and the necessary alignment with the inclined plane of the monocoque made by the vehicle body team. The other two pulleys were then arranged along the same plane. The centre of the driving pulley coincides with the centre of the steering wheel along the axis of the steering column, while the centres of the two other pulleys have been arranged in such a way that the wire coming out of the pulleys in the y direction intercepts precisely the central slide to which it will be hooked, knowing the height of the latter, since it is a pre-fabricated component, and also the spatial positioning constrained by the rail guide and its 12 DIN 912 M3x20 screws whose housing had already been arranged on the monocoque in agreement with the team vehicle body. The arrangement obtained is visible in the lateral projection of Figure 4-32, where one can see the inclined plane of the pulleys and the coincidence of the tangency of the secondary pulleys with the clamps that hook the cable to the central sled (red circle).

Figure 4-32: The pulleys are arranged in a common plane parallel to the monocoque.

Having therefore set the spatial inclination plane, the spatial coordinates of the centre and the diameters for each pulley, it was possible to obtain a preliminary drawing that mainly illustrated certain properties and geometric parameters that would be useful later, such as the winding angles and the inclinations of the wire itself (see Figure 4-33).

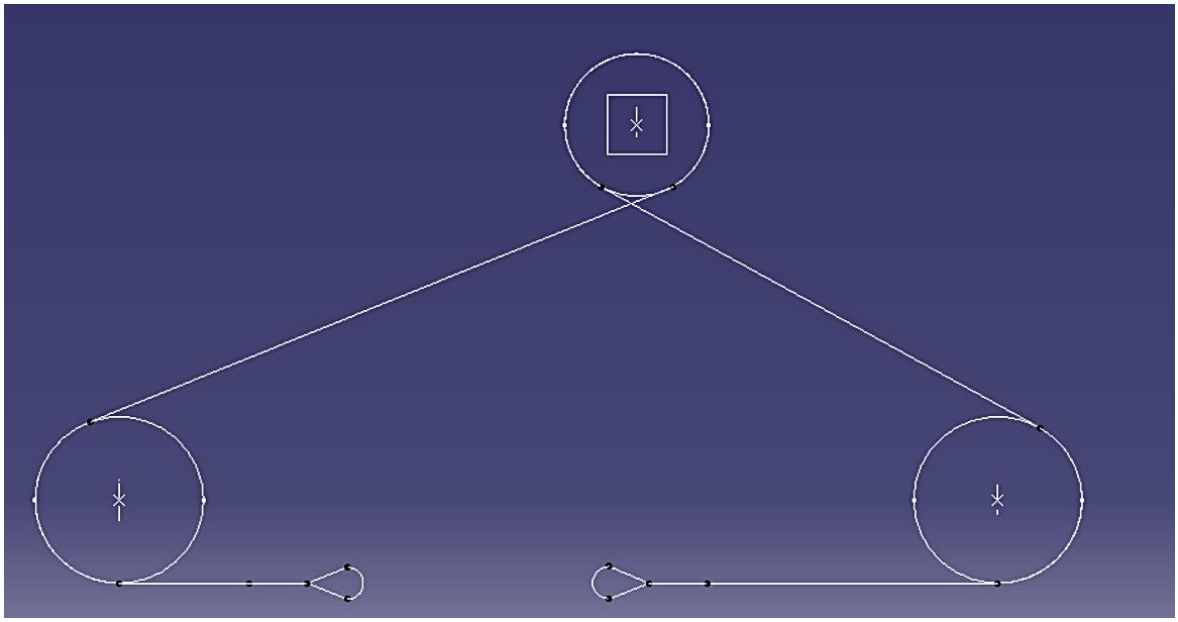

Figure 4-33: 2D Preliminary drawing of system of pulleys

In order to determine the stresses on the branches of the wire, it is necessary to write a set of equations derived from the balancing of the fundamental elements of the steering system: the central slide and the three pulleys.

The following set of equations can be defined from Figures 4-34 4-35 4-36 4-37 on the following pages:

$$T_3 + T_4 - m\ddot{x} = 2F_{steer} \cdot cos\gamma \quad (4\text{-}28)$$

$$T_1 R_3 - T_3 R_3 - I_3 \ddot{\theta}_3 = 0 \quad (4\text{-}29)$$

$$C_p + T_2 R_1 - T_1 R_1 - I_1 \ddot{\theta}_1 = 0 \quad (4\text{-}30)$$

$$T_2 R_2 - T_4 R_2 - I_2 \ddot{\theta}_2 = 0 \quad (4\text{-}31)$$

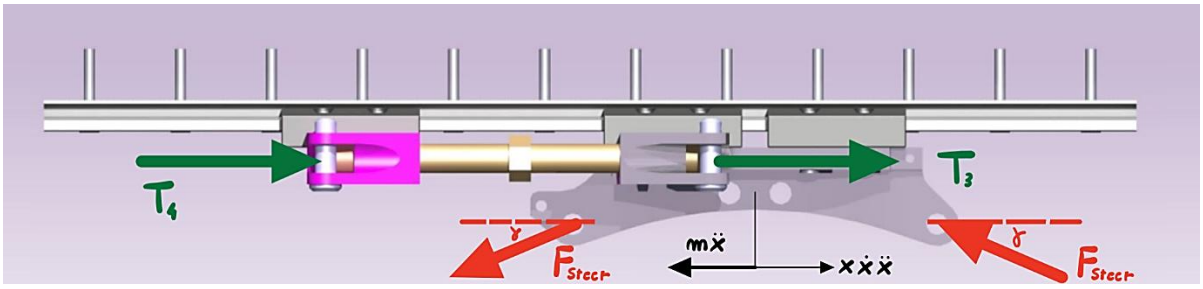

Figure 4-34: Balancing forces on the central sled (see Figure 3-2)

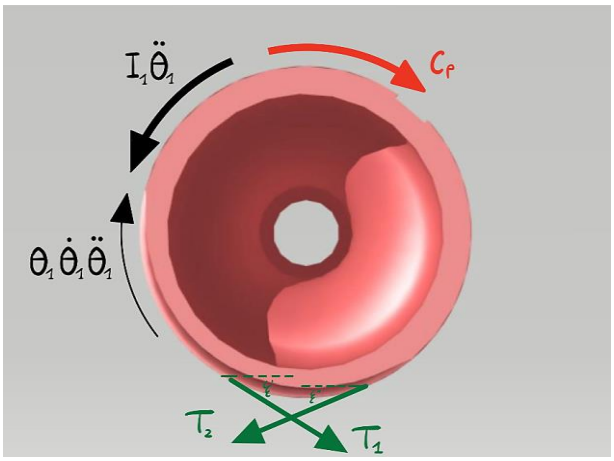

Figure 4-35: Balancing forces on the driving pulley

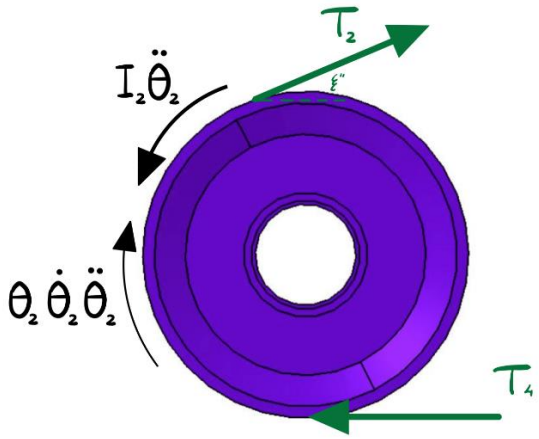

Figure 4-36: Balancing forces on the secondary pulley (2nd pulley)

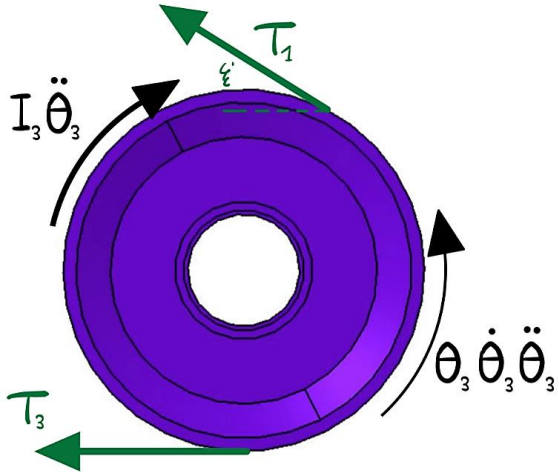

Figure 4-37: Balancing forces on the secondary pulley (3rd pulley)

Several inertial terms appear within these expressions, for which one can already get an idea of the order of magnitude.
The central slide, made of aluminium, has a weight of 0.3 kg and covers a maximum distance of 160 mm as shown by the kinematic analysis in Paragraph 4.2.3. Statistically, the response time of a steering system for normal or commercial applications is 2-5 seconds (Summala H. -Driver/Vehicle Steering Response Latencies- 1981, p.9). Therefore, even considering the minimum time interval, the estimated acceleration of the central slide is 0,08 m/s^2. This implies that the inertial contribution related to the sled is $m\ddot{x}$=0,024 N. The F_{steer} that appears in equation 4-28 is 19.203 N, which makes the inertial contribution completely negligible.
A similar argument can be made for the inertia contribution associated with pulleys. By knowing their diameters (Table 4-9) and approximating them to solid discs, it is possible to estimate their volume and mass and consequently their moment of inertia. Let's take pulleys 2nd and 3rd as an example:
Being full disks, the volume will be $V_2 = V_3 = \pi(R_3^2) \cdot s$ where s is the thickness of the pulley set as a safety value at 50 mm but certainly less in the final pulleys (also due to the overall dimensions). Knowing that the pulleys will be made of aluminium (specific weight $\rho = 2700\ kg/m^3$) we can say that the approximate mass of a secondary pulley is $m_2 = m_3 = \rho V_2 = 0{,}68\ kg$. The moment of inertia then is $I_2 = I_3 = \frac{1}{2} m_2 R_2^2 = 0{,}0005\ kg \cdot m^2$.
Furthermore, since the pulleys rotate as a function of the displacement of the central sled, the angular acceleration can be estimated as $\ddot{\theta}_2 = \ddot{\theta}_3 = 2\ rad/s^2$ (angular acceleration corresponding to a linear acceleration of the sled of 0,08 m/s^2). This finally implies that the inertial contribution for the secondary pulleys is approximately $I_2\ \ddot{\theta}_2 = I_3\ \ddot{\theta}_3 = 0{,}002$ Nm, therefore negligible with respect to the torques at play in the system, generated by the cable tensions.
In the light of what has been said, regarding the set of equations it can be stated that $T_1 = T_3$ and $T_2 = T_4$.
However, in order to know the range of values that these voltages can assume, it is necessary to consider two further aspects: the adherence conditions of the cable on the pulleys and the torque that the driver can supply to the steering wheel, and therefore to pulley 1st via the steering column.

The theory of adhesion conditions is a fundamental step in the calculation of the stresses to which the cable is subjected. These must ensure that there is no uplift of the wire relative to the sheave groove in which it is inserted. The following is a brief demonstration of the basis of the formulations used in this project to ensure the adherence conditions (Ferraresi, Raparelli - Machine Applied Mechanics- CLUT Editrice, p.159).

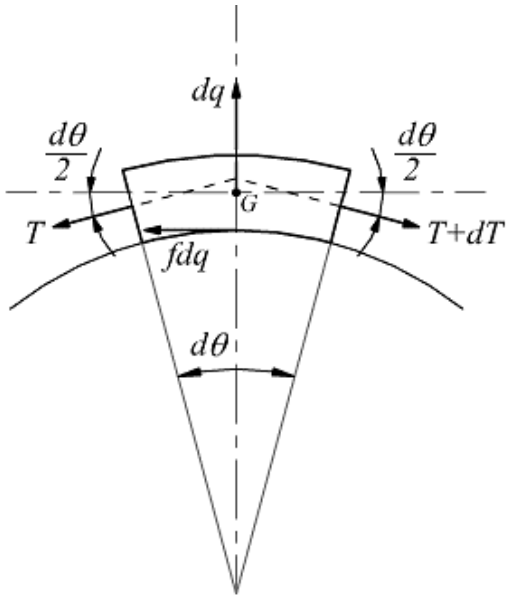

Figure 4-38: Infinitesimal element of a cable (Ferraresi, Raparelli - Machine Applied Mechanics- CLUT Editrice)

To see if in a coupling between a cable and a pulley a force coupling has been assured with an adherence that prevents reciprocal slipping, let us consider an infinitesimal element (as small as desired) of a cable that subtends an elementary angle dθ.
On the normal face of the element, the elementary normal force dq acts in a direction that opposes the sliding on the crown of the pulley.
Furthermore, on the same element, the weight force and the centrifugal force act.
If *f* is the coefficient of friction between cable and pulley, the equations of equilibrium are:

$$fdq + Tcos\frac{d\theta}{2} - (T + dT)cos\frac{d\theta}{2} = 0 \qquad (4\text{-}32)$$

$$dq - Tsen\frac{d\theta}{2} - (T + dT)sen\frac{d\theta}{2} = 0 \qquad (4\text{-}33)$$

Since the angle dθ/2 is an infinitesimal quantity, it can be approximated:
$cos\frac{d\theta}{2} \cong 1 \quad sen\frac{d\theta}{2} \cong \frac{d\theta}{2}$ and the term $dT \cdot sen\frac{d\theta}{2}$ is negligible because it is a product of infinitesimal quantities.

The two equations 4-32 and 4-33 then become:

$$fdq - dT = 0 \qquad (4\text{-}34)$$

$$dq - Td\vartheta = 0 \qquad (4\text{-}35)$$

If we then obtain the value of dq from the second equation and replace it in the first, we obtain the following relationship which links, in infinitesimal terms, the increase dT undergone by the voltage to the increase dθ of the winding angle:

$$\frac{dT}{T} = fd\theta \qquad (4\text{-}36)$$

Referring now to the following Figure, which schematically represents a pulley in which the entire arc embraced by the cable subtends the winding angle α with the branch subject to the tension T_1 conductor, while that subject to the tension T_2 conducted, it can be deduced that:

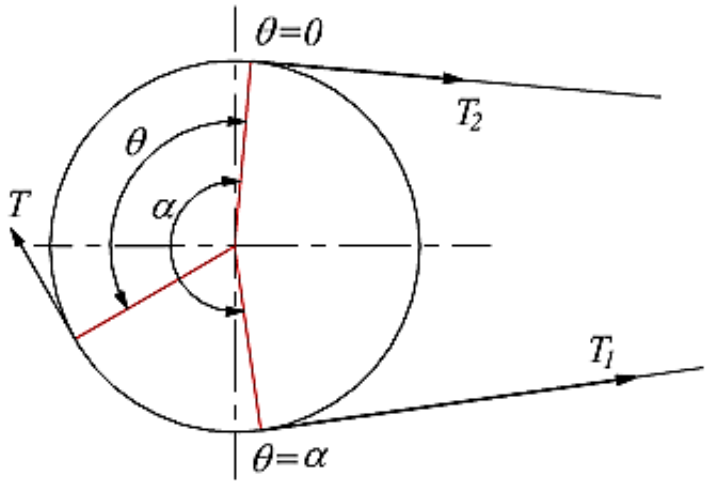

Figure 4-39: Schematic diagram of pulley with conductor branch and conduit one (Ferraresi, Raparelli - Machine Applied Mechanics- CLUT Editrice)

Comparison with relation 4-36 shows that while the tension in the track varies from T_2 to T_1, the angle θ varies from zero to the value α. Integrating 4-36 between these limits, we have:

$$\int_{T2}^{T1} \frac{dT}{T} = \int_0^{\alpha} f d\theta \qquad (4\text{-}37)$$

So:

$$ln\frac{T_1}{T_2} = f\alpha \rightarrow \frac{T_1}{T_2} = e^{f\alpha} \qquad (4\text{-}38)$$

If we call F the transmitted peripheral force or driving force on the pulley (what is defined as T in Figure 4-39), the equation of the moment with respect to the centre of the driving pulley is:

$$F \cdot \frac{D}{2} + T_2 \cdot \frac{D}{2} - T_1 \cdot \frac{D}{2} = 0 \rightarrow F = T_1 - T_2 \qquad (4\text{-}39)$$

Therefore, by substituting in equation 4-38 we obtain the two expressions of the tensions T_1 , T_2 in relation to the driving force applied to the primary pulley:

$$T_1 = \frac{Fe^{f\alpha}}{e^{f\alpha}-1} \qquad (4\text{-}40)$$

$$T_2 = \frac{F}{e^{f\alpha}-1} \qquad (4\text{-}41)$$

As can be seen from Figure 4-35, the driving force on the pulley is given by the torque applied by the driver. Statistically, the torque that a driver can apply ranges from a value of 1.1 Nm up to 28-30 Nm. (Dreyfuss, Tilley -The Measure of Man and Woman: Human Factors in Design- 2002, p.76). This range covers both steering manoeuvres under normal conditions and sudden and violent manoeuvres. Knowing therefore the diameter of the pulley 1 (Table 4-9) we can calculate F within this range and using then the relations (4-40 and 4-41) we can also calculate the range of tensions that the wire will have to bear in anticipation of normal and violent steering manoeuvres.

C_p -torque applied by the driver-	$\boldsymbol{T_1 = T_3}$	$\boldsymbol{T_2 = T_4}$
1,1 Nm	40,09 N	3,42 N
2 Nm	72,89 N	6,22 N
3 Nm	109,33 N	9,33 N
4 Nm	145,78 N	12,44 N
5 Nm	182,22 N	15,55 N
6 Nm	218,66 N	18,66 N
7 Nm	255,11 N	21,78 N
8 Nm	291,55 N	24,89 N
9 Nm	328,00 N	28,00 N
10 Nm	364,44 N	31,11 N
11 Nm	400,88 N	34,22 N
12 Nm	437,33 N	37,33 N
13 Nm	473,77 N	40,44 N
14 Nm	510,22 N	43,55 N
15 Nm	546,66 N	46,66 N
16 Nm	583,11 N	49,77 N
17 Nm	619,55 N	52,88 N
18 Nm	655,99 N	55,99 N
19 Nm	692,44 N	59,10 N
20 Nm	728,88 N	62,22 N
21 Nm	765,33 N	65,33 N
22 Nm	801,77 N	68,44 N
23 Nm	838,21 N	71,55 N
24 Nm	874,66 N	74,66 N
25 Nm	911,10 N	77,77 N
26 Nm	947,55 N	80,88 N
27 Nm	983,99 N	83,99 N
28 Nm	1020,43 N	87,10 N
29 Nm	1056,88 N	90,21 N
30 Nm	1093,32 N	93,32 N

$$\alpha = 5{,}235\ rad\ \ - wrap\ angle -$$

$$f = 0{,}47 - friction\ coefficient\ aluminum\ on\ steel -$$

Table 4-10: Values of the tensions in the wire as the torque applied by the driver to the steering wheel varies

From these values, it is clear that the cable will be affected at most by tensions of around 1000 N or less (a torque of 30 Nm supplied by the pilot is a very extreme and anatomically infrequent case). On the basis of this, the tensions obtained are perfectly in line with the breaking load of the commercial steel cable consisting of 28 external wires, each with a diameter of 0.33 mm and arranged around seven textile cores and with an overall diameter d=3mm, i.e. the one recommended by the supplier. As can be seen in the next Figure (Ceccantini s.r.l. -Cables and Ropes Catalog-www.ceccantini.it/cataloghi/nuovocatalogo/02-funi.pdf, p.32) the breaking load is 4220 N.

fune Ø mm	peso x 100 m. kg	carico di rottura min. kgf	carico di rottura min. daN	fili esterni Ø mm
2	1,5	245	240	0,28
3	3	430	422	0,33

Figure 4-40: Breaking loads for some commercial cables (Ceccantini n.d.)

The calculation of the range of tensions affecting the cable also opens up the possibility of a hint of the possible play or free angle that can affect the steering wheel of the system due to the elastic deformation of the cable itself under the action of the tensions during steering.

As in fact in the classical architectures (rack and pinion) illustrated in Chapter 2, one of the main causes of play in the steering is due to inaccurate positioning in the coupling of the toothed elements, as well as to the different tightening of the rotating elements of the entire system, also for this particular structure it is logical to attribute and imagine the effects of play due to the transmission element of the motion that replaces the pinion, that is the cable.

By means of formula $\Delta L = \frac{T*L_0}{A*E}$, where $L_0 = 1184\ mm$ is the cable length, $A = 7{,}068\ mm^2$ is the cable section, $E = 196000\ N/mm^2$ is the Young Modulus of galvanized steel, the cable material, the elongation of the cable deriving from its elastic deformation under the action of the Tensions T has therefore been evaluated. This value obviously fluctuates with the value of the torque applied by the driver to the steering wheel and therefore with the increasing tensions inside the cable. On the basis of knowledge of these elongation values, it was then possible, using formula $\theta_l = \Delta L / R_1$, to estimate the angle of rotation θ_l of the primary pulley (R_1 primary pulley radius computed in next section) and therefore of the steering column and steering wheel, necessary to recover this elongation in order to have a steering effect.

At the end of this evaluation, for the range of tension values previously calculated and reported in Table 4-10, the range of values assumed by the free steering angle θ_l oscillates between $1{,}5° \div 2°$.

An idea reported together with the TUfast team for future applications deriving from this Thesis work is the certification by means of a dynamic simulation software of this theoretical play and a further evaluation on plays originated by any non-optimal tightening, friction and pulley play of the system.

Once the stresses that the wire must withstand and that act on the pulleys had been defined, it was possible to use the knowledge of these values to calculate the constraint reactions that the pulley supports would have to withstand. In this phase of choosing the appropriate supports for each load and for the shape and arrangement of each component, the help of one of the gold sponsors of the TUfast Eco Team for the 2022 season, Aluminium Engineering, was invaluable.
ALEN GmbH is a future-oriented and constantly growing company in the development and production of structural components for vehicle technology, particularly in the automotive sector (see aluengineering.de).
As a competent partner, they supported us in the project management, industrialisation and implementation of lightweight construction products. Their knowledge in the automotive sector and in the implementation of aluminium components (such as pulleys) and more, in the more general and complex frame of the whole car, was invaluable and deserves to be mentioned.
The way to act in this particular phase of defining the supports was therefore as follows: preliminary calculation of the loads that each specific support would have to withstand and subsequent meetings with Aluminium Engineering to exchange ideas and gather advice on the ideal support and mechanical component to be used for that specific function.
Below are the design calculations for the various constraint reactions and then the supports and components suggested by the sponsor in our meetings.

The first component analysed is obviously the driving pulley (1^{st} pulley).
It has already been said that this pulley will be more elongated, therefore with a greater axial length than the others, because it will have an insert for connection with the steering column (Figure 4-29).
The steering column that starts from the cockpit passes through a hole that will be made in a special housing of the monocoque (see Figure 4-41) and ends in the central part with the driving pulley. This means that the steering column-pulley assembly must be connected to the monocoque by means of a support, so as to allow the pulley to rotate with respect to the fixed frame. The support will certainly be inserted in correspondence with the hole through which the steering column passes, and it is logical to think that a flange that can be fixed with screws is the best solution. The flange will also have to adapt to the shape of the housing present on the monocoque, inside which the hole will be made, as shown still in Figure 4-41.

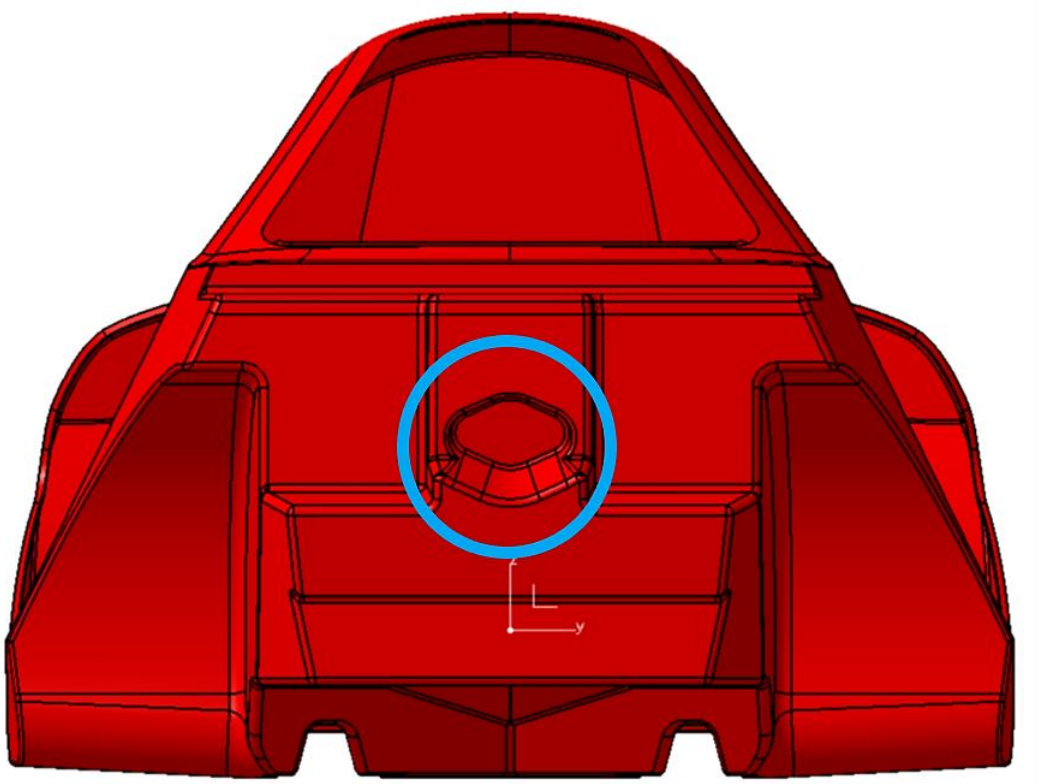

Figure 4-41: CAD model of the real monocoque with the detail of the housing for the hole of steering column (CATIA V5)

With the idea of implementing this flange, the support for the primary pulley was dimensioned.
From Figure 4-42, the force balance equations can be derived:

$$2R_H = T_{1max}cos\xi' - T_{2max}cos\xi'' \quad (4\text{-}42)$$

$$2R_V = T_{1max}sin\xi' + T_{2max}sin\xi'' + m_1 g \quad (4\text{-}43)$$

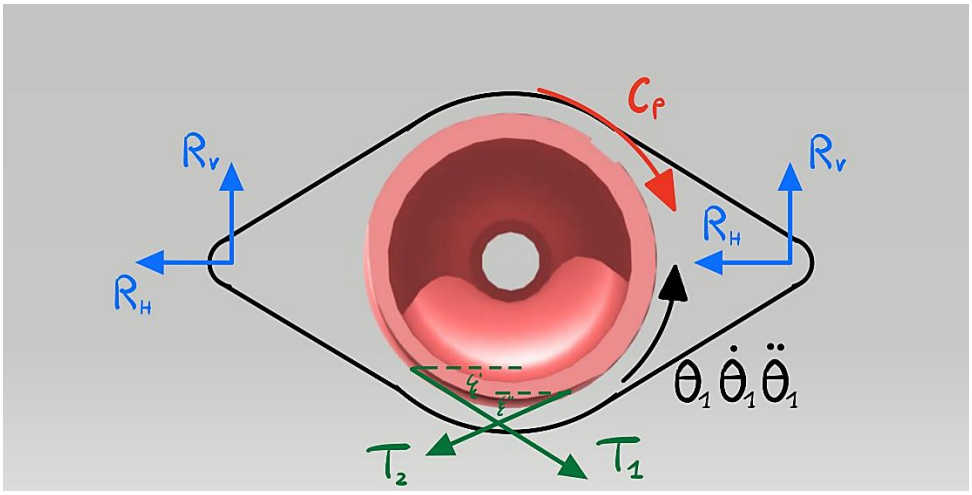

Figure 4-42: Balancing forces on the driving pulley

Term and value	Description
$\boldsymbol{R_H}$	Horizontal constraint reaction on one of the two screws designed for fixing the flange [N]
$\boldsymbol{R_V}$	Vertical constraint reaction on one of the two screws designed for fixing the flange [N]
$\boldsymbol{T_{1max} = 1093,32\ N}$	Maximum value of tension T_1 to consider the worst-case scenario (see Table 4-10) [N]
$\boldsymbol{T_{2max} = 93,32\ N}$	Maximum value of tension T_2 to consider the worst-case scenario (see Table 4-10) [N]
$\boldsymbol{\xi' = 29,62\ deg}$	Angle of inclination with respect to the horizontal of the branch of wire that goes from pulley 1 to 3 [deg]
$\boldsymbol{\xi'' = 22,69\ dege}$	Angle of inclination with respect to the horizontal of the branch of wire that goes from pulley 1 to 2 [deg]

Table 4-11: Descriptive table of quantities appearing in the equations

From equations 4-42 and 4-43 we obtain that $R_H = 432{,}19\ N$ and $R_V = 288{,}16\ N$.
Knowing therefore the values of the constraint reactions, it is possible to calculate the maximum shear stress τ and the maximum axial stress σ_a for the flange screws using the following formulas (Baragetti S., Terranova A. -Progetto e Calcolo di Sistemi Meccanici- Hoepli):

$$\tau = \frac{R_b}{nA_{RES}} \qquad (4\text{-}44)$$

$$\sigma_a = \frac{F_a}{2A_{RES}} \qquad (4\text{-}45)$$

Term and value	Description
$\boldsymbol{R_b = 519,45\ N}$	Resulting constraint reaction on the screw [N] $R_b = \sqrt{{R_H}^2 + {R_V}^2}$
$\boldsymbol{A_{RES}}$	Resistant area of the screw; its value depends on the chosen screw [mm^2]
$\boldsymbol{n = 1}$	Number of areas in contact in the threaded coupling
$\boldsymbol{F_a = 27000\ N}$	Maximum axial load the body can exert on the steering column during an accident. This load is also transmitted to the screws that bind the pulley and steering column to the monocoque [N]

Table 4-12: Descriptive table of quantities appearing in the equations

On the basis of these formulations and by comparing ourselves with Aluminium Engineering, in the end the screws chosen for this particular application were DIN 912 M10x40, for which the values of maximum shear stress ($\tau = 17\ N/mm^2$) and maximum axial stress ($\sigma_a = 280\ N/mm^2$) are well below the values admissible by the material before breaking or yielding.

The flange identified together with the screws mentioned here is shown in the following Figure.

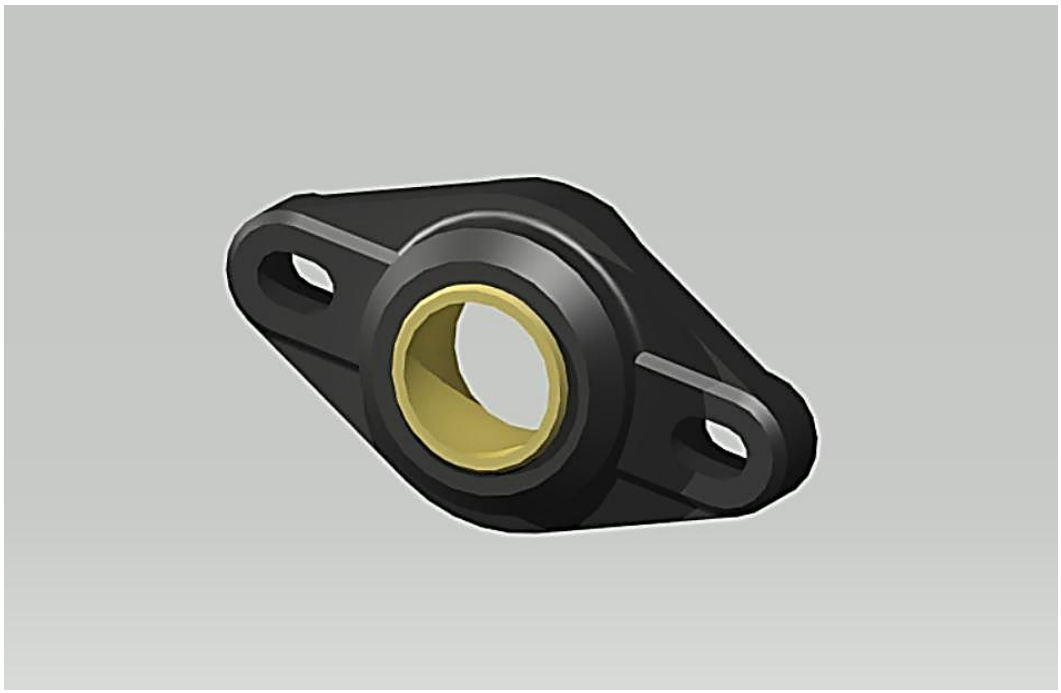

Figure 4-43: Driving pulley support flange (final CAD drawing, CATIA V5)

A bearing is inserted between the body of the steering column insert and the flange, allowing the pulley and column to rotate in relation to the flange, which is integral with the monocoque. In this case too, the choice of bearing is the result of collaboration with Aluminium Engineering, which, together with the team, assessed the field of applicability of these elements in the detail of the system in question. Our opinions converged on a needle bearing. This type of bearing is preferred in situations such as the one in question, where the correct rolling of the rolling elements, and therefore the correct rotation of the system, is preferred to the element's ability to withstand loads.

The analysis now focuses on the supports for the secondary pulleys. These pulleys have a more conventional shape than the driving pulley, as they do not have to be fitted to any additional components (such as the steering column). However, both are designed to be attached directly to the monocoque, without the use of intermediate flanges. They also need to be mounted on a fixed bearing relative to the monocoque, allowing relative rotation. Discussing these issues with Aluminium Engineering, the solution found through co-working was that of a support which would guarantee a triple constraint, as illustrated in the following Figure:

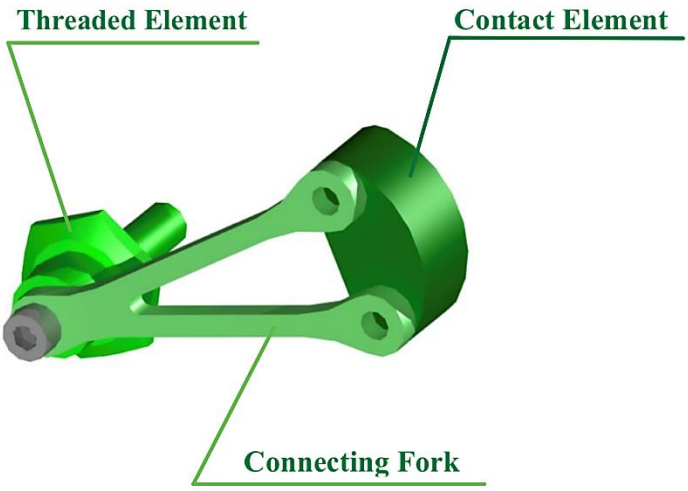

Figure 4-44: Support for secondary pulleys (CATIA V5)

As can be seen in Figure 4-44, the support suggested by Aluminium Engineering has three loading points. This avoids a concentrated load at a single point which could be problematic and cause damage to the carbon fibre wall of the monocoque. The support is based on three elements:

- a Contact Element with the wall on which two load points are arranged;
- a Threaded Element characterised by a surface on which the bearing+pulley will be mounted and a shoulder with two different surfaces: one smooth, suitable for contact with the monocoque, and one slightly tapered to hold the bearing in position;
- a Connecting Fork between the first two elements to avoid making a single piece and making the whole structure heavier;

Therefore, basing the calculation of the constrained reactions on the support structure presented above, we will have:

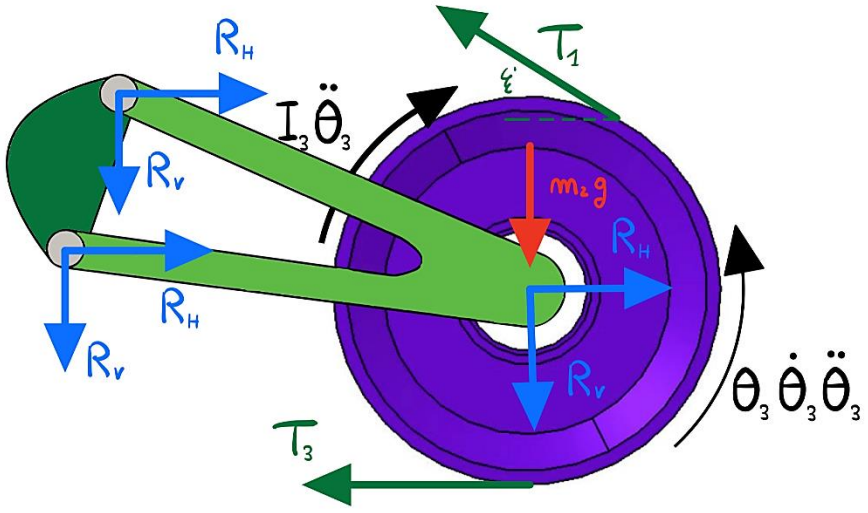

Figure 4-45: Balancing forces on the driving pulley

The force balance equations can be derived from Figure 4-45:

$$R_H = T_{1max}cos\xi' + T_{3max} \quad (4\text{-}45)$$
$$R_V = T_{1max}sin\xi' - m_2 g \quad (4\text{-}46)$$

Term and value	Description
$\boldsymbol{R_H}$	Horizontal constraint reaction on the entire support. It will be split between the three load points (the three screws) [N]
$\boldsymbol{R_V}$	Vertical constraint reaction on the entire support. It will be split between the three load points (the three screws) [N]
$\boldsymbol{T_{1max} = T_{3max} = 1093,32\ N}$	Maximum value of tensions T_1 and T_3 to consider the worst-case scenario (see Table 4-10) [N]
$\boldsymbol{\xi' = 29,62\ deg}$	Angle of inclination with respect to the horizontal of the branch of wire that goes from pulley 1 to 3 [deg]

Table 4-13: Descriptive table of quantities appearing in the equations

From equations 4-45 and 4-46 we obtain that $R_H = 2102\ N$ and $R_V = 539{,}15\ N$.
Knowing therefore the values of the constraint reactions, it is possible to calculate the maximum shear stress τ for the screws of the tri-loaded support by means of the following formula (Baragetti S., Terranova A. -Progetto e Calcolo di Sistemi Meccanici- Hoepli):

$$\tau = \frac{R_b}{nA_{RES}} \quad (4\text{-}47)$$

Term and value	Description
$\boldsymbol{R_b = 519,45\ N}$	Resulting constraint reaction on the screw [N] $R_b = \sqrt{{R_H}^2 + {R_V}^2}$
$\boldsymbol{A_{RES}}$	Resistant area of the screw; its value depends on the chosen screw [mm²]
$\boldsymbol{n = 1}$	Number of areas in contact in the threaded coupling

Table 4-14: Descriptive table of quantities appearing in the equations

The maximum shear stress obtained with this formulation ($\tau = 59{,}3\ N/mm^2$) is therefore to be divided between the screws of the three loading points. The threaded element, manufactured by Aluminium Engineering, has a diameter of M8, while the screws chosen for the other element in contact with the wall are two DIN M5x45. In this way the load distribution on each screw is safely below the values allowed by the material before breaking or yielding.
As mentioned above, the secondary pulleys require a bearing integral with the support which allows their relative rotation. As already mentioned, the threaded element of the support provides a fixing surface for the bearing + pulley assembly.
The choice of bearing agreed with Aluminium Engineering was an SKF 61902 radial ball

bearing. The radial bearing is a good solution since the secondary pulley bearing does not support axial loads.

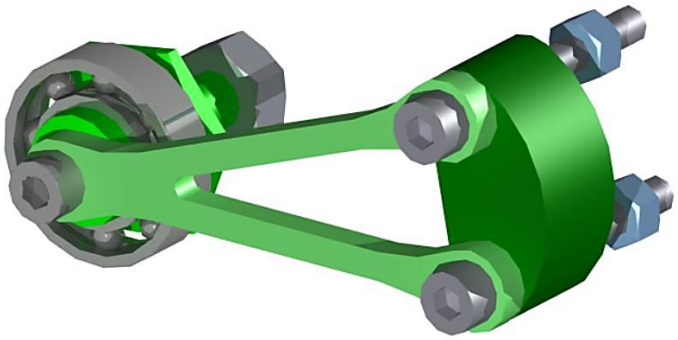

Figure 4-46: Supports for the secondary pulleys (final CAD drawing, CATIA V5)

The supports and associated mechanical components were sized in the same way for the two secondary pulleys, following the formulas given in this section.

The next component of the steering system to be dimensioned was the steering column (see Figure 4-5).
In university-level automotive applications, the steering column is usually a tubular carbon fibre structure. However, in the previous TUfast Eco Team model, the muc019, the steering column was one of the most critical components of the steering system.
During the steering phase, in fact, the feedback from the steering column, both in terms of effort and noise, was not at all what was desired. Therefore, one of the main objectives of this project was to solve this problem and to avoid its repetition in the muc022.
The first step was to analyse the steering column of the muc019 project.
Having had the opportunity during the days in the workshop to personally test the steering of the muc019 model, the impression, later confirmed by the pilot of this model, was that the steering column was too stressed. The torsional stress τ_{019} and the twisting angle θ_{019} were calculated using the following formulae (Shaikh, Parvez, Shakebuddin -Design, Analysis and Optimization of Collapsible Steering Column- IRJET, 2016, Vol. 03, p.2621):

$$\tau_{019} = \frac{16 C_p d_{ext}}{\pi (d_{ext}^4 - d_{int}^4)} \qquad (4\text{-}48)$$

$$\theta_{019} = \frac{32 C_p L}{\pi (d_{ext}^4 - d_{int}^4) G} \qquad (4\text{-}49)$$

Term and Value	Description
$C_p = 30\ Nm$	Torque applied by the driver. Statistically it can be between a value of 1,1 and 30 Nm. (Dreyfuss, Tilley -The Measure of Man and Woman: Human Factors in Design- 2002, p.76) In this analysis we use the limit value $C_p = 30$ Nm to evaluate the maximum possible torsional effort and maximum twisting angle. [Nm]
$d_{int} = 16\ mm$	Internal diameter of the steering column of muc019 [mm]
$d_{ext} = 18\ mm$	External diameter of the steering column of muc019 [mm]
$L = 565\ mm$	Steering column length of muc019 [mm]
$G = 4\ GPa$	Elasticity tangential modulus of carbon fibre [GPa] (-Mechanical Properties of Carbon Fibre Composite Materials, Fibre- www.performance-composites.com)

Table 4-15: Descriptive table of quantities appearing in the equations

From the application of the equations 4-48 and 4-49) we obtain the following results.
The torsional stress $\tau_{019} = 69{,}73\ MPa$, a tolerable value because below the admissible value for the carbon fibre of the steering column ($\tau_{adm} = 150 \div 200\ MPa$ -Mechanical Properties of Carbon Fibre Composite Materials, Fibre- www.performance-composites.com).
The discourse relative to the twisting angle is instead different. The value obtained for the steering column of muc019 is $\theta_{019} = 1{,}09\ deg$. However, the conventionally acceptable values for the twisting angle of a steering column are between 0.05 ÷ 0.30 deg. This value confirms the sensations obtained from the driver's feedback and highlights the problems of a steering column that is too twisted under the application of torque to the steering wheel.
The muc022 steering column should then have had a much lower twisting angle, thus setting a target for its sizing.
By looking at the parameters that appear in formula 4-49, it is possible to get an idea of the aspects that need to be acted upon in order to obtain the mentioned target.

- One hypothesis may therefore be to decrease the length of the steering column. However, this length of 565 mm in project muc019 will also be the same in project muc022, since the position of its ends coincides with the positions of the previous model. One end is constrained by the space in front of the battery pack as we have already discussed, while the other end is constrained by the steering wheel and thus by the position of the driver, which remains unchanged in its x and z coordinates, and simply shifted along y towards the centre of the car as part of the pre-conceptual decisions. No substantial change therefore leads to a possible decrease in the length of the steering column.

- Another option would be to choose a different carbon fibre to increase the elasticity tangential modulus G. However, this solution faces obstacles that are this time more organisational than design related. The tubular structures are part of the set of components that the team purchased in large quantities and stored in the warehouse before the pandemic period. The environmental and economic philosophy of the TUfast Eco Team, as I have said many times before, is to reduce waste to a minimum; therefore, the Board itself has asked me to use as much as possible of what is already in stock (see Paragraph 3.3). The tubular structures available in stock are all of the same carbon fibre type.
- The last parameter, which is still affected by the team's operational philosophy of refusing waste, is the size of the tubular structures. After pointing out to the team that to improve the steering column it was necessary to increase its size, I was informed that there was only one tubular structure in stock that was larger than the one used for the muc019 steering column. The diameters of this new structure are d_{int}=18 mm and d_{ext}=22 mm.

In order to assess whether it can be used and whether it leads to an obvious improvement in the tangential deformation of the column, the following calculations were carried out:

$$\tau_{022} = \frac{16 C_p d_{ext}}{\pi (d_{ext}^4 - d_{int}^4)} \qquad (4\text{-}50)$$

$$\theta_{022} = \frac{32 C_p L}{\pi (d_{ext}^4 - d_{int}^4) G} \qquad (4\text{-}51)$$

Term and Value	Description
$\boldsymbol{C_p = 30\ Nm}$	Torque applied by the driver. Statistically it can be between a value of 1,1 and 30 Nm. (Dreyfuss, Tilley -The Measure of Man and Woman: Human Factors in Design- 2002, p.76) In this analysis we use the limit value C_p = 30 Nm to evaluate the maximum possible torsional effort and maximum twisting angle. [Nm]
$\boldsymbol{d_{int} = 18\ mm}$	Internal diameter of the steering column of muc022 [mm]
$\boldsymbol{d_{ext} = 22\ mm}$	External diameter of the steering column of muc022 [mm]
L= 565 mm	Steering column length of muc022 [mm]

G= 4 GPa	Elasticity tangential modulus of carbon fibre [GPa] (-Mechanical Properties of Carbon Fibre Composite Materials, Fibre-www.performance-composites.com)

Table 4-16: Descriptive table of quantities appearing in the equations

With a tubular structure with these new dimensions, a torsional stress $\tau_{022} = 26\,MPa$ is obtained, therefore always below the tolerable value for carbon fibre ($\tau_{adm} = 150 \div 200\,MPa$), while the twisting angle is $\theta_{022} = 0{,}334\,deg$, considerably reduced with respect to $\theta_{019} = 1{,}09\,deg$ and brought to the limits of the conventional values.
In the light of this, the choice has been to use this new tubular structure, which represents an excellent compromise between performance research and compliance with the team's directives and policies.

A further check on the tubular structure chosen is that of compression failure. This is a procedure which is more part of the set of precautions for the benefit of the driver's safety than of the set of evaluations which seek performance.
The purpose of this type of check is to assess the behaviour of the steering column in the event of a strong impact, in order to prevent the compressive load caused by the pilot's body being thrown against the column from causing the column to break and thus causing serious damage to the pilot.
The wording in support of the standard (Shaikh, Parvez, Shakebuddin -Design, Analysis and Optimization of Collapsible Steering Column- IRJET, 2016, Vol. 03, p.2621) in this case is as follows:

$$a = \frac{0 - v_{max}^2}{2s} \qquad (4\text{-}52)$$

$$Force\ of\ impact = a \cdot m \qquad (4\text{-}53)$$

Term and Value	Description
$\boldsymbol{a}$	Acceleration of the body in the event of a violent impact at maximum speed [m/s²]
$\boldsymbol{v_{max}}$=40 km/h=11,11 m/s	maximum speed of the car [m/s]
s=0,46 m	Standard stretching distance of seat belt [m]
m=70kg	Mass of occupant [kg]

Table 4-17: Descriptive table of quantities appearing in the equations

Based on equations 4-52 and 4-53, the impact force that the pilot's body exerts in the event of a violent impact on the steering column is $Force\ of\ impact = 9{,}39\,kN$. The maximum allowable compression force for the carbon fibre is 25 kN. The tubular structure chosen for the steering column is thus verified also with respect to this particular case study.

The last components to be sized are the tie rods. Also in this case they are carbon fibre tubular structures, with smaller diameters than the steering column, so also in this case the choice of the most suitable diameter is strongly bounded by the availability in stock.
In order to choose the right diameter, according to equation 4-54 which is based on equation 4-28, the maximum axial load applied on the tie rods $F_{steer,max}$ was evaluated:

$$T_{3max} + T_{4max} = 2F_{steer,max} \cdot cos\gamma \qquad (4\text{-}54)$$

Term and Value	Description
$\boldsymbol{T_{3max} = 1093,32\ N}$	Maximum value of tension T_3 to consider the worst-case scenario (see Table 4-10) [N]
$\boldsymbol{T_{4max} = 93,32\ N}$	Maximum value of tension T_4 to consider the worst-case scenario (see Table 4-10) [N]

Table 4-18: Descriptive table of quantities appearing in the equations

The value of $F_{steer,max} = 510{,}2\ N$ should then be compared with the maximum permissible axial load for the different tubular structures, which can be obtained from the formula:

$$F_{a,max} = UTS \cdot A \qquad (4\text{-}55)$$

Where UTS is the Ultimate Tensile Strength of the carbon fibre, and therefore the same for all tubular structures, while A is the cross section of the tube and varies according to size.
The tubular structure with the smallest diameters in stock ($d_{int} = 12\ mm\ d_{ext} = 14\ mm$), guarantees a maximum permissible axial load $F_{a,max} = 5121\ N$, therefore well above the maximum axial load applied on the tie rods. These tubular structures have therefore been chosen as definitive, although there is clearly room for a further reduction in diameter, which will be explored in more detail in Chapter 5 on possible future improvements to the design.

Figure 4-47: An example of the carbon fibre tubular structures used for steering columns and tie rods

4.4 Realization on Catia V5 of the CAD Drawings of the muc022 Steering System

After having sized all the elements of the Steering System and having chosen the basic mechanical components associated with them (bearings, supports, screws), the last phase of the project was the drawing in CATIA V5 of the same and the final assembly into the final Steering System that was then uploaded into the CAD assembly of the car.

The CAD phase, even though it follows the work of defining architectures, choosing kinematic theories, simulating movements, calculating dynamic actions and dimensioning elements, is just as demanding and perhaps even more important. It represents the moment when all the work done previously produces a visible result that is close to the real world and gives the semblance of what the final product will be. In the specific case of this project, this phase also has a further significance. It is the first real milestone in the realisation of the vehicle. Once the CAD drawings have been produced, they become the main reference point for the manufacturing phase, but also for the Board, which has a first vision of the final product, and for the Sponsors, with whom it is more immediate to interface and who thus have feedback that rewards their technical and economic contribution.
This Paragraph will therefore present the CATIA V5 drawings of the main elements making up the steering system, together with a brief description of some special features, some details, some functions or design peculiarities. Some of these drawings have already been shown in their entirety or in some details in the previous Paragraphs and Chapters for the sole purpose of increasing the clarity of the particular contents, even though at the time of drafting these calculations there were ideas or simple sketches at the base and the Figures included are only the final result.
Finally, the complete Steering System will also be presented as the final result of the entire Thesis Project. The same as can be found on the muc022.

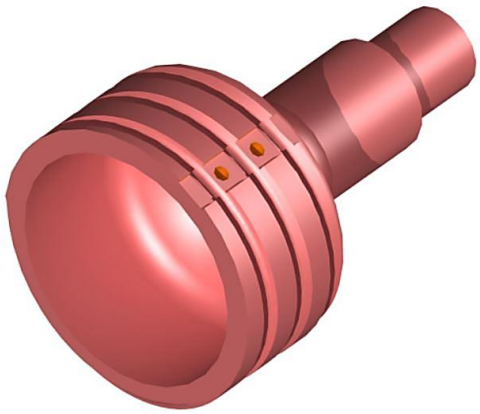

Figure 4-48: Driving Pulley (1st Pulley) (Final CAD Drawing, CATIA V5)

The realization of the CAD model of the driving pulley was based on the indications regarding the diameters defined in Paragraph 4.3.2 (see Table 4-9). The insert placed on the rear part will be used to connect it to the steering column and in fact the dimensioning of this detail was carried out following the evaluations made on the tubular structure presented in Paragraph 4.3.2 in the section on the Steering Column. Instead, the diameter of the connection between the insert and the pulley body respects the internal diameter of the chosen support flange (see Figure 4-43).
Finally, the pocket that houses the two holes visible on the surface is the housing for one of the cable tensioners.

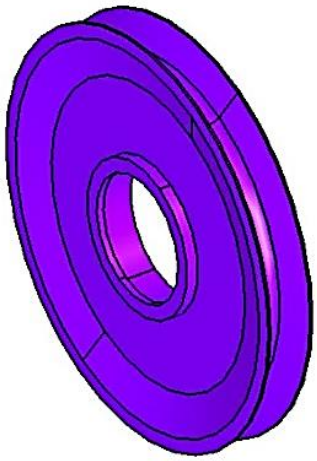

Figure 4-49: Secondary Pulley (2nd – 3rd Pulleys) (Final CAD Drawing, CATIA V5)

The secondary pulleys are of a more traditional form with no details requiring special connection. The height of the shoulders follows that described in Figure 4-31, while the internal diameter has been chosen to suit the particular tri-loaded support in Figure 4-46.

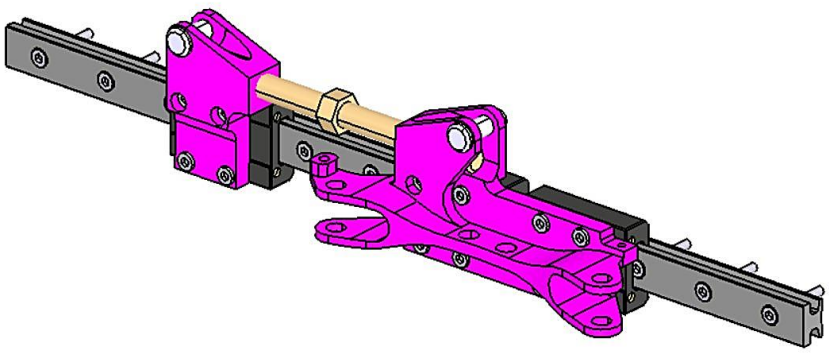

Figure 4-50: Central slide and rail guide on which it slides (Final CAD drawing, CATIA V5)

As explained in Paragraph 3.3, the horizontal translation slide and its rail guide are the subject of a sponsorship agreement between TUfast Eco Team and the company Reichenbacher Hamuel.

The CAD models in Figure 4-50 show the main features. The 300 mm long rail guide largely covers the distance covered by the slide, which as seen in Paragraph 4.2.3 is 160 mm. The white elements installed on the upper ends of the slide are the points of attachment to the cable, while the brown screw is a device for setting the tension in the cable because if screwed in, it allows the two parts of which the slide is composed to move closer or further away and therefore the two ends of the cable connected to them.

Figure 4-51: Steering Column and Support Flanges (Final CAD Drawing, CATIA V5)

The diameters used for the CAD model of the steering column are those of the carbon tubular structure available in stock and validated in Paragraph 4.3.2.

Figure 4-51 also shows the two flanges that support the column. The lower one was chosen following the calculation procedures illustrated in the same Paragraph 4.3.2 (see Figure 4-43), while the upper one as well as the connection element with the steering wheel were designed by the steering wheel team.

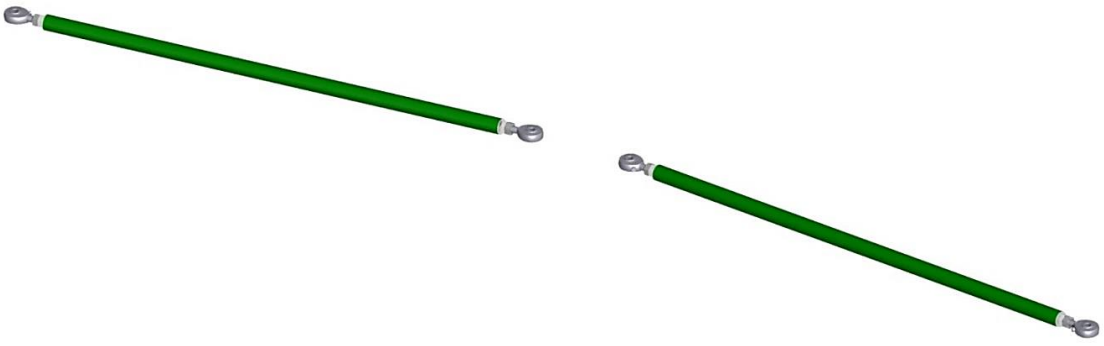

Figure 4-52: Tie rods (Final CAD Drawing, CATIA V5)

As for the steering column, also for the two tie rods, the diameters used for the CAD model are those of the carbon tubular structures available in stock and validated in Paragraph 4.3.2. Figure 4-52 also shows the bearing rings at the ends of the tie rods. These are the elements conventionally used to connect the tie rods to the rest of the system simulating the optimal joints of the Jeantaud mechanism (see Paragraph 4.2.3) in non-industrial or mass production applications.

All the components presented so far, all the calculations, drawings, procedures, researches, team meetings, sponsor meetings, analyses, simulations, design choices, have converged in the realisation of the Steering System, assembly of the various CAD models presented in this Paragraph. The realisation of the final and definitive CAD of the Steering System marks the conclusion of its design phase and with it also of this Thesis Research Work.
Below are the figures of the final result, which is fundamental for this Master Thesis, as well as for the TUfast Eco Team and specifically for the manufacturing team that will now begin production and the concrete realisation of what was designed and presented in this Thesis.
Postponing the conclusions to Chapter 6, we now insert Figures 4-53 and 4-54, i.e. the Steering System of muc022.

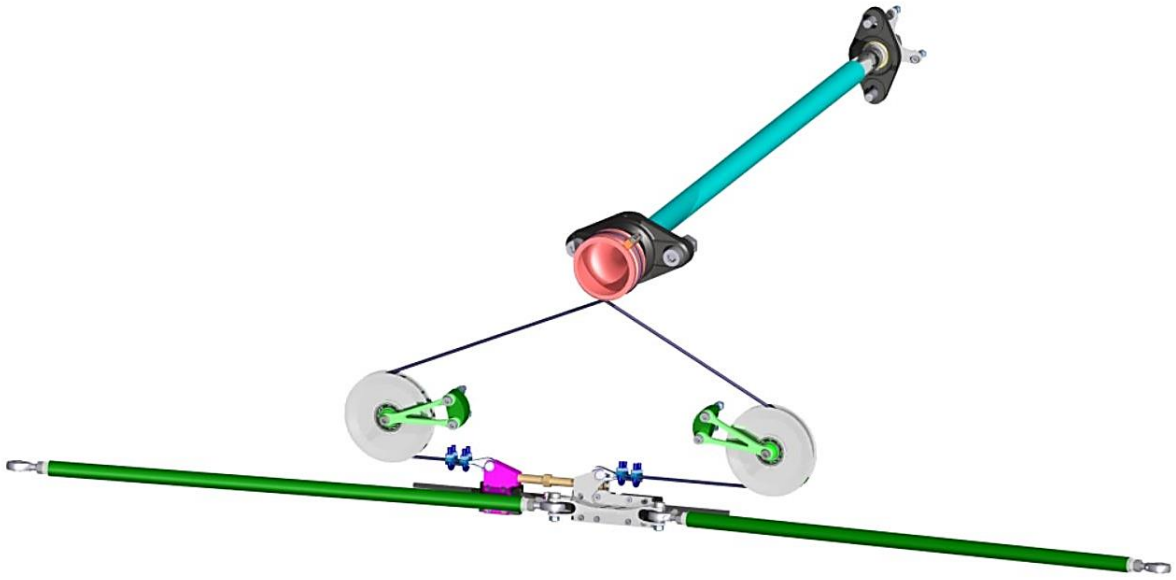

Figure 4-53: muc022 Steering System (isometric view) (Final CAD Drawing, CATIA V5)

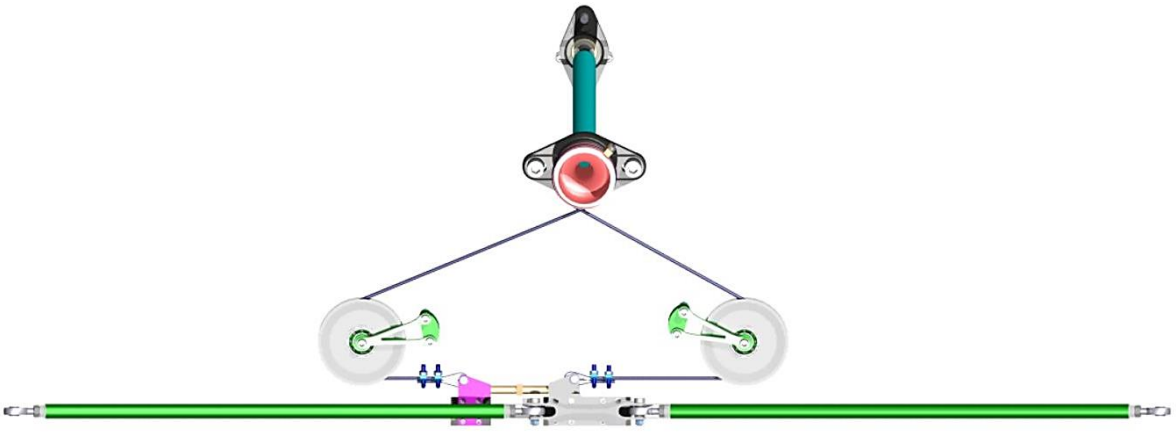

Figure 4-54: muc022 Steering System (frontal view) (Final CAD Drawing, CATIA V5)

At the time of writing this Thesis, a final CAD assembly of the entire muc022 has not yet been produced. However, below is the CAD assembly of all the mechanical systems of the muc022, so you can also see how the Steering System presented in this Thesis integrates with all the other systems of the car.

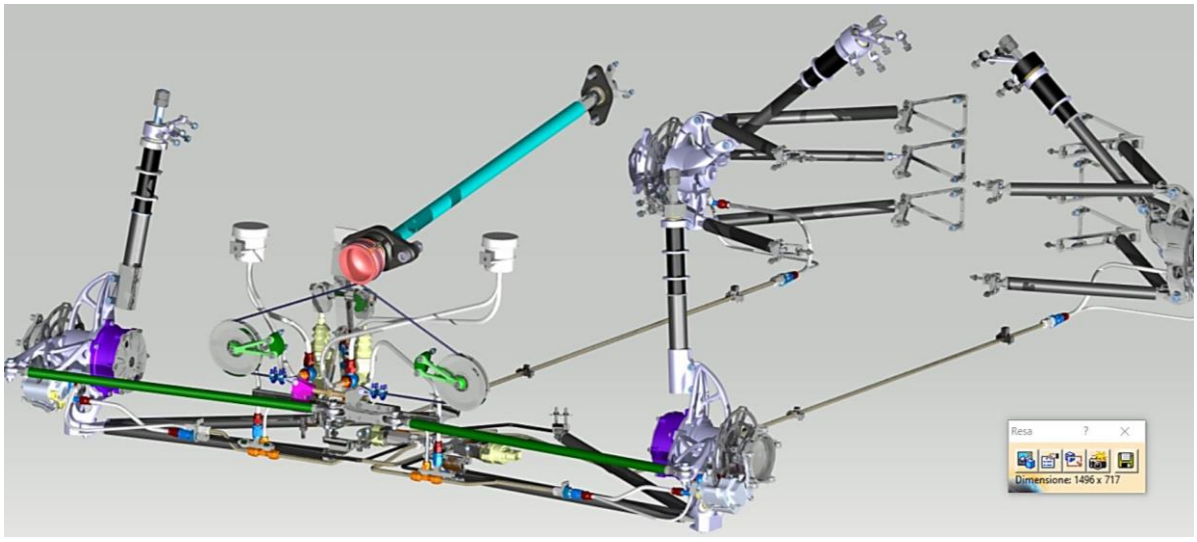

Figure 4-55: Assembly of all mechanical systems of muc022 (Final CAD Drawing, CATIA V5, TUfast E.T. 2022)

5 Future Improvements

In this Chapter some suggestions for possible future improvements of the project developed in this Thesis are presented. These suggestions are relevant and useful not only on a didactic and formal level, but also and above all for the future of the team and its future members, so as to have a well-defined starting point for the next few years and guidelines that will lead to better and better results and performances, with the aim of avoiding that each team is forced to start from a blank sheet of paper every time, as all muc022 designers have been forced to do.

In Paragraph 4.3.2 the dimensioning of the pulley support elements was dealt with among other things. In the case of the secondary pulleys, it was stated that the support element of the latter has three load points and that one of these consists of a threaded element which provides a fixing surface for the bearing+pulley assembly and the choice of bearing agreed with Aluminium Engineering was an SKF 61902 radial ball bearing (see Figures 4-44 and 4-46). The radial bearing is a good solution given that the secondary pulley bearing does not support axial loads. However, it is precisely from this observation that a possible point of development can be identified.
As these bearings are not designed to support axial loads, instead of a radial ball bearing, the selection and dimensioning of a needle roller or needle roller bearing could be considered.

Figure 5-1: Example of needle bearing

This type of bearing is designed to withstand radial loads but above all to promote rolling and rotation due to the large surface area of the ring covered by the large number of cylinders. This reduces the friction that could arise over time and slow down the rotation of the pulleys. In addition, needle bearings have another advantage: they have smaller diameters than ball bearings. In this way, it is possible to reduce the vertical space taken up along the wall of the monocoque by the bearing and pulley assembly.

The dimensioning of the tie rods was also discussed in Paragraph 4.3.2. As specified, these elements must withstand a maximum axial load $F_{steer,max} = 510{,}2\ N$. The carbon fibre tubular structures chosen to make the tie rods have diameters $d_{int} = 12\ mm\ d_{ext} = 14\ mm$ and guarantee a maximum permissible axial load $F_{a,max} = 5121\ N$. These components were the smallest available in stock and were therefore used to comply with the team's philosophy of zero material and economic waste; however, it is clear that the safety margin on axial load is very large and could be exploited to reduce the section of the tie rods.
This would lighten the overall weight of the system and also reduce one of the most critical overall dimensions of the various components. The tie rods have a length of 419.217 mm each, compared with a front track half-length of 540 mm. In their movement, therefore, they sweep an area that covers a very large portion of the front part of the car.
Reducing their diameters could reduce the risk of contact with the other structures present, in particular with the motor hub which, we should remember, is located in the centre of the wheel hub (see Figure 4-15), which could thus be extended to accommodate more powerful motors or allow greater heat dispersion.

A final suggestion that is more of a suggestion for the future is to consider implementing an autonomous steering system on the existing muc022 architecture. This is something more complex than the suggestions given above, and would involve a re-evaluation of the space, masses and overall dimensions of all the system components. However, it would be a nice evolution of the system and an alignment with what is now the very present future of the automotive industry.
In this sense, I was able to take some ideas that could lead to some valid solutions. Here are some hints.

Of course, in order to create an autonomous system, it is necessary to implement a rotational or linear actuator, the control and operation of which is controlled by the sensor system developed by the sensor department. From a mechanical point of view, this rotational actuator could be linked to a pinion coupled with a rack fixed to the central slide. In this way, actuating the actuator rotates the pinion and moves the rack and with it the central slide and the two tie rods. However, the actuator-pinion connection must have a clutch, so that it can be operated at will by the pilot and allow the switch from manual to autonomous driving. If the two clutch discs are also available, it would be possible to remove the entire autonomous apparatus to allow participation in the Shell Eco Marathon, a competition in which current regulations do not allow assisted steering or steering.

Another solution would be to use a toothed intermediate element connected to a linear actuator. This intermediate element would be coupled to a toothing made on the central slide so that when the linear actuator is commanded to move out or in, it would take the toothed element with it and through the coupling would also move the central slide, as can be seen in Figure 5-2.

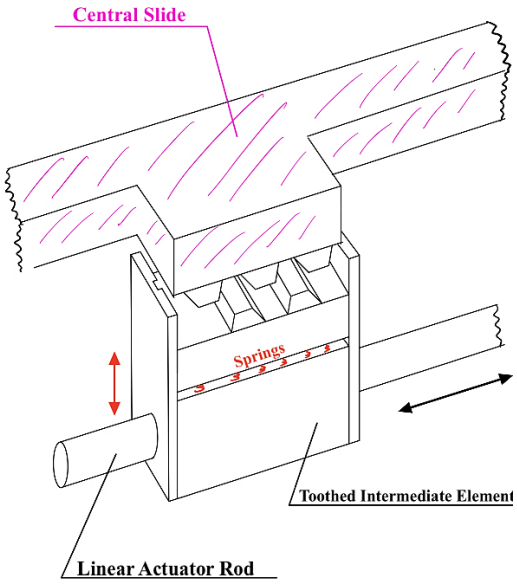

Figure 5-2: A simple sketch giving shape to the idea of an intermediate toothed element

The intermediate element is divided into two parts: the upper part with the toothing and the lower part, connected together by a system of springs. The springs tend in their natural position to push the upper part against the toothing made on the slide. However, by means of a mechanical or electrical control by the driver, it is possible to force the upper part to descend against the action of the springs and then lock it in that position using another spring or valves (see Figure 5-3).

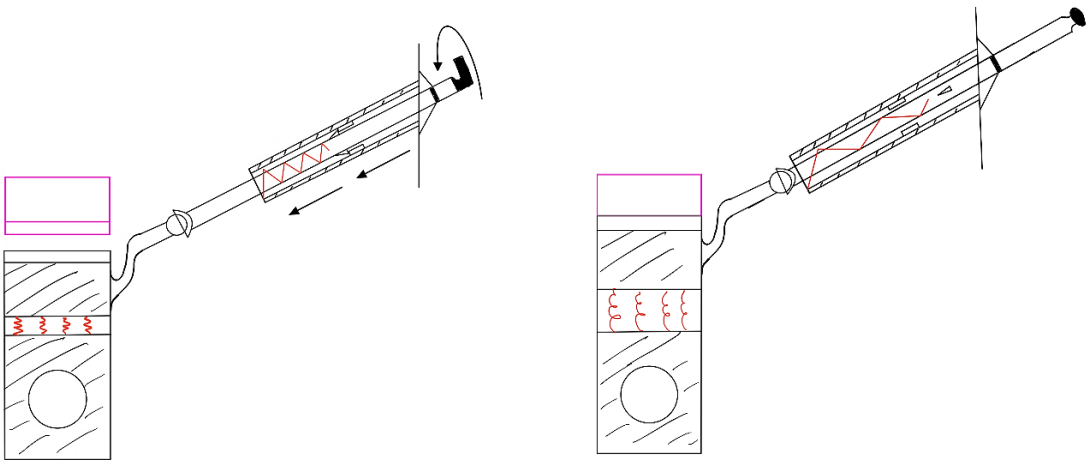

Figure 5-3: A simple sketch of the control of the manual-autonomous drive switch mechanism

The ideas given here and the sketches are only incipits, ideas to be verified and to be used as a basis for integrating an autonomous drive on the particular architecture of the muc022 Steering System.

6 Conclusion

The heart and objective of this Research Work and Thesis was the development of a Steering System that was strongly characterised by lightness and originality. In this sense, this project fits in perfectly with the evolution of systems in the automotive world, which is increasingly extreme and oriented towards reducing weights and dimensions to make room for new battery packs, new electric or hybrid engines and, more generally, to better optimise available space. Promoting sustainable, lightweight, modular and easily integrated systems such as the one described in this Thesis is also an important step towards improving environmental conditions and respect for ecology. It represents a step towards a greener industry. Added to this is the sporting and competitive nature of a project that was born and grew up alongside the rules of a motorsport event, the Shell Eco Marathon, which becomes a spur for continuous improvement aimed at surpassing the results achieved on a daily basis.

With these well-defined themes as a basis and support, this project has developed.
The first stages were to study and analyse the initial situation, the technical and managerial requirements, the limitations and constraints imposed, and to set the objective and the results. The architecture of the Steering System was born from these. The first step in creating this architecture was to choose the kinematic theory of the system and assess how and through which geometric parameters this could be achieved, using advanced kinematic simulation tools. Once the kinematics and therefore the angles, lines and trajectories that the car had to follow through the Steering System had been established, a dynamic analysis phase was necessary to assess what forces were required to perform these trajectories and above all how to generate them. The mathematical model derived from this section made it possible to link the kinematic results to the forces required to achieve them. Once the value of these forces was known, the next step was to size the components of the architecture designed for the Steering System, so that they would be able to generate them. At this stage it was also necessary to think about how to integrate the various elements with each other and with the other systems, choosing and sizing various supports and connection structures. When all the dimensions were finally set, it was possible to create CAD models of each element and of the entire Steering System. These will become fundamental tools for the subsequent Manufacturing and physical production phase of the system.

The path followed to reach the final result was extremely educational. It required the acquisition and accumulation of a great deal of technical knowledge, from the most common Steering System architectures to the understanding of its operation, passing through the various kinematic theories and the longitudinal and lateral dynamic analysis of the car, up to and including the most classic methods of dimensioning and verifying loads and stresses, as well as an excellent knowledge of professional software such as CATIA V5, DMU Kinematics and CIM Database. All these were tools which, from being requirements for completing the project, became knowledge and pieces of personal technical training.
The added value of a project like this, however, was certainly the teamwork it required.

Being part of such a prestigious team, with the aim of achieving an equally prestigious result was extremely motivating and a continuous source of constructive comparisons and ideas for growth.
TUfast E.T. philosophy of work, collaboration, future-oriented lateral thinking, respect for the environment and management of human, technical and economic resources permeates every page of this Thesis.
This Project represents a real furrow left in the world of university competitions, a guide and a starting point for the future of the same and a glimpse of what is the automotive world.

7 List of Figures

8 List of Tables

9 List of Abbreviations

CAD	Computer-Aided Drafting
DMU	Digital Mock-Ups
MUC	Munich Urban Concept
SAE	Society of Automotive Engineers
SEM	Shell Eco Marathon

10 Bibliography

Abe M. (2008). *Vehicle dynamics and control for improving handling and active safety from four-wheel-steering to direct yaw moment control*. Academic Paper.

Altair Engineering. (2017). *Lighter, farther, faster, greener: TUfast Eco team drives to success with HyperWorks*. Altair University Merit Paper.

Aluminium Engineering. (n.d.) *About Us*. Retrieved July 25, 2021, from ALEN Gmbh: https://aluengineering.de/

Audi. (2021, May 5). *Fine-tuning the characteristics of the Audi steering system*. Retrieved October 19, 2021, from Audi: https://www.audi-mediacenter.com/en/press-releases/fine-tuning-the-characteristics-of-the-audi-steering-system-13955

Baragetti S., Terranova A. (2007, November 27). *Design and calculation of mechanical systems*. Hoepli. ISBN-13: 978-8820339357

Bargende M., Reuss H., Wiedemann J. (2017 January). *Internationales Stuttgarter Symposium: Automobil und Motorentechnik.* Springer. doi: 10.1007/978-3-658-16988-6

BMW. (2020, June 3). How car steering determines a car's driving feel. Retrieved October 5, 2021, from BMW: https://www.bmw.com/en/performance/requirements-for-good-car-steering.html

Carbiketech. (2019, August 6). *Worm & Sector Steering*. Retrieved October 10, 2021, from: https://carbiketech.com/worm-and-sector-steering/

Ceccantini. (n.d.). *Cables and Ropes Catalog*. Retrieved October 11, 2021, from Ceccantini: www.ceccantini.it/cataloghi/nuovocatalogo/02-funi.pdf

Euromotor. (n.d.). *Automotive Engineering II Topic 10-11-12*. Retrieved July 24, 2021, from Euromotor: https://www.euromotor.org/mod/resource/view.php?id=21338

Ferraresi C., Raparelli T. (2007, March 1). *Machine Applied Mechanics*. CLUT Editrice. ISBN-13: 978-8879922548

Ferrari. (2012). *Ferrari F12berlinetta Vehicle Dynamic* (Motion Picture). Retrieved October 20, 2021, from Ferrari: https://www.ferrari.com/it-IT/auto/f12-berlinetta

Formula1. (2020, February 20). DAS explained: What we know so far about Mercedes' trick new steering system. Retrieved October 22, 2020, from Formula1: https://www.formula1.com/en/latest/article.das-explained-what-we-know-so-far-about-mercedes-trick-new-steering-system.4vgDQ6cc20xUfhdZGT0ejB.html

Johanson C., Stockel M. (2014, February 3). *Auto Suspension & Steering*. G-W. ISBN: 9781619607156

Koyo. (1999). *Trends Regarding Rolling Bearings for Steering System*. Engineering Journal

Performance Composites. (n.d.). *Mechanical Properties of Carbon Fibre Composite Materials, Fibre / Epoxy resin.* Retrieved October 10, 2021, from Performance Composites: http://www.performance-composites.com/carbonfibre/mechanicalproperties_2.asp

Porsche. (n.d.). *Steering Systems*. Retrieved October 19, 2021, from Porsche Engineering: https://www.porscheengineering.com/peg/en/services/engineeringservices/chassis/steering/

Reichenbacher Hamuel. (n.d.). *Company*. Retrieved May 27, 2021, from Reichenbacher: https://reichenbacher.de/en/company/factories-locations

Shaikh, Parvez, Shakebuddin. (2016, June). *Design, Analysis and Optimization of Collapsible Steering Column*. IRJET. Academic Paper

Sharp R., Granger R. (2003). *Proceedings of the Institution of Mechanical Engineers Part D.* Journal of Automobile Engineering

Shekh M., Umrao O., Singh D. (2020, June 2). *Kinematic Analysis of Steering Mechanism: A Review.* Springer. doi: 10.1007/978-981-15-2647-3_48

Shell. (2020). *Shell Eco-Marathon 2021 Official Rules Chapter 1*. Retrieved from https://www.makethefuture.shell/en-gb/shell-eco-marathon/global-rules

Shell. (n.d.). 2020 *Virtual Programme*. Retrieved October 12, 2021, from Make the future: https://www.makethefuture.shell/en-gb/shell-eco-marathon/virtual-programme

Shell. (n.d.). *How it works*. Retrieved October 10, 2021, from Make the future: https://www.makethefuture.shell/en-gb/shell-eco-marathon/how-it-works

Shell. (n.d.). *Track competitions*. Retrieved October 20, 2021, from Make the future: https://www.makethefuture.shell/en-gb/shell-eco-marathon/competitions

Spentzas K., Alkhazali I., Demic M. (2001). *Kinematics of four-wheel-steering vehicles*. Springer. doi: 10.1007/s100100100060

Summala H. (1981). *Driver/Vehicle Steering Response Latencies*. Academic Paper

Tilley A., Dreyfuss H. (2002, February 13). *The Measure of Man and Woman: Human Factors in Design*. John Wiley & Sons Inc. ISBN-13: 978-0471099550

TUfast. (2018, November 2). TUfast Eco Team Twitter account. Retrieved October 10, 2021, from Twitter: https://twitter.com/tufast_eco/status/1058388668027715585

TUfast. (2019). muc019. Retrieved October 10, 2021, from TUfast Eco: https://tufast-eco.de/project_muc019=en.html

TUfast. (n.d.). *About TUfast*. Retrieved October 11, 2021, from TUfast Racing Team: https://tufast-racingteam.de/about-tufast/

Vigliani A., (2020). *Lectures on Motor Vehicles Mechanics*. Lecture slides. Politecnico di Torino, Turin.

Zhao X., Zhang S. (2009). *The Evolvement of Automobile Steering System Based on TRIZ*. Academic Paper. Northeastern University, Shenyang city, P.R. China.

At the conclusion of this Thesis, I would like to spend a few lines to thank those who have been a key component of this work.

I would like to thank my supervisor, Prof. Andrea Tonoli, for his infinite willingness to assist and support this activity and project of mine, making it a point of reference for the entire automotive world within the Politecnico di Torino.

I would also like to thank the Technische Universität München, which welcomed me during my training abroad and gave me the opportunity to get to know a different, new and extremely stimulating academic and teaching environment.

A heartfelt thank you also to the whole TUfast Eco Team, a family before being a student team. Having the opportunity to be part of it for about a year has taught me a lot about the automotive world, about collaboration between team members, about the importance of achieving many small and large personal results aimed at achieving a single shared and global result. This dissertation encapsulates all my experience in the team and all that it has left me.

Finally, I would like to thank the Politecnico di Torino, because in all these years it has taught me an incredible number of things, and not only of a technical nature. Perseverance, curiosity, analysis of difficulties and situations, awareness of one's own means, the desire not to be satisfied, the development of critical thinking and an eclectic vision are, together of course with the technical and educational background, the most important legacy of the Politecnico and this, from my point of view, is the highest ambition and the most vivid source of pride for a University!